# Models of Electric Machines

# Models of Electric Machines

**Marc Bodson**

ISBN: 9798542675947. Independently published.
Electronic file produced on August 6, 2022.



Front cover: schematic of a brushless doubly-fed reluctance machine (see p. 26).
Back cover: schematic of a brushless doubly-fed induction machine (see p. 43).

# Preface

This short book presents mathematical models for various electric machines, including brushless doubly-fed reluctance machines and brushless doubly-fed induction machines. These less conventional machines have recently attracted significant research interest. Other models include ordinary doubly-fed induction machines, cascaded doubly-fed induction machines, wound-field synchronous machines, three-phase machines with single-phase excitation, non-symmetric induction machines, and hybrid motors. The presentation complements another book from the author where the models of simpler machines are developed. Concepts from winding function theory are given to enable the modeling of more advanced configurations. A contribution of the work is the derivation of multiple state-space models in a common framework. Complex variable models are introduced in cases where considerable simplifications can be achieved. The equivalence between different types of machines is demonstrated. Another contribution of the work is the presentation of models for arbitrary three-phase to two-phase transformations, showing the impact of the choices made on the resulting models.

# About the author

Marc Bodson received a Ph.D. degree in Electrical Engineering and Computer Science from the University of California, Berkeley, in 1986. He obtained two M.S. degrees - one in Electrical Engineering and Computer Science and the other in Aeronautics and Astronautics - from the Massachusetts Institute of Technology, Cambridge MA, in 1982. In 1980, he received the degree of Ingénieur Civil Mécanicien et Electricien from the Université Libre de Bruxelles, Belgium. He is a Professor of Electrical & Computer Engineering at the University of Utah in Salt Lake City, where he was Chair of the department between 2003 and 2009. He was the Editor-in-Chief of *IEEE Trans. on Control Systems Technology* from 2000 to 2003. He was elected *Fellow* of the IEEE in 2006, and *Associate Fellow* of the American Institute of Aeronautics and Astronautics in 2013. He also received the Engineering Educator of the Year award from the Utah Engineers Council in 2007. His activities are described in further detail at www.ece.utah.edu/~bodson.

**Acknowledgment:** the author thanks Ray Beach, Linda Taylor, and David Sadey from the NASA Glenn Research Center for discussions on hybrid-electric propulsion that motivated some of the work leading to this book. The author is also most grateful to his friend and collaborator, Dr. John Chiasson for stimulating his interest in electric machines over the span of many years.

# Chapter 1

# Introduction

## 1.1 Objective

This chapter introduces basic principles of modeling of electric machines, including transformations that are useful for three-phase machines.

## 1.2 General model of an electric machine

The electrical equations of a machine with $n$ windings are

$$\frac{d\psi_k}{dt} = v_k - R_k i_k, \qquad \text{for } k = 1, \cdots, n, \tag{1.1}$$

where $\psi_k$ is the total flux linkage in winding $k$, $v_k$ is the voltage applied to the winding, and $i_k$ is the current flowing in the winding. The signs of the voltages and currents are chosen such that $v_k i_k > 0$ if power is absorbed by the winding.

The total flux linkages in the windings are assumed to be of the form

$$\psi_k = \psi_{m,k}(\theta) + \sum_{j=1}^{n} L_{kj}(\theta)\ i_j, \tag{1.2}$$

where $\psi_{m,k}(\theta)$ originates from the permanent magnets in the machine (if any), $\theta$ is the angular position of the rotor, $L_{kk}(\theta)$ is the self-inductance of winding $k$, and $L_{kj}(\theta)$ is the mutual inductance between winding $k$ and winding $j$ (with $L_{kj} = L_{jk}$).

Combining (1.1) and (1.2),

$$\frac{d\psi_k}{dt} = \frac{\partial \psi_{m,k}(\theta)}{\partial \theta}\ \omega + \sum_{j=1}^{n} L_{kj}(\theta)\ \frac{di_j}{dt} + \sum_{j=1}^{n} \frac{\partial L_{kj}(\theta)}{\partial \theta}\ i_j\ \omega, \tag{1.3}$$

where

$$\omega = \frac{d\theta}{dt} \tag{1.4}$$

is the angular velocity of rotation of the rotor. The electrical equations of the machine are then

$$\sum_{j=1}^{n} L_{kj}(\theta)\ \frac{di_j}{dt} = v_k - R_k i_k - \frac{\partial \psi_{m,k}(\theta)}{\partial \theta}\ \omega - \sum_{j=1}^{n} \frac{\partial L_{kj}(\theta)}{\partial \theta}\ i_j\ \omega. \tag{1.5}$$

Based on principles of energy conservation, the motoring torque can be computed to be [6]

$$\tau_M = \sum_{k=1}^{n} \frac{\partial \psi_{m,k}(\theta)}{\partial \theta}\ i_k + \frac{1}{2} \sum_{k=1}^{n} \sum_{j=1}^{n} \frac{\partial L_{kj}(\theta)}{\partial \theta}\ i_j\ i_k. \tag{1.6}$$

The model can also be written in matrix form as

$$\begin{aligned} L(\theta)\frac{di}{dt} &= v - Ri - \frac{\partial \psi_m(\theta)}{\partial \theta}\ \omega - \frac{\partial L(\theta)}{\partial \theta} i\ \omega \\ \tau_M &= i^T \frac{\partial \psi_m(\theta)}{\partial \theta} + \frac{1}{2} i^T \frac{\partial L(\theta)}{\partial \theta} i, \end{aligned} \tag{1.7}$$

where $L(\theta)$ is a matrix with elements $L_{kj}(\theta)$ and $\psi_m(\theta)$, $v$, and $i$ are vectors with elements $\psi_{m,k}(\theta)$, $v_k$, and $i_k$, respectively. $R$ is a diagonal matrix with elements $R_k$ on the diagonal. All vectors, including $\partial \psi_m(\theta)/\partial \theta$, are assumed to be column vectors.

## 1.3 Three-phase to two-phase transformations

Three-phase to two-phase transformations are useful to represent three-phase machines as equivalent two-phase machines. A generic $3-2$ transformation is defined by

$$\begin{pmatrix} v_a \\ v_b \\ v_h \end{pmatrix} = M_{3-2} \begin{pmatrix} v_A \\ v_B \\ v_C \end{pmatrix}, \text{ with } M_{3-2} = C_V \begin{pmatrix} 1 & -1/2 & -1/2 \\ 0 & \sqrt{3}/2 & -\sqrt{3}/2 \\ 1/\sqrt{2} & 1/\sqrt{2} & 1/\sqrt{2} \end{pmatrix}. \tag{1.8}$$

In (1.8), $v_A$, $v_B$, and $v_C$ are three-phase variables, $v_a$ and $v_b$ are equivalent two-phase variables, and $v_h$ is the homopolar variable added to make the transformation invertible. The coefficient $C_V$ determines the type of transformation that is used. Choices made in the literature are typically $C_V = 1$, $\sqrt{2/3}$, and $2/3$. The inverse of the $3-2$ transformation, or $2-3$ transformation, is given by

$$\begin{pmatrix} v_A \\ v_B \\ v_C \end{pmatrix} = M_{3-2}^{-1} \begin{pmatrix} v_a \\ v_b \\ v_h \end{pmatrix}, \text{ with } M_{3-2}^{-1} = \frac{2}{3C_V} \begin{pmatrix} 1 & 0 & 1/\sqrt{2} \\ -1/2 & \sqrt{3}/2 & 1/\sqrt{2} \\ -1/2 & -\sqrt{3}/2 & 1/\sqrt{2} \end{pmatrix}. \tag{1.9}$$

For balanced three-phase voltages

$$v_A = V_{pk}\cos(\theta_S),\ v_B = V_{pk}\cos(\theta_S - 2\pi/3),\ v_C = V_{pk}\cos(\theta_S + 2\pi/3), \tag{1.10}$$

the two-phase voltages satisfy

$$v_a = C_M V_{pk}\cos(\theta_S),\quad v_b = C_M V_{pk}\sin(\theta_S),\quad v_h = 0, \tag{1.11}$$

where

$$C_M = \frac{3}{2}C_V. \tag{1.12}$$

Power in the three-phase and two-phase variables is defined through

$$P = v_A i_A + v_B i_B + v_C i_C,\quad P_2 = v_a i_a + v_b i_b + v_h i_h. \tag{1.13}$$

It turns out that

$$P_2 = C_P P,\quad \text{with } C_P = \frac{3}{2}C_V^2. \tag{1.14}$$

The coefficients $C_P$ and $C_M$ are given in the following table for the three typical choices of $C_V$ [6]. For each choice, one coefficient is equal to 1. The labels used in the table are chosen to reflect the property, but are not standard in the literature.

| | Equal vector | Equal power | Equal magnitude |
|---|---|---|---|
| $C_V$ | 1 | $\sqrt{2/3}$ | 2/3 |
| $C_P$ | 3/2 | 1 | 2/3 |
| $C_M$ | 3/2 | $\sqrt{3/2}$ | 1 |

Note that the homopolar variable can be multiplied by a separate coefficient in the $3-2$ transformation and divided by the same coefficient in the $2-3$ transformation. The change has no impact on the results of this document, except for the power equivalence in (1.14). The homopolar variable is typically assumed to be zero or is neglected.

# Chapter 2

# Winding Function Theory

## 2.1 Objective

The objective of this chapter is to present elements of winding function theory and apply the results to compute inductances for various winding configurations.

## 2.2 Winding function

Fig. 2.1 shows the cross-section of the cylindrical stator and rotor of a machine. The rotor is slightly smaller than the stator, and the difference between the radius of two circles is called the *airgap* length. The airgap is said to be uniform. A *concentrated winding* is shown on the periphery of the stator and has two turns The conductors are represented by circles with dots and crosses representing the direction of the current as the front and back of an arrow (the current flows into the page for the cross and out of the page for the dot). The rotor position is identified by the angle $\alpha$ of an arbitrary location with respect to the horizontal.

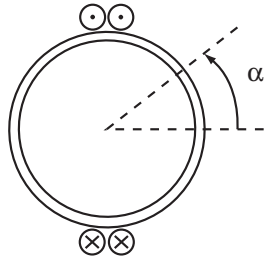


Figure 2.1: Concentrated winding with two turns

Fig. 2.2 shows how the so-called *winding function* associated with the winding

of Fig. 2.1 is obtained. On the left, the number of conductors is counted in the counterclockwise direction, starting from $\alpha = -\pi$. The count is incremented by 1 when a cross is encountered and -1 when a dot is encountered. So, the count becomes 2 for $\alpha = -\pi/2$ and returns to zero when $\alpha = \pi/2$.

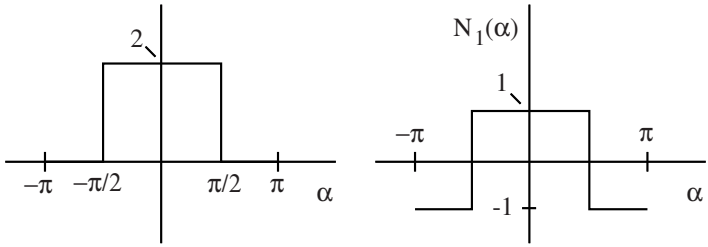


Figure 2.2: Winding function for a concentrated winding with two turns

On the right of the figure, the winding function $N_1(\alpha)$ is obtained from the function on the left by adding a constant (-1 in this case) such that the average of $N_1(\alpha)$ is equal to zero. For a concentrated winding with $N_1$ turns, the winding function becomes

$$N_1(\alpha) = \frac{N_1}{2} \operatorname{sign}(\cos(\alpha)), \tag{2.1}$$

where the sign function is such that

$$\begin{aligned} \operatorname{sign}(x) &= 1 \quad && \text{for } x > 0 \\ \operatorname{sign}(x) &= 0 \quad && \text{for } x = 0 \\ \operatorname{sign}(x) &= -1 \quad && \text{for } x < 0. \end{aligned} \tag{2.2}$$

Fig. 2.3 shows a configuration with two windings having a 90° span instead of a single winding with a 180° span. The two windings are connected in series. The overall winding is said to have 4 *poles* or 2 *pole pairs* (as opposed to 2 poles and 1 pole pair in Fig. 2.1). In this case,

$$N_1(\alpha) = \frac{N_1}{2} \operatorname{sign}(\cos(n_1\alpha)), \tag{2.3}$$

where $N_1$ is the number of turns per pole pair and $n_1$ is the number of pole pairs. If the windings are rotated by an angle $\varphi_1/n_1$ in the counter-clockwise direction, the function is replaced by

$$N_1(\alpha) = \frac{N_1}{2} \operatorname{sign}(\cos(n_1\alpha - \varphi_1)). \tag{2.4}$$

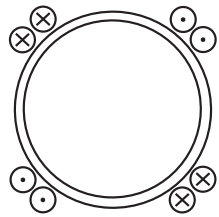

Figure 2.3: Concentrated winding with two pole pairs

*Sinusoidally-distributed windings* are obtained by carefully setting the conductors so that the winding function can be approximated by a sinusoidal function. Then, the winding function is assumed to be

$$N_1(\alpha) = \frac{N_1}{2}\cos(n_1\alpha - \varphi_1), \tag{2.5}$$

where $N_1$ is the number of turns per pole pair, $n_1$ is the number of pole pairs, and $\varphi_1$ specifies the orientation of the winding.

## 2.3 Computation of inductances

Winding function theory [22] states that the mutual inductance (in H) between two windings is

$$L_{12} = c\int_{-\pi}^{\pi} N_1(\alpha)N_2(\alpha)\ d\alpha, \tag{2.6}$$

where

$$c = \frac{\mu_0\ r\ l}{g}. \tag{2.7}$$

The parameters of the equation are $g$, the airgap length (in m), $\mu_0$, the permeability of free space (equal to $4\pi\ 10^{-7}$ H/m), $r$, the radius of the rotor (in m), and $l$, the length of the rotor (in m). The self-inductance of a winding is obtained as a special case where $N_2(\alpha) = N_1(\alpha)$.

The expression (2.6) is based on idealized assumptions and should not be expected to be very accurate. The airgap is assumed to be small, and the result is applied in the same way regardless of whether a winding is located on the stator or on the rotor. Still, the theory is useful to understand general charateristics of electric machines and how inductances depend on machine parameters.

For two sinusoidally-distributed windings,

$$\begin{aligned} L_{12} &= \frac{cN_1N_2}{4}\int_{-\pi}^{\pi}\cos(n_1\alpha-\varphi_1)\cos(n_2\alpha-\varphi_2)\;d\alpha \\ &= \frac{cN_1N_2}{8}\int_{-\pi}^{\pi}\cos\left((n_1+n_2)\alpha-(\varphi_1+\varphi_2)\right)\;d\alpha \\ &\quad +\frac{cN_1N_2}{8}\int_{-\pi}^{\pi}\cos\left((n_1-n_2)\alpha-(\varphi_1-\varphi_2)\right)\;d\alpha. \end{aligned} \tag{2.8}$$

Note that $L_{12} = 0$ if $n_1 \neq n_2$. In other words, two windings with different numbers of pole pairs are not coupled magnetically. On the other hand, if $n_1 = n_2$,

$$L_{12} = \frac{cN_1N_2\pi}{4}\cos\left(\varphi_1-\varphi_2\right). \tag{2.9}$$

As a special case, the self-inductance of a winding is

$$L_{11} = \frac{cN_1^2\pi}{4}. \tag{2.10}$$

**Example of a two-phase machine with identical AB windings:** let $N_A = N_B = N$, $\varphi_A = 0$, and $\varphi_B = \pi/2$. Then

$$L_{AA} = L_{BB} = \frac{cN^2\pi}{4},\; L_{AB} = 0. \tag{2.11}$$

**Example of a three-phase machine with identical ABC windings:** let $N_A = N_B = N_C = N$, $\varphi_A = 0$, $\varphi_B = 2\pi/3$, and $\varphi_C = -2\pi/3$. Then

$$\begin{aligned} L_{AA} &= L_{BB} = L_{CC} = \frac{cN^2\pi}{4} \\ L_{AB} &= L_{BC} = L_{CA} = -\frac{cN^2\pi}{8}. \end{aligned} \tag{2.12}$$

In the theory of electric machines, the self-inductances are assumed to be slightly larger than the predicted values to account for the presence of so-called *leakage fluxes*.

## 2.4 Non-uniform airgap

In some cases, electric machines are deliberately built with a varying airgap length. For example, Fig. 2.4 shows a rotor built so that the airgap length reaches a maximum (or minimum) value three times along the periphery of the rotor. The dotted circle shows the average airgap length with respect to the stator. An angle $\theta$ is introduced that identifies the position of the rotor through

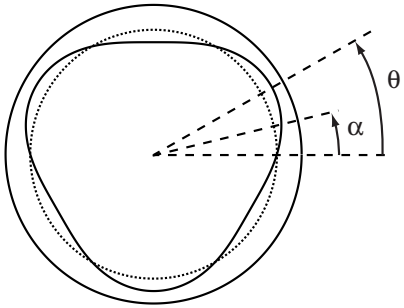


Figure 2.4: Machine with varying airgap

one of the locations where the airgap length is the smallest. Note that a varying airgap length will also be used to model rotors with heterogeneous constructions, such as in Fig. 4.1.

For the analysis of machines with non-uniform airgaps, (2.6) and (2.7) are used, but with $g$ replaced according to

$$\frac{1}{g} \rightarrow \frac{1}{g}\left(1 + d\ \cos(n_R(\alpha - \theta)\right), \tag{2.13}$$

where $0 < d < 1$ and $n_R$ is the number of peaks of the airgap length ($n_R = 3$ in Fig. 2.4). With this change, $1/g$ represents the average inverse airgap length. The case $d = 0$ corresponds to a uniform airgap. While it may have been more intuitive to choose a sinusoidal variation of the airgap length, the choice of inverse airgap length produces useful analytic results.

The mutual inductance (2.6) between two sinusoidal windings becomes

$$L_{12} = L_{12,0} + L_{12,d}, \tag{2.14}$$

where

$$L_{12,0} = \frac{cN_1N_2}{4}\int_{-\pi}^{\pi} \cos(n_1\alpha - \varphi_1)\cos(n_2\alpha - \varphi_2)\ d\alpha, \tag{2.15}$$

and

$$L_{12,d} = \frac{cN_1N_2d}{4}\int_{-\pi}^{\pi} \cos(n_1\alpha - \varphi_1)\cos(n_2\alpha - \varphi_2)\cos(n_R(\alpha - \theta))\ d\alpha. \tag{2.16}$$

The component $L_{12,0}$ is the same as was obtained for the uniform airgap in (2.9), so that

$$\begin{aligned} L_{12,0} &= \frac{cN_1N_2\pi}{4}\cos\left(\varphi_1 - \varphi_2\right) \quad \text{for} \quad n_1 = n_2 \\ L_{12,0} &= 0 \qquad\qquad\qquad\qquad\quad \text{for} \quad n_1 \neq n_2. \end{aligned} \tag{2.17}$$

The component depending on the parameter $d$ is equal to

$$\begin{aligned} L_{12,d} &= \frac{cN_1N_2d}{16}\int_{-\pi}^{\pi} \left(\cos\left((n_1+n_2+n_R)\alpha-(\varphi_1+\varphi_2+n_R\theta)\right)\right. \\ &\quad +\cos\left((n_1+n_2-n_R)\alpha-(\varphi_1+\varphi_2-n_R\theta)\right) \\ &\quad +\cos\left((n_1-n_2+n_R)\alpha-(\varphi_1-\varphi_2+n_R\theta)\right) \\ &\quad \left.+\cos\left((n_1-n_2-n_R)\alpha-(\varphi_1-\varphi_2-n_R\theta)\right)\right)\ d\alpha. \end{aligned} \tag{2.18}$$

The result of the integration is that

$$L_{12,d}=0 \ \text{ unless } n_R=n_1+n_2,\ n_R=n_2-n_1,\ \text{or } n_R=n_1-n_2. \tag{2.19}$$

A case of interest is

$$L_{12,d}=\frac{cN_1N_2\pi d}{8}\cos(n_R\theta-(\varphi_1+\varphi_2)) \quad \text{if } n_R=n_1+n_2. \tag{2.20}$$

**Example of a two-phase machine with identical AB windings:** let $N_A = N_B = N$, $n_A = n_B = n_P$, $n_R = 2n_P$, $\varphi_A = 0$, and $\varphi_B = \pi/2$. Then

$$\begin{aligned} L_{AA} &= \frac{cN^2\pi}{4}+\frac{cN^2\pi d}{8}\cos(2n_P\theta) \\ L_{BB} &= \frac{cN^2\pi}{4}-\frac{cN^2\pi d}{8}\cos(2n_P\theta) \\ L_{AB} &= \frac{cN^2\pi d}{8}\sin(2n_P\theta). \end{aligned} \tag{2.21}$$

**Example of a three-phase machine with identical ABC windings:** let $N_A = N_B = N_C = N$, $n_A = n_B = n_C = n_P$, $n_R = 2n_P$, $\varphi_A = 0$, $\varphi_B = 2\pi/3$, and $\varphi_C = -2\pi/3$. Noting that an angle $4\pi/3$ is the same as $-2\pi/3$,

$$\begin{aligned} L_{AA} &= \frac{cN^2\pi}{4}+\frac{cN^2\pi d}{8}\cos(2n_P\theta) \\ L_{BB} &= \frac{cN^2\pi}{4}+\frac{cN^2\pi d}{8}\cos(2n_P\theta+2\pi/3) \\ L_{CC} &= \frac{cN^2\pi}{4}+\frac{cN^2\pi d}{8}\cos(2n_P\theta-2\pi/3)) \\ L_{AB} &= -\frac{cN^2\pi}{8}+\frac{cN^2\pi d}{8}\cos(2n_P\theta-2\pi/3) \\ L_{BC} &= -\frac{cN^2\pi}{8}+\frac{cN^2\pi d}{8}\cos(2n_P\theta) \\ L_{CA} &= -\frac{cN^2\pi}{8}+\frac{cN^2\pi d}{8}\cos(2n_P\theta+2\pi/3). \end{aligned} \tag{2.22}$$

# Chapter 3

# Doubly-Fed Induction Machines

## 3.1 Objective

The objective of this chapter is to derive a model of the machine shown schematically on Fig. 3.1. The machine is called a *doubly-fed induction machine* (DFIM) or *wound-rotor induction machine* (WRIM) Both the stator and the rotor have three-phase windings (A, B, C, and X, Y, Z, respectively). With short-circuited rotor windings, the model also represents a three-phase cage rotor induction machine, or squirrel-cage induction machine. The results of the chapter:

- derive the model of the machine.
- show that the machine is equivalent to a two-phase machine if an equal power $3-2$ transformation is used. With other $3-2$ transformations, the equations are the same, except for an extra coefficient appears in the equation for the torque.
- derive a model of the machine in complex variables.
- extend the model to a rotating reference frame.

## 3.2 Model in phase variables

Define vectors of stator voltages, stator currents, and stator total flux linkages

$$v_S = \begin{pmatrix} v_{SA} \\ v_{SB} \\ v_{SC} \end{pmatrix}, \; i_S = \begin{pmatrix} i_{SA} \\ i_{SB} \\ i_{SC} \end{pmatrix}, \; \psi_S = \begin{pmatrix} \psi_{SA} \\ \psi_{SB} \\ \psi_{SC} \end{pmatrix}. \tag{3.1}$$

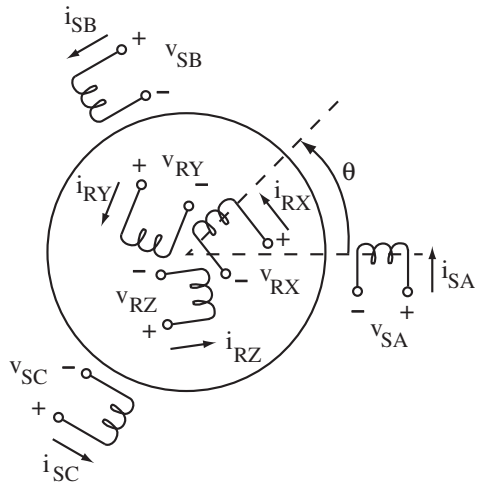


Figure 3.1: Schematic of a machine with three-phase stator and rotor windings

Rotor variables are similarly defined as

$$v_R = \begin{pmatrix} v_{RX} \\ v_{RY} \\ v_{RZ} \end{pmatrix}, \; i_R = \begin{pmatrix} i_{RX} \\ i_{RY} \\ i_{RZ} \end{pmatrix}, \; \psi_R = \begin{pmatrix} \psi_{RX} \\ \psi_{RY} \\ \psi_{RZ} \end{pmatrix}. \tag{3.2}$$

The electrical equations describing the machine are

$$\frac{d\psi_S}{dt} = v_S - R_S i_S, \; \frac{d\psi_R}{dt} = v_R - R_R i_R, \tag{3.3}$$

where $R_S$ is the resistance of a stator winding and $R_R$ is the resistance of a rotor winding.

An explicit model of the machine can be obtained by expressing the total flux linkages as functions of the currents. Based on the geometry of the machine on Fig. 3.1 and the results of Section 2.3, we assume that

$$\begin{pmatrix} \psi_S \\ \psi_R \end{pmatrix} = L(\theta) \begin{pmatrix} i_S \\ i_R \end{pmatrix}, \; L(\theta) = \begin{pmatrix} L_{SS} & L_{SR}(\theta) \\ L_{SR}^T(\theta) & L_{RR} \end{pmatrix}, \tag{3.4}$$

where

$$L_{SS} = \begin{pmatrix} L_{SW} & M_{SW} & M_{SW} \\ M_{SW} & L_{SW} & M_{SW} \\ M_{SW} & M_{SW} & L_{SW} \end{pmatrix}, \; L_{RR} = \begin{pmatrix} L_{RW} & M_{RW} & M_{RW} \\ M_{RW} & L_{RW} & M_{RW} \\ M_{RW} & M_{RW} & L_{RW} \end{pmatrix}, \tag{3.5}$$

and

$$L_{SR}(\theta) = M_{SR}\begin{pmatrix} \cos(n_P\theta) & \cos(n_P\theta+2\pi/3) & \cos(n_P\theta-2\pi/3) \\ \cos(n_P\theta-2\pi/3) & \cos(n_P\theta) & \cos(n_P\theta+2\pi/3) \\ \cos(n_P\theta+2\pi/3) & \cos(n_P\theta-2\pi/3) & \cos(n_P\theta) \end{pmatrix}. \tag{3.6}$$

The variables of the model are:

- $\theta$, the angle of the rotor (in rad).
- $n_P$, the number of poles pairs ($n_P = 1$ on Fig. 3.1).
- $L_{SW}$, the self-inductance of a stator winding.
- $M_{SW}$, the mutual inductance between two stator windings.
- $L_{RW}$, the self-inductance of a rotor winding.
- $M_{RW}$, the mutual inductance between two rotor windings.
- $M_{SR}$, the mutual inductance between a stator winding and a rotor winding when the windings are aligned (e.g., between windings $A$ and $X$ when $\theta = 0$).

Using (3.3) and the expressions for the inductances, explicit differential equations describing the machine can be derived, specifically

$$\begin{aligned} \frac{d}{dt}\begin{pmatrix} i_S \\ i_R \end{pmatrix} &= L^{-1}(\theta)\left(\begin{pmatrix} v_S - R_S i_S \\ v_R - R_R i_R \end{pmatrix}\right. \\ &\quad \left. -\omega\begin{pmatrix} 0 & \partial L_{SR}(\theta)/\partial\theta \\ \partial L_{SR}^T(\theta)/\partial\theta & 0 \end{pmatrix}\begin{pmatrix} i_S \\ i_R \end{pmatrix}\right), \end{aligned} \tag{3.7}$$

where $\omega = d\theta/dt$ is the angular velocity of the machine. The general formula for the torque (1.7) gives

$$\begin{aligned} \tau_M &= \frac{1}{2} i_S^T \frac{\partial L_{SR}(\theta)}{\partial\theta} i_R + \frac{1}{2} i_R^T \frac{\partial L_{SR}^T(\theta)}{\partial\theta} i_S \\ &= i_S^T \frac{\partial L_{SR}(\theta)}{\partial\theta} i_R \\ &= -n_P M_{SR}\left[\sin(n_P\theta)(i_{SA}i_{RX} + i_{SB}i_{RY} + i_{SC}i_{RZ})\right. \\ &\quad + \sin(n_P\theta + 2\pi/3)(i_{SA}i_{RY} + i_{SB}i_{RZ} + i_{SC}i_{RX}) \\ &\quad \left. + \sin(n_P\theta - 2\pi/3)(i_{SA}i_{RZ} + i_{SB}i_{RX} + i_{SC}i_{RY})\right]. \end{aligned} \tag{3.8}$$

**Inversion of the inductance matrix:** Fact 1 of Section 3.7 shows that the inverse of the matrix $L(\theta)$ has an explicit expression

$$L^{-1}(\theta) = \begin{pmatrix} D(\theta)^{-1}L_{RR} & -D(\theta)^{-1}L_{SR}(\theta) \\ -D(\theta)^{-1}L_{SR}^T(\theta) & D(\theta)^{-1}L_{SS} \end{pmatrix}, \tag{3.9}$$

where $D(\theta)$ is the matrix

$$D(\theta) = L_{SS}L_{RR} - L_{SR}(\theta)L_{SR}^T(\theta). \tag{3.10}$$

Further, Fact 2 of Section 3.7 shows that the determinant of $D(\theta)$, which is also the denominator of $L^{-1}(\theta)$, is equal to

$$\begin{aligned} \det\left(D(\theta)\right) &= (L_{SW} + 2M_{SW})(L_{RW} + 2M_{RW}) \\ &\quad \left((L_{SW} - M_{SW})(L_{RW} - M_{RW}) - \frac{9}{4}M_{SR}^2\right)^2. \end{aligned} \tag{3.11}$$

Define

$$\begin{aligned} L_S &= L_{SW} - M_{SW},\ L_R = L_{RW} - M_{RW},\ M = \frac{3}{2}M_{SR}, \\ L_{Sh} &= L_{SW} + 2M_{SW},\ L_{Rh} = L_{RW} + 2M_{RW}. \end{aligned} \tag{3.12}$$

Then, (3.11) becomes

$$\det\left(D(\theta)\right) = L_{Sh}L_{Rh}(L_SL_R - M^2). \tag{3.13}$$

Thus, for the matrix $L(\theta)$ to be invertible, one needs

$$L_{Sh} \neq 0, \quad L_{Rh} \neq 0, \text{ and } L_SL_R - M^2 \neq 0. \tag{3.14}$$

**Leakage fluxes:** assuming that the stator and the rotor windings have $N_S$ and $N_R$ turns, respectively, the results of Section 2.3 give the values

$$\begin{aligned} L_{SW} &= \frac{cN_S^2\pi}{4},\ M_{SW} = -\frac{cN_S^2\pi}{8},\ L_{RW} = \frac{cN_R^2\pi}{4},\ M_{RW} = -\frac{cN_R^2\pi}{8}, \\ M_{SR} &= \frac{cN_SN_R\pi}{4}, \end{aligned} \tag{3.15}$$

resulting in

$$L_S = \frac{3cN_S^2\pi}{8},\ L_R = \frac{3cN_R^2\pi}{8},\ M = \frac{3cN_SN_R\pi}{8},\ L_{Sh} = 0,\ L_{Rh} = 0. \tag{3.16}$$

Note that

$$M = \sqrt{L_SL_R}, \tag{3.17}$$

so that all three terms in (3.13) are zero.

In practice, addfitional leakage fluxes result in $L_{Sh}$, $L_{Rh}$, and $L_S L_R - M^2$ having positive values. With these leakage fluxes, (3.14) is satisfied. The so-called *leakage factor*

$$\sigma = 1 - \frac{M^2}{L_S L_R},\ 0 \leqslant \sigma \leqslant 1, \tag{3.18}$$

is small but nonzero. The mutual inductance

$$M = \sqrt{1-\sigma}\ \sqrt{L_S L_R} \tag{3.19}$$

is slightly smaller than the maximal value $\sqrt{L_S L_R}$.

**Numerical example:** consider a DFIM with $L_S = 1.6$ mH, $L_R = 19$ mH, and $M = 5.2$ mH. Then, $\sigma = 0.11$ and

$$\frac{M}{\sqrt{L_S L_R}} = \sqrt{1-\sigma} = 0.94. \tag{3.20}$$

In other words, the leakage fluxes cause a reduction of the mutual inductance from the maximal value by about 6%.

## 3.3 Two-phase equivalent machine

The three-phase machine can be transformed into an equivalent two-phase machine by using the three-phase to two-phase transformation (1.8). The model (3.4) becomes

$$\begin{pmatrix} \psi_{Sa} \\ \psi_{Sb} \\ \psi_{Sh} \end{pmatrix} = M_{3-2} L_{SS} M_{3-2}^{-1} \begin{pmatrix} i_{Sa} \\ i_{Sb} \\ i_{Sh} \end{pmatrix} + M_{3-2} L_{SR}(\theta) M_{3-2}^{-1} \begin{pmatrix} i_{Rx} \\ i_{Ry} \\ i_{Rh} \end{pmatrix}, \tag{3.21}$$

where $i_{Rx}$, $i_{Ry}$, and $i_{Rh}$ are the two-phase rotor currents corresponding to $i_{RX}$, $i_{RY}$, and $i_{RZ}$. Computing the products[1], one finds that

$$\begin{aligned} \begin{pmatrix} \psi_{Sa} \\ \psi_{Sb} \\ \psi_{Sh} \end{pmatrix} &= \begin{pmatrix} L_S & 0 & 0 \\ 0 & L_S & 0 \\ 0 & 0 & L_{Sh} \end{pmatrix} \begin{pmatrix} i_{Sa} \\ i_{Sb} \\ i_{Sh} \end{pmatrix} \\ &\quad + M \begin{pmatrix} \cos(n_P\theta) & -\sin(n_P\theta) & 0 \\ \sin(n_P\theta) & \cos(n_P\theta) & 0 \\ 0 & 0 & 0 \end{pmatrix} \begin{pmatrix} i_{Rx} \\ i_{Ry} \\ i_{Rh} \end{pmatrix}, \end{aligned} \tag{3.22}$$

[1] A symbolic mathematical software, such as *Matlab*'s *Symbolic Math Toolbox*, is useful for such purpose (see Section 3.6).

where $L_S$, $L_{Sh}$, and $M$ were defined in (3.12). In a similar manner, the following equations can be obtained for the rotor fluxes

$$\begin{pmatrix} \psi_{Rx} \\ \psi_{Ry} \\ \psi_{Rh} \end{pmatrix} = \begin{pmatrix} L_R & 0 & 0 \\ 0 & L_R & 0 \\ 0 & 0 & L_{Rh} \end{pmatrix} \begin{pmatrix} i_{Rx} \\ i_{Ry} \\ i_{Rh} \end{pmatrix} + M \begin{pmatrix} \cos(n_P\theta) & \sin(n_P\theta) & 0 \\ -\sin(n_P\theta) & \cos(n_P\theta) & 0 \\ 0 & 0 & 0 \end{pmatrix} \begin{pmatrix} i_{Sa} \\ i_{Sb} \\ i_{Sh} \end{pmatrix}. \quad (3.23)$$

Due to the fact that the three-phase to two-phase transformation is linear and does not depend on time, the transformed variables satisfy

$$\begin{aligned} \frac{d}{dt}\begin{pmatrix} \psi_{Sa} \\ \psi_{Sb} \\ \psi_{Sh} \end{pmatrix} &= \begin{pmatrix} v_{Sa} - R_S\, i_{Sa} \\ v_{Sb} - R_S\, i_{Sb} \\ v_{Sh} - R_S\, i_{Sh} \end{pmatrix} \\ \frac{d}{dt}\begin{pmatrix} \psi_{Rx} \\ \psi_{Ry} \\ \psi_{Rh} \end{pmatrix} &= \begin{pmatrix} v_{Rx} - R_R\, i_{Rx} \\ v_{Ry} - R_R\, i_{Ry} \\ v_{Rh} - R_R\, i_{Rh} \end{pmatrix}. \end{aligned} \quad (3.24)$$

Therefore, the two-phase model is given by

$$\frac{d}{dt}\left( L_2(\theta) \begin{pmatrix} i_{Sa} \\ i_{Sb} \\ i_{Rx} \\ i_{Ry} \end{pmatrix} \right) = \begin{pmatrix} v_{Sa} - R_S\, i_{Sa} \\ v_{Sb} - R_S\, i_{Sb} \\ v_{Rx} - R_R\, i_{Rx} \\ v_{Ry} - R_R\, i_{Ry} \end{pmatrix}, \quad (3.25)$$

with

$$L_2(\theta) = \begin{pmatrix} L_S & 0 & M\cos(n_P\theta) & -M\sin(n_P\theta) \\ 0 & L_S & M\sin(n_P\theta) & M\cos(n_P\theta) \\ M\cos(n_P\theta) & M\sin(n_P\theta) & L_R & 0 \\ -M\sin(n_P\theta) & M\cos(n_P\theta) & 0 & L_R \end{pmatrix}, \quad (3.26)$$

and

$$\begin{aligned} L_{Sh}\frac{di_{Sh}}{dt} &= v_{Sh} - R_S\, i_{Sh} \\ L_{Rh}\frac{di_{Rh}}{dt} &= v_{Rh} - R_R\, i_{Rh}. \end{aligned} \quad (3.27)$$

Equations (3.25) and (3.26) are the same for all choices of $C_V$ in (1.8) and are the same as the equations describing a two-phase machine with windings $a$, $b$, $x$ and $y$ [6]. An explicit form of (3.25) is

$$\frac{d}{dt}\begin{pmatrix} i_{Sa} \\ i_{Sb} \\ i_{Rx} \\ i_{Ry} \end{pmatrix} = L_2^{-1}(\theta)\left( \begin{pmatrix} v_{Sa} - R_S\, i_{Sa} \\ v_{Sb} - R_S\, i_{Sb} \\ v_{Rx} - R_R\, i_{Rx} \\ v_{Ry} - R_R\, i_{Ry} \end{pmatrix} - \omega\frac{\partial L_2(\theta)}{\partial\theta}\begin{pmatrix} i_{Sa} \\ i_{Sb} \\ i_{Rx} \\ i_{Ry} \end{pmatrix} \right), \quad (3.28)$$

with

$$\frac{\partial L_2(\theta)}{\partial \theta} = n_P M \begin{pmatrix} 0 & 0 & -\sin(n_P\theta) & -\cos(n_P\theta) \\ 0 & 0 & \cos(n_P\theta) & -\sin(n_P\theta) \\ -\sin(n_P\theta) & \cos n_P\theta) & 0 & 0 \\ -\cos(n_P\theta) & -\sin(n_P\theta) & 0 & 0 \end{pmatrix}. \tag{3.29}$$

In the transformed variables, the torque (3.8) becomes

$$\begin{aligned} \tau_M &= \begin{pmatrix} i_{Sa} & i_{Sb} & i_{Sh} \end{pmatrix} \left(M_{3-2}^{-1}\right)^T \frac{\partial L_{SR}(\theta)}{\partial \theta} M_{3-2}^{-1} \begin{pmatrix} i_{Rx} \\ i_{Ry} \\ i_{Rh} \end{pmatrix} \\ &= n_P\ M\ C_P^{-1} (-i_{Sa}\ i_{Rx}\ \sin(n_P\theta) - i_{Sa}\ i_{Ry}\ \cos(n_P\theta) \\ &\quad + i_{Sb}\ i_{Rx}\ \cos(n_P\theta) - i_{Sb}\ i_{Ry}\ \sin(n_P\theta)), \end{aligned} \tag{3.30}$$

where $C_P$ is the coefficient of power associated with the $3-2$ transformation. Note that the torque is also equal to

$$\tau_M = C_P^{-1} \begin{pmatrix} i_{Sa} & i_{Sb} & i_{Rx} & i_{Ry} \end{pmatrix}^T \frac{\partial L_2(\theta)}{\partial \theta} \begin{pmatrix} i_{Sa} \\ i_{Sb} \\ i_{Rx} \\ i_{Ry} \end{pmatrix}. \tag{3.31}$$

In other words, the torque is the same as the torque of the transformed two-phase machine multiplied by the coefficient $C_P^{-1}$. The coefficient $C_P$ originates from the relationship between three-phase and two-phase powers in (1.14).

The homopolar variables satisfy stable first-order differential equations that are independent of the equations for the two-phase variables and the variables do not affect the torque. In general, the homopolar variables can be neglected for control development.

One can verify that

$$L_2^{-1}(\theta) = \frac{1}{L_S L_R - M^2} \begin{pmatrix} L_R & 0 & -M\cos(n_P\theta) & M\sin(n_P\theta) \\ 0 & L_R & -M\sin(n_P\theta) & -M\cos(n_P\theta) \\ -M\cos(n_P\theta) & -M\sin(n_P\theta) & L_S & 0 \\ M\sin(n_P\theta) & -M\cos(n_P\theta) & 0 & L_S \end{pmatrix}, \tag{3.32}$$

by computing that $L_2(\theta)\ L_2^{-1}(\theta) = I$, where $I$ is the identity matrix. Therefore, the conditions for the transformed system (3.27), (3.28) to be well-defined are the same as those for the three-phase system (3.14).

## 3.4 Complex model of a DFIM

A compact representation of the two-phase model can be obtained by grouping pairs of variables into complex variables. Specifically, let

$$\begin{aligned} \widetilde{v}_S &= v_{Sa} + j v_{Sb}, \quad & \widetilde{\imath}_S &= i_{Sa} + j i_{Sb}, \\ \widetilde{v}_R &= v_{Rx} + j v_{Ry}, \quad & \widetilde{\imath}_R &= i_{Rx} + j i_{Ry}. \end{aligned} \tag{3.33}$$

The left-hand side of (3.25) is transformed to the complex domain by computing

$$\begin{aligned} & \begin{pmatrix} 1 & j & 0 & 0 \\ 0 & 0 & 1 & j \end{pmatrix} \frac{d}{dt} \left( L_2(\theta) \begin{pmatrix} i_{Sa} \\ i_{Sb} \\ i_{Rx} \\ i_{Ry} \end{pmatrix} \right) \\ = \; & \frac{d}{dt} \left( \begin{pmatrix} L_S & jL_S & Me^{jn_P\theta} & jMe^{jn_P\theta} \\ Me^{-jn_P\theta} & jMe^{-jn_P\theta} & L_R & jL_R \end{pmatrix} \begin{pmatrix} i_{Sa} \\ i_{Sb} \\ i_{Rx} \\ i_{Ry} \end{pmatrix} \right) \\ = \; & \frac{d}{dt} \left( \begin{pmatrix} L_S & Me^{jn_P\theta} \\ Me^{-jn_P\theta} & L_R \end{pmatrix} \begin{pmatrix} \widetilde{\imath}_S \\ \widetilde{\imath}_R \end{pmatrix} \right). \end{aligned} \tag{3.34}$$

For the right-hand side of (3.25),

$$\begin{pmatrix} 1 & j & 0 & 0 \\ 0 & 0 & 1 & j \end{pmatrix} \begin{pmatrix} v_{Sa} - R_S\, i_{Sa} \\ v_{Sb} - R_S\, i_{Sb} \\ v_{Rx} - R_R\, i_{Rx} \\ v_{Ry} - R_R\, i_{Ry} \end{pmatrix} = \begin{pmatrix} \widetilde{v}_S - R_S\, \widetilde{\imath}_S \\ \widetilde{v}_R - R_R\, \widetilde{\imath}_R \end{pmatrix}. \tag{3.35}$$

Therefore, the complex model is given by

$$\frac{d}{dt} \left( \begin{pmatrix} L_S & M\, e^{jn_P\theta} \\ M\, e^{-jn_P\theta} & L_R \end{pmatrix} \begin{pmatrix} \widetilde{\imath}_S \\ \widetilde{\imath}_R \end{pmatrix} \right) = \begin{pmatrix} \widetilde{v}_S - R_S\, \widetilde{\imath}_S \\ \widetilde{v}_R - R_R\, \widetilde{\imath}_R \end{pmatrix}. \tag{3.36}$$

When using complex variables, the transpose of the inductance matrix is equal to its complex conjugate. Such a matrix is called *Hermitian*, and the property replaces the symmetry property that applies in the real domain. The torque (3.30) becomes

$$\tau_M = n_P M\, C_P^{-1}\, \mathrm{Im} \left( \widetilde{\imath}_S \; \left( \widetilde{\imath}_R\, e^{jn_P\theta} \right)^* \right), \tag{3.37}$$

where Im denotes the imaginary part and * the complex conjugate.

The overall complex model (3.36), (3.37) is the same as the two-phase model, but is more compact. Derivations using the model are often simplified [2], [5], [7], [12], [14].

**Three-phase to complex transformation:** the complex variables can be computed directly from the three-phase variables. Indeed, (1.8) implies that

$$v_a + jv_b = C_V \ \left(v_A + e^{j2\pi/3} v_B + e^{-j2\pi/3} v_C\right). \tag{3.38}$$

Therefore

$$\begin{aligned} \widetilde{v}_S &= C_V \ z_3^T \ v_S, \quad \widetilde{\imath}_S = C_V \ z_3^T \ i_S, \\ \widetilde{v}_R &= C_V \ z_3^T \ v_R, \quad \widetilde{\imath}_R = C_V \ z_3^T \ i_R, \end{aligned} \tag{3.39}$$

where $z_3^T$ is the complex vector

$$z_3^T = \begin{pmatrix} 1 & e^{j2\pi/3} & e^{-j2\pi/3} \end{pmatrix}. \tag{3.40}$$

From (1.9), the inverse of the three-phase to complex transformation is

$$v_S = \frac{2}{3C_V} \begin{pmatrix} 1 & 0 \\ -1/2 & \sqrt{3}/2 \\ -1/2 & -\sqrt{3}/2 \end{pmatrix} \begin{pmatrix} \mathrm{Re}\,(\widetilde{v}_S) \\ \mathrm{Im}\,(\widetilde{v}_S) \end{pmatrix} + \frac{\sqrt{2}}{3C_V} v_{Sh} \begin{pmatrix} 1 \\ 1 \\ 1 \end{pmatrix}. \tag{3.41}$$

Note that

$$\frac{\sqrt{2}}{3C_V} v_{Sh} = \frac{v_{SA} + v_{SB} + v_{SC}}{3}, \tag{3.42}$$

so that the offset in (3.41) is the average of the three-phase voltages. Neglecting $v_{Sh}$, the inverse of the three-phase to complex transformation is

$$v_S = \frac{2}{3C_V} \mathrm{Re}\,(\widetilde{v}_S \ z_3^*) = \frac{1}{3C_V} \left( \widetilde{v}_S \ z_3^* + \widetilde{v}_S^* \ z_3 \right). \tag{3.43}$$

## 3.5 Complex model of a DFIM in a rotating reference frame

The complex model can be expressed in a rotating reference frame by letting

$$\begin{aligned} \overline{v}_S &= e^{-j\theta_S} \ \widetilde{v}_S, \quad \overline{\imath}_S = e^{-j\theta_S} \ \widetilde{\imath}_S, \\ \overline{v}_R &= e^{-j\theta_R} \ \widetilde{v}_R, \quad \overline{\imath}_R = e^{-j\theta_R} \ \widetilde{\imath}_R, \end{aligned} \tag{3.44}$$

where $\theta_S$ and $\theta_R$ are angles to be defined. The angles correspond to angular frequencies

$$\omega_S = \frac{d\theta_S}{dt}, \ \omega_R = \frac{d\theta_R}{dt}. \tag{3.45}$$

Inserting the new variables in (3.36),

$$\begin{aligned}\frac{d}{dt}\left(L_S\, e^{j\theta_S}\, \overline{\imath}_S + M\, e^{j(\theta_R+n_P\theta)}\, \overline{\imath}_R\right) &= e^{j\theta_S}\left(\overline{v}_S - R_S\, \overline{\imath}_S\right)\\ \frac{d}{dt}\left(M\, e^{j(\theta_S-n_P\theta)}\, \overline{\imath}_S + L_R\, e^{j\theta_R}\, \overline{\imath}_R\right) &= e^{j\theta_R}\left(\overline{v}_R - R_R\, \overline{\imath}_R\right).\end{aligned} \tag{3.46}$$

The equations are simplified for the choice

$$\theta_R = \theta_S - n_P\theta,\ \omega_R = \omega_S - n_P\omega. \tag{3.47}$$

Then, multiplying the first equation by $e^{-j\theta_S}$ and the second equation by $e^{-j\theta_R}$, the complex model becomes

$$\begin{pmatrix} L_S & M \\ M & L_R \end{pmatrix} \frac{d}{dt}\begin{pmatrix} \overline{\imath}_S \\ \overline{\imath}_R \end{pmatrix} = \begin{pmatrix} \overline{v}_S - R_S\, \overline{\imath}_S - j\omega_S(L_S\, \overline{\imath}_S + M\, \overline{\imath}_R) \\ \overline{v}_R - R_R\, \overline{\imath}_R - j(\omega_S - n_P\omega)(M\, \overline{\imath}_S + L_R\, \overline{\imath}_R) \end{pmatrix}, \tag{3.48}$$

with the torque

$$\tau_M = n_P M\, C_P^{-1}\, \mathrm{Im}\left(\overline{\imath}_S\, \overline{\imath}_R^*\right). \tag{3.49}$$

When $\theta_S = 0$, the model is said to be expressed in the *stator frame of reference* or in *stationary coordinates*. If $\theta_S$ is such that the variables are constant in steady-state, the model is said to be expressed in *synchronous* or *DQ coordinates*.

## 3.6 Symbolic code

The code below produces the results of (3.22), (3.23), (3.30), and (3.54).

```
%
% Symbolic code for DFIM
%
syms lss lsw msw lrr lrw mrw lsr msr np th m3t2 cv l2ss ...
     l2sr l2rr is2 isa isb ish ir2 irx iry irh tm lslrt real
%
% Original model
%
a=2*pi/3;
lss=[lsw msw msw;msw lsw msw;msw msw lsw];
lrr=[lrw mrw mrw;mrw lrw mrw;mrw mrw lrw];
lsr=msr*[cos(np*th) cos(np*th+a) cos(np*th-a); ...
    cos(np*th-a) cos(np*th) cos(np*th+a);
```

```
    cos(np*th+a) cos(np*th-a) cos(np*th)];
%
% 2-phase equivalent inductance matrices
%
m3to2=cv*[1 -1/2 -1/2;0 sqrt(3)/2 -sqrt(3)/2;1/sqrt(2) ...
    1/sqrt(2) 1/sqrt(2)];
l2ss=simplify(m3to2*lss*inv(m3to2))
l2sr=simplify(m3to2*lsr*inv(m3to2))
l2rr=simplify(m3to2*lrr*inv(m3to2))
%
% 2-phase equivalent torque
%
is2=[isa;isb;ish];ir2=[irx;iry;irh];
tm=simplify(is2'*inv(m3to2)'*diff(lsr,th)*inv(m3to2)*ir2)
%
% Proof of Fact 2
%
lsrlsrt=simplify(lsr*lsr')
```

## 3.7 Auxiliary results

**Definition:** a $3 \times 3$ *circulant* matrix is a matrix of the form

$$M = \begin{pmatrix} a & b & c \\ c & a & b \\ b & c & a \end{pmatrix}. \tag{3.50}$$

Circulant matrices $M_1$, $M_2$ are such that $M_1 + M_2$, $M_1 M_2$, and $(M_1)^{-1}$ are also circulant matrices. The product of two such matrices commutes, i.e., $M_1 M_2 = M_2 M_1$.

**Fact 1:** the inverse of the matrix $L(\theta)$ in (3.4) is given by (3.9).

**Proof of Fact 1:** the result is obtained by checking block-by-block that $L(\theta)\ L^{-1}(\theta)$ is the identity matrix. Partition the matrix as four blocks of equal size, with

$$L(\theta)L^{-1}(\theta) = \begin{pmatrix} M_1 & M_2 \\ M_3 & M_4 \end{pmatrix}. \tag{3.51}$$

Given (3.9),

$$\begin{aligned} M_1 &= L_{SS}D(\theta)^{-1}L_{RR} - L_{SR}(\theta)D(\theta)^{-1}L_{SR}^T(\theta) \\ M_2 &= -L_{SS}D(\theta)^{-1}L_{SR}(\theta) + L_{SR}(\theta)D(\theta)^{-1}L_{SS} \\ M_3 &= L_{SR}^T(\theta)D(\theta)^{-1}L_{RR} - L_{RR}D(\theta)^{-1}L_{SR}^T(\theta) \\ M_4 &= -L_{SR}^T(\theta)D(\theta)^{-1}L_{SR}(\theta) + L_{RR}D(\theta)^{-1}L_{SS}. \end{aligned} \tag{3.52}$$

Given (3.5) and (3.6), all the matrices appearing in the above expressions are circulant matrices. Using the commutation property

$$\begin{aligned} M_1 &= (L_{SS}L_{RR} - L_{SR}(\theta)L_{SR}^T(\theta))D(\theta)^{-1} = I \\ M_2 &= -(L_{SS}L_{SR}(\theta + L_{SR}(\theta)L_{SS})D(\theta)^{-1} = 0 \\ M_3 &= (L_{SR}^T(\theta)L_{RR} - L_{RR}L_{SR}^T(\theta))D(\theta)^{-1} = 0 \\ M_4 &= (-L_{SR}^T(\theta)L_{SR}(\theta) + L_{RR}L_{SS})D(\theta)^{-1} = I, \end{aligned} \tag{3.53}$$

which proves the result.

**Fact 2:** (3.11) is satisfied.

**Proof of Fact 2:** from (3.6),

$$L_{SR}(\theta)L_{SR}^T(\theta) = \frac{3}{2}M_{SR}^2 \begin{pmatrix} 1 & -1/2 & -1/2 \\ -1/2 & 1 & -1/2 \\ -1/2 & -1/2 & 1 \end{pmatrix}. \tag{3.54}$$

With (3.5), it follows that

$$L_{SS}L_{RR} - L_{SR}(\theta)L_{SR}^T(\theta) = \begin{pmatrix} f & g & g \\ g & f & g \\ g & g & f \end{pmatrix}, \tag{3.55}$$

where

$$\begin{aligned} f &= L_{SW}L_{RW} + 2M_{SW}M_{RW} - \frac{3M_{SR}^2}{2} \\ g &= L_{SW}M_{RW} + M_{SW}L_{RW} + M_{SW}M_{RW} + \frac{3M_{SR}^2}{4}. \end{aligned} \tag{3.56}$$

In general,

$$\det \begin{pmatrix} f & g & g \\ g & f & g \\ g & g & f \end{pmatrix} = f^3 + 2g^3 - 3fg^2 = (f-g)^2(f+2g). \tag{3.57}$$

Therefore,

$$\begin{aligned}
&\det\left(L_{SS}L_{RR} - L_{SR}(\theta)L_{SR}^T(\theta)\right) \\
&= \left(L_{SW}L_{RW} + M_{SW}M_{RW} - L_{SW}M_{RW} - M_{SW}L_{RW} - \frac{9M_{SR}^2}{4}\right)^2 \\
&\quad (L_{SW}L_{RW} + 4M_{SW}M_{RW} + 2L_{SW}M_{RW} + 2M_{SW}L_{RW}) \\
&= (L_{SW} + 2M_{SW})(L_{RW} + 2M_{RW})\left((L_{SW} - M_{SW})(L_{RW} - M_{RW}) - \frac{9}{4}M_{SR}^2\right)^2 .
\end{aligned} \tag{3.58}$$

# Chapter 4

# Brushless Doubly-Fed Reluctance Machines

## 4.1 Objective

The objective of this chapter is to study *brushless doubly-fed reluctance machines* (BDFRM). The results of the chapter:

- derive a model of the BDFRM.
- show that the machine is equivalent to a doubly-fed induction machine.

## 4.2 Model in phase variables

Fig. 4.1 shows a schematic representation of a brushless doubly-fed reluctance machine [4], [24]. The rotor is such that the reluctance reaches a maximum and a minimum $n_R$ times along the periphery of the rotor (with $n_R = 3$ on the figure). Although quite different in construction compared to Fig. 2.4, the reluctance variation of Fig. 4.1 is assumed to be modeled as the airgap length variation of Section 2.4.

The stator has a set of three-phase windings called the *power windings* (with $n_P = 1$ on the figure), and another set of three-phase windings called the *control windings* (with $n_C = 2$ on the figure). Other values of $n_P$ and $n_C$ are possible, but one needs $n_P \neq n_C$ and $n_R = n_P + n_C$ to obtain useful results. The choice $n_R = n_P - n_C$ or $n_R = n_C - n_P$ (whichever is positive) is also possible, but is not considered here.

The power and control windings are labelled PA, PB, PC, and CA, CB, CC, respectively. The angle of the PA winding is assumed to be zero, while the angle of the first CA winding is $\varphi/n_C$. The angle of the rotor is defined so that the

reluctance of the flux paths for winding PA is minimum at angles $\theta = 0°$, $120°$, and $-120°$.

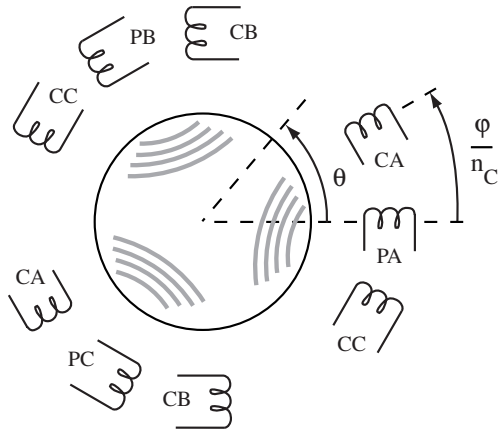


Figure 4.1: Schematic representation of a brushless doubly-fed reluctance machine

As usual for windings with multiple pole pairs, the two elements of the CA, CB, and CC windings are placed in series to constitute three windings. The machine then has a total of 6 windings, with currents and voltages

$$i_P = \begin{pmatrix} i_{PA} \\ i_{PB} \\ i_{PC} \end{pmatrix},\ i_C = \begin{pmatrix} i_{CA} \\ i_{CB} \\ i_{CC} \end{pmatrix},\ v_P = \begin{pmatrix} v_{PA} \\ v_{PB} \\ v_{PC} \end{pmatrix},\ v_C = \begin{pmatrix} v_{CA} \\ v_{CB} \\ v_{CC} \end{pmatrix}. \tag{4.1}$$

The $6 \times 6$ inductance matrix is of the form

$$L(\theta) = \begin{pmatrix} L_{PP} & L_{PC}(\theta) \\ L_{PC}^T(\theta) & L_{CC} \end{pmatrix}. \tag{4.2}$$

Using (2.14), (2.17), and (2.20) with $n_1 = n_2 = n_P$ and $n_R \neq 2n_P$, one finds that only the $L_{12,0}$ terms remain in $L_{PP}$. Specifically, for $N_P$ the number of turns per pole pair of the power winding,

$$L_{PP} = \begin{pmatrix} L_{PW} & M_{PW} & M_{PW} \\ M_{PW} & L_{PW} & M_{PW} \\ M_{PW} & M_{PW} & L_{PW} \end{pmatrix}, \tag{4.3}$$

where

$$L_{PW} = \frac{cN_P^2\pi}{4},\ M_{PW} = -\frac{cN_P^2\pi}{8}. \tag{4.4}$$

In practice, the value of $L_{PW}$ is slightly larger than $-2M_{PW}$ due to the leakage flux.

Similarly, for $N_C$ the number of turns per pole pair of the control winding,

$$L_{CC} = \begin{pmatrix} L_{CW} & M_{CW} & M_{CW} \\ M_{CW} & L_{CW} & M_{CW} \\ M_{CW} & M_{CW} & L_{CW} \end{pmatrix}, \tag{4.5}$$

where

$$L_{CW} = \frac{cN_C^2\pi}{4},\ M_{CW} = -\frac{cN_C^2\pi}{8}. \tag{4.6}$$

Using (2.14), (2.17), and (2.20) again, but this time with $n_1 = n_P \neq n_2 = n_C$, one finds that the $L_{12,0}$ terms are zero in $L_{PC}(\theta)$. With $n_1 + n_2 = n_R$,

$$\begin{aligned} L_{PC}(\theta) \;=\; M_{PC} \begin{pmatrix} \cos(n_R\theta - \varphi) & \cos(n_R\theta - \varphi - 2\pi/3) \\ \cos(n_R\theta - \varphi - 2\pi/3) & \cos(n_R\theta - \varphi + 2\pi/3) \\ \cos(n_R\theta - \varphi + 2\pi/3) & \cos(n_R\theta - \varphi) \end{pmatrix} \\ \begin{pmatrix} \cos(n_R\theta - \varphi + 2\pi/3) \\ \cos(n_R\theta - \varphi) \\ \cos(n_R\theta - \varphi - 2\pi/3) \end{pmatrix}, \end{aligned} \tag{4.7}$$

where

$$M_{PC} = \frac{cN_PN_C\pi d}{8}. \tag{4.8}$$

The electrical equations of the machine are

$$\frac{d\psi_P}{dt} = v_P - R_P i_P,\ \frac{d\psi_C}{dt} = v_C - R_C i_C, \tag{4.9}$$

where $R_P$ is the resistance of a power winding, $R_C$ is the resistance of a control winding, and the total flux linkages satisfy

$$\begin{pmatrix} \psi_P \\ \psi_C \end{pmatrix} = L(\theta) \begin{pmatrix} i_P \\ i_C \end{pmatrix}. \tag{4.10}$$

The torque is given by the general form (1.7), or

$$\begin{aligned} \tau_M &= \frac{1}{2} \begin{pmatrix} i_P^T & i_C^T \end{pmatrix} \frac{\partial L(\theta)}{\partial \theta} \begin{pmatrix} i_P \\ i_C \end{pmatrix} \\ &= i_P^T \frac{\partial L_{PC}(\theta)}{\partial \theta} i_C. \end{aligned} \tag{4.11}$$

## 4.3 Equivalence between a BDFRM and a DFIM

The inductances (4.2), (4.3), (4.5), and (4.7) are the same as those of doubly-fed induction machine (see (3.4), (3.5), and (3.6)). The subscripts $S$, $R$ of the DFIM are replaced by $P$, $C$, $n_P$ is replaced by $n_R$, and the angle $\theta$ is replaced by $\theta - \varphi/n_R$. The offset $\varphi/n_R$ is insignificant and can easily be compensated for in a control system.

There is a notable difference in terms of the parameter values to be expected. Using (3.12), we have that

$$\begin{aligned} L_P &= L_{PW} - M_{PW} = \frac{3cN_P^2\pi}{8} \\ L_C &= L_{CW} - M_{CW} = \frac{3cN_C^2\pi}{8} \\ M &= \frac{3}{2}M_{PC} = \frac{3cN_PN_C\pi d}{16}. \end{aligned} \tag{4.12}$$

It follows that

$$M = \frac{d}{2}\sqrt{L_PL_C}. \tag{4.13}$$

Even for the extreme value of $d = 1$ and without leakage flux, the mutual inductance is 1/2 the value for a DFIM. The leakage factor (3.18) is

$$\sigma = 1 - \frac{M^2}{L_PL_C} = 1 - \frac{d^2}{4}. \tag{4.14}$$

For $\sigma = 0.75$ for $d = 1$, compared to $\sigma = 0$ for the DFIM without leakage (see (3.17)). The BDFRM appears as a doubly-fed induction machine with a large leakage factor that is not due to leakage, but to the construction of the machine.

Considering the homopolar variables in (3.12), we have that

$$L_{Ph} = 0,\ L_{Ch} = 0. \tag{4.15}$$

In the absence of leakage flux, the homopolar inductances are zero, as for the DFIM.

# Chapter 5

# Cascaded Doubly-Fed Induction Machines

## 5.1 Objective

The objective of this chapter is to study *cascaded doubly-fed induction machines* (CDFIM). The results of the chapter:

- derive a model of the CDFIM.
- compute an equivalent two-phase model in the form of a complex variable model.
- extend the model to a general model in a rotating reference frame.

## 5.2 Model of a cascaded doubly-fed induction machine

A *cascaded doubly-fed induction machine* (CDFIM) is obtained by connecting two doubly-fed induction machines electrically and mechanically [13]. One machine is called the *power machine* and the other is called the *control machine*. The two machines are connected front to back mechanically. Electrically, the rotors are connected in parallel, but with the second and third phases crossed. The concept is shown on Fig. 5.1.

Using the results of Section 3.2 while adjusting the notation, the power machine is modeled as

$$\frac{d}{dt}\left(L_{PP}i_P + L_{PR}(\theta)i_{RP}\right) = v_P - R_P i_P, \tag{5.1}$$

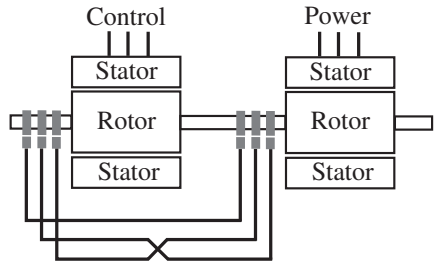


Figure 5.1: Cascaded doubly-fed induction machine

with

$$\frac{d}{dt}\left(L_{PR}^{T}(\theta)i_P + L_{RRP}i_{RP}\right) = v_{RP} - R_{RP}i_{RP}. \tag{5.2}$$

The submatrices are given by

$$L_{PP} = \begin{pmatrix} L_{PW} & M_{PW} & M_{PW} \\ M_{PW} & L_{PW} & M_{PW} \\ M_{PW} & M_{PW} & L_{PW} \end{pmatrix}, \; L_{RRP} = \begin{pmatrix} L_{RWP} & M_{RWP} & M_{RWP} \\ M_{RWP} & L_{RWP} & M_{RWP} \\ M_{RWP} & M_{RWP} & L_{RWP} \end{pmatrix}, \tag{5.3}$$

and

$$L_{PR}(\theta) = M_{PR}\begin{pmatrix} \cos(n_P\theta) & \cos(n_P\theta + 2\pi/3) & \cos(n_P\theta - 2\pi/3) \\ \cos(n_P\theta - 2\pi/3) & \cos(n_P\theta) & \cos(n_P\theta + 2\pi/3) \\ \cos(n_P\theta + 2\pi/3) & \cos(n_P\theta - 2\pi/3) & \cos(n_P\theta) \end{pmatrix}. \tag{5.4}$$

In the model of the control machine, an angle $\theta_{CP}$ is added to the rotor angle $\theta$ to account for the fact that the rotor of the control machine may not be aligned with its stator in the same way as for the power machine. This angle depends on how the machines are coupled. If the stators are aligned, $\theta_{CP}$ is the angle of the $X$ winding of the control machine relative to the angle of the $X$ winding of the power machine. Accordingly,

$$\frac{d}{dt}\left(L_{CC}i_C + L_{CRO}(\theta + \theta_{CP})i_{RC}\right) = v_C - R_C i_C \tag{5.5}$$

and

$$\frac{d}{dt}\left(L_{CRO}^{T}(\theta + \theta_{CP})i_C + L_{RRC}i_{RC}\right) = v_{RC} - R_{RC}i_{RC}. \tag{5.6}$$

The stator/rotor coupling matrix for the control machine is denoted $L_{CRO}(\theta)$ to keep the label $L_{CR}(\theta)$ for a different purpose.

In (5.6), the submatrices are given by

$$L_{CC} = \begin{pmatrix} L_{CW} & M_{CW} & M_{CW} \\ M_{CW} & L_{CW} & M_{CW} \\ M_{CW} & M_{CW} & L_{CW} \end{pmatrix}, \; L_{RRC} = \begin{pmatrix} L_{RWC} & M_{RWC} & M_{RWC} \\ M_{RWC} & L_{RWC} & M_{RWC} \\ M_{RWC} & M_{RWC} & L_{RWC} \end{pmatrix}, \tag{5.7}$$

and

$$L_{CRO}(\theta) = M_{CR} \begin{pmatrix} \cos(n_C\theta) & \cos(n_C\theta + 2\pi/3) & \cos(n_C\theta - 2\pi/3) \\ \cos(n_C\theta - 2\pi/3) & \cos(n_C\theta) & \cos(n_C\theta + 2\pi/3) \\ \cos(n_C\theta + 2\pi/3) & \cos(n_C\theta - 2\pi/3) & \cos(n_C\theta) \end{pmatrix}. \tag{5.8}$$

Given the rotor electrical connection,

$$v_{RC} = S_{BC}\, v_{RP},\, i_{RC} = -S_{BC}\, i_{RP}, \tag{5.9}$$

where $S_{BC}$ is a matrix representing the swapping of the phases $B$ and $C$, i.e.,

$$S_{BC} = \begin{pmatrix} 1 & 0 & 0 \\ 0 & 0 & 1 \\ 0 & 1 & 0 \end{pmatrix}. \tag{5.10}$$

Note that

$$S_{BC} = S_{BC}^T = S_{BC}^{-1}. \tag{5.11}$$

The model of the control machine can be expressed in terms of the rotor variables using (5.9). Equation (5.5) becomes

$$\frac{d}{dt}\left(L_{CC} i_C + L_{CR}(\theta) i_{RP}\right) = v_C - R_C i_C, \tag{5.12}$$

where

$$L_{CR}(\theta) = -L_{CRO}(\theta + \theta_{CP}) S_{BC}. \tag{5.13}$$

Multiplying (5.6) by $S_{BC}^{-1}$ gives

$$\begin{aligned} &\frac{d}{dt}\left(S_{BC}^{-1} L_{CRO}^T(\theta + \theta_{CP}) i_C - S_{BC}^{-1} L_{RRC} S_{BC} i_{RP}\right) \\ &= S_{BC}^{-1}\left(S_{BC} v_{RP} + R_{RC} S_{BC} i_{RP}\right). \end{aligned} \tag{5.14}$$

The special form of $L_{RRC}$ in (5.7) implies that swapping the last two rows as well as the last two columns leaves the matrix unchanged. Using (5.11), (5.13), and the fact that $R_{RC}$ is a scalar,

$$\frac{d}{dt}\left(-L_{CR}^T(\theta)i_C - L_{RRC}i_{RP}\right) = v_{RP} + R_{RC}i_{RP}. \tag{5.15}$$

Subtracting (5.15) from (5.2) and defining

$$i_R = i_{RP},\ R_R = R_{RP} + R_{RC},\ L_{RR} = L_{RRP} + L_{RRC}, \tag{5.16}$$

the following equation is obtained

$$\frac{d}{dt}\left(L_{PR}^T(\theta)i_P + L_{CR}^T(\theta)i_C + L_{RR}i_R\right) = -R_R i_R. \tag{5.17}$$

**Overall model:** (5.1), (5.12), and (5.17) give the overall model of the machine

$$\frac{d}{dt}\left(L(\theta)\begin{pmatrix} i_P \\ i_C \\ i_R \end{pmatrix}\right) = \begin{pmatrix} v_P - R_P i_P \\ v_C - R_C i_C \\ -R_R i_R \end{pmatrix}, \tag{5.18}$$

where

$$L(\theta) = \begin{pmatrix} L_{PP} & 0 & L_{PR}(\theta) \\ 0 & L_{CC} & L_{CR}(\theta) \\ L_{PR}^T(\theta) & L_{CR}^T(\theta) & L_{RR} \end{pmatrix}. \tag{5.19}$$

According to (1.7), the torque is given by

$$\begin{aligned} \tau_M &= \frac{1}{2}\begin{pmatrix} i_P^T & i_C^T & i_R^T \end{pmatrix}\frac{\partial L(\theta)}{\partial \theta}\begin{pmatrix} i_P \\ i_C \\ i_R \end{pmatrix} \\ &= i_P^T\frac{\partial L_{PR}(\theta)}{\partial \theta}i_R + i_C^T\frac{\partial L_{CR}(\theta)}{\partial \theta}i_R. \end{aligned} \tag{5.20}$$

The torque is the sum of the torque $\tau_{MP}$ produced by the power machine and the torque $\tau_{MC}$ produced by the control machine

$$\tau_M = \tau_{MP} + \tau_{MC}, \tag{5.21}$$

where

$$\tau_{MP} = i_P^T\frac{\partial L_{PR}(\theta)}{\partial \theta}i_R,\ \tau_{MC} = i_C^T\frac{\partial L_{CR}(\theta)}{\partial \theta}i_R. \tag{5.22}$$

The power and control torques are not independent however, since they are coupled through the current $i_R$.

## 5.3 Complex model of a CDFIM

**Power machine:** with small adjustments of notation, a complex model of the power machine can be obtained using the results of Section 3.4. As in (3.39), complex variables for the power machine are related to the original vectors through

$$\begin{aligned} \widetilde{v}_P &= C_V\ z_3^T\ v_P, \qquad & \widetilde{\imath}_P &= C_V\ z_3^T\ i_P, \\ \widetilde{v}_{RP} &= C_V\ z_3^T\ v_{RP}, & \widetilde{\imath}_{RP} &= C_V\ z_3^T\ i_{RP}, \end{aligned} \tag{5.23}$$

where

$$z_3^T = \begin{pmatrix} 1 & e^{j2\pi/3} & e^{-j2\pi/3} \end{pmatrix}. \tag{5.24}$$

The complex model (3.36) gives

$$\frac{d}{dt}\left(L_P\widetilde{\imath}_P + M_P\ e^{jn_P\theta}\widetilde{\imath}_{RP}\right) = \widetilde{v}_P - R_P\ \widetilde{\imath}_P, \tag{5.25}$$

and

$$\frac{d}{dt}\left(M_P\ e^{-jn_P\theta}\widetilde{\imath}_P + L_{RP}\widetilde{\imath}_{RP}\right) = \widetilde{v}_{RP} - R_{RP}\ \widetilde{\imath}_{RP}. \tag{5.26}$$

The parameters are

$$L_P = L_{PW} - M_{PW},\ L_{RP} = L_{RWP} - M_{RWP},\ M_P = \frac{3}{2}M_{PR}. \tag{5.27}$$

From (3.37), the torque of the power machine is

$$\tau_{MP} = n_P M_P\ C_P^{-1}\,\mathrm{Im}\left(\widetilde{\imath}_P\ \left(\widetilde{\imath}_{RP}\ e^{jn_P\theta}\right)^*\right), \tag{5.28}$$

where $C_P$ is the coefficient of power of the $3-2$ transformation, Im denotes the imaginary part, and * denotes the complex conjugate.

**Control machine:** for the control machine, a slightly different transformation is used for the stator, so that

$$\begin{aligned} \widetilde{v}_C &= C_V\ z_3^{*T}\ e^{-j\varphi}\ v_C, \quad & \widetilde{\imath}_C &= C_V\ z_3^{*T} e^{-j\varphi}\ i_C, \\ \widetilde{v}_{RC} &= C_V\ z_3^T\ v_{RC}, & \widetilde{\imath}_{RC} &= C_V\ z_3^T\ i_{RC}, \end{aligned} \tag{5.29}$$

where $\varphi$ is a constant angle to be determined. Note that

$$\widetilde{v}_C^* = C_V\ z_3^T\ e^{j\varphi}\ v_C, \tag{5.30}$$

so that

$$C_V\ z_3^T\ v_C = \widetilde{v}_C^*\ e^{-j\varphi}. \tag{5.31}$$

Therefore, the following substitutions should be made in the complex DFIM model for the control machine

$$\widetilde{v}_C \to \widetilde{v}_C^*\, e^{-j\varphi},\ \widetilde{\imath}_C \to \widetilde{\imath}_C^*\, e^{-j\varphi},\ \theta \to \theta + \theta_{CP}. \tag{5.32}$$

The variables $\widetilde{v}_{RC}$ and $\widetilde{\imath}_{RC}$ are unchanged.

The resulting complex model for the control machine is then

$$\frac{d}{dt}\left(L_C\, \widetilde{\imath}_C^*\, e^{-j\varphi} + M_C\, e^{jn_C(\theta+\theta_{CP})}\widetilde{\imath}_{RC}\right) = \widetilde{v}_C^*\, e^{-j\varphi} - R_C\, \widetilde{\imath}_C^*\, e^{-j\varphi}, \tag{5.33}$$

with

$$\frac{d}{dt}\left(M_C\, e^{-jn_C(\theta+\theta_{CP})}\, \widetilde{\imath}_C^*\, e^{-j\varphi} + L_{RC}\widetilde{\imath}_{RC}\right) = \widetilde{v}_{RC} - R_{RC}\, \widetilde{\imath}_{RC}, \tag{5.34}$$

and

$$\tau_{MC} = n_C M_C\, C_P^{-1}\, \mathrm{Im}\left(\widetilde{\imath}_C^*\, e^{-j\varphi}\left(\widetilde{\imath}_{RC}\, e^{jn_C(\theta+\theta_{CP})}\right)^*\right). \tag{5.35}$$

The parameters are

$$L_C = L_{CW} - M_{CW},\ L_{RC} = L_{RWC} - M_{RWC},\ M_C = \frac{3}{2}M_{CR}. \tag{5.36}$$

Let

$$\varphi = \pi - n_C\theta_{CP}, \tag{5.37}$$

so that (5.33) multiplied by $e^{j\varphi}$ becomes

$$\frac{d}{dt}\left(L_C\, \widetilde{\imath}_C^* - M_C\, e^{jn_C\theta}\, \widetilde{\imath}_{RC}\right) = \widetilde{v}_C^* - R_C\, \widetilde{\imath}_C^*, \tag{5.38}$$

and (5.34) becomes

$$\frac{d}{dt}\left(-M_C\, e^{-jn_C\theta}\, \widetilde{\imath}_C^* + L_{RC}\widetilde{\imath}_{RC}\right) = \widetilde{v}_{RC} - R_{RC}\, \widetilde{\imath}_{RC}. \tag{5.39}$$

**Rotor connection:** the electrical connection between the machines is described by (5.9). Expressed in the complex domain, the equations become

$$\widetilde{v}_{RC} = \widetilde{v}_{RP}^*,\ \widetilde{\imath}_{RC} = -\imath_{RP}^*. \tag{5.40}$$

Due to the rotor currents being the same, the two rotor equations merge into a single differential equation. Indeed, taking the complex conjugates of (5.38) and (5.39), and using (5.40), one finds that

$$\frac{d}{dt}\left(L_C\, \widetilde{\imath}_C\ + M_C\, e^{-jn_C\theta}\, \widetilde{\imath}_{RP}\right) = \widetilde{v}_C - R_C\, \widetilde{\imath}_C, \tag{5.41}$$

and

$$\frac{d}{dt}\left(-M_C\ e^{jn_C\theta}\ \widetilde{\imath}_C - L_{RC}\widetilde{\imath}_{RP}\right) = \widetilde{v}_{RP} + R_{RC}\ \widetilde{\imath}_{RP}. \tag{5.42}$$

Subtracting (5.42) from (5.26) gives

$$\begin{aligned}&\frac{d}{dt}\left(M_P\ e^{-jn_P\theta}\widetilde{\imath}_P + L_{RP}\widetilde{\imath}_{RP} + M_C\ e^{jn_C\theta}\widetilde{\imath}_C + L_{RC}\widetilde{\imath}_{RP}\right)\\ &= -R_{RP}\ \widetilde{\imath}_{RP} - R_{RC}\widetilde{\imath}_{RP}.\end{aligned} \tag{5.43}$$

Simplifying the notation with (5.16) and $\widetilde{\imath}_R = \widetilde{\imath}_{RP}$,

$$\frac{d}{dt}\left(M_P\ e^{-jn_P\theta}\widetilde{\imath}_P + M_C\ e^{jn_C\theta}\widetilde{\imath}_C + L_R\widetilde{\imath}_R\right) = -R_R\ \widetilde{\imath}_R. \tag{5.44}$$

With (5.37) and (5.40), the torque (5.35) of the control machine becomes

$$\begin{aligned}\tau_{MC} &= n_C M_C\ C_P^{-1}\ \mathrm{Im}\left(\widetilde{\imath}_C^*\ e^{-j\varphi}\ \left(\widetilde{\imath}_{RC}\ e^{jn_C(\theta+\theta_{CP})}\right)^*\right)\\ &= n_C M_C\ C_P^{-1}\ \mathrm{Im}\left(\widetilde{\imath}_C^*\ \left(\widetilde{\imath}_{RP}^*\ e^{jn_C\theta}\right)^*\right)\\ &= -n_C M_C\ C_P^{-1}\ \mathrm{Im}\left(\widetilde{\imath}_C\ \left(\widetilde{\imath}_{RP}\ e^{-jn_C\theta}\right)^*\right).\end{aligned} \tag{5.45}$$

**Overall model:** collecting (5.25), (5.41), and (5.44) with $\widetilde{\imath}_R = \widetilde{\imath}_{RP}$, and $\tau_M = \tau_{MP} + \tau_{MC}$ with (5.28) and (5.45), the overall complex model of the CDFIM is

$$\begin{aligned}\frac{d}{dt}\left(\begin{pmatrix} L_P & 0 & M_P\ e^{jn_P\theta}\\ 0 & L_C & M_C\ e^{-jn_C\theta}\\ M_P\ e^{-jn_P\theta} & M_C\ e^{jn_C\theta} & L_R\end{pmatrix}\begin{pmatrix}\widetilde{\imath}_P\\ \widetilde{\imath}_C\\ \widetilde{\imath}_R\end{pmatrix}\right)\\ = \begin{pmatrix}\widetilde{v}_P - R_P\widetilde{\imath}_P\\ \widetilde{v}_C - R_C\widetilde{\imath}_C\\ -R_R\widetilde{\imath}_R\end{pmatrix}\\ \tau_M = n_P M_P\ C_P^{-1}\ \mathrm{Im}\left(\widetilde{\imath}_P\ \left(\widetilde{\imath}_R\ e^{jn_P\theta}\right)^*\right)\\ -n_C M_C\ C_P^{-1}\ \mathrm{Im}\left(\widetilde{\imath}_C\ \left(\widetilde{\imath}_R\ e^{-jn_C\theta}\right)^*\right).\end{aligned} \tag{5.46}$$

## 5.4 Complex model of a CDFIM in a rotating coordinate frame

Similarly to the DFIM in Section 3.4, the model can be expressed in a rotating reference frame by letting

$$\begin{aligned}\overline{v}_P &= e^{-j\theta_P}\ \widetilde{v}_P, \quad \overline{\imath}_P = e^{-j\theta_P}\ \widetilde{\imath}_P,\\ \overline{v}_C &= e^{j\theta_C}\ \widetilde{v}_C, \quad \overline{\imath}_C = e^{j\theta_C}\ \widetilde{\imath}_C,\\ \overline{v}_R &= e^{-j\theta_R}\ \widetilde{v}_R, \quad \overline{\imath}_R = e^{-j\theta_R}\ \widetilde{\imath}_R,\end{aligned} \tag{5.47}$$

where $\theta_P$, $\theta_C$, and $\theta_R$ are angles to be defined. *Again, a different definition is applied for the variables of the control machine*, so that the variables $\overline{v}_C$ and $\overline{\imath}_C$ are the complex conjugates of what the definition would normally specify.

The angular frequencies corresponding to the angles of the reference frames are denoted

$$\frac{d\theta_P}{dt} = \omega_P, \ \frac{d\theta_C}{dt} = \omega_C, \ \frac{d\theta_R}{dt} = \omega_R. \tag{5.48}$$

Using (5.47), the first equation of (5.46) becomes

$$\frac{d}{dt}\left(L_P\ e^{j\theta_P}\ \overline{\imath}_P + M_P\ e^{jn_P\theta}\ e^{j\theta_R}\ \overline{\imath}_R\right) = e^{j\theta_P}\ \overline{v}_P - R_P\ e^{j\theta_P}\ \overline{\imath}_P. \tag{5.49}$$

Differentiating the products on the left-hand side, and multiplying both sides by $e^{-j\theta_P}$,

$$\begin{aligned}&\frac{d}{dt}\left(L_P\ \overline{\imath}_P\right) + j\omega_P\ L_P\ \overline{\imath}_P + e^{j(n_P\theta+\theta_R-\theta_P)}\frac{d}{dt}\left(M_P\ \overline{\imath}_R\right)\\ &+j\left(n_P\omega+\omega_R\right)\ e^{j(n_P\theta+\theta_R-\theta_P)}\ M_P\ \overline{\imath}_R = \overline{v}_P - R_P\ \overline{\imath}_P.\end{aligned} \tag{5.50}$$

The result is simplified for the special choice

$$\theta_R = \theta_P - n_P\theta, \tag{5.51}$$

which implies that

$$\omega_R = \omega_P - n_P\omega. \tag{5.52}$$

Then, (5.50) becomes

$$\frac{d}{dt}\left(L_P\ \overline{\imath}_P + M_P\ \overline{\imath}_R\right) = \overline{v}_P - R_P\ \overline{\imath}_P - j\omega_P\ \left(L_P\ \overline{\imath}_P + M_P\ \overline{\imath}_R\right). \tag{5.53}$$

For the second equation of (5.46),

$$\frac{d}{dt}\left(L_C\ e^{-j\theta_C}\ \overline{\imath}_C + M_C\ e^{-jn_C\theta}\ e^{j\theta_R}\ \overline{\imath}_R\right) = e^{-j\theta_C}\ \overline{v}_C - R_C\ e^{-j\theta_C}\ \overline{\imath}_C. \tag{5.54}$$

Differentiating the products and multiplying by $e^{j\theta_C}$,

$$\begin{aligned}&\frac{d}{dt}\left(L_C\ \overline{\imath}_C\right) - j\omega_C\ L_C\ \overline{\imath}_C + e^{j(-n_C\theta+\theta_R+\theta_C)}\frac{d}{dt}\left(M_C\ \overline{\imath}_R\right)\\ &-j\left(n_C\omega-\omega_R\right)\ e^{j(-n_C\theta+\theta_R+\theta_C)}\ M_C\ \overline{\imath}_R = \overline{v}_C - R_C\ \overline{\imath}_C.\end{aligned} \tag{5.55}$$

The result is simplified for

$$\theta_C = n_C\theta - \theta_R, \tag{5.56}$$

which implies that

$$\omega_C = n_C\omega - \omega_R. \tag{5.57}$$

With (5.56), (5.55) becomes

$$\frac{d}{dt}\left(L_C\ \overline{\imath}_C + M_C\ \overline{\imath}_R\right) = \overline{v}_C - R_C\ \overline{\imath}_C + j\omega_C\left(L_C\ \overline{\imath}_C + M_C\ \overline{\imath}_R\right). \tag{5.58}$$

For the third equation of (5.46)

$$\frac{d}{dt}\left(M_P\ e^{j(\theta_P - n_P\theta)}\ \overline{\imath}_P + M_C\ e^{j(n_C\theta - \theta_C)}\ \overline{\imath}_C + L_R\ e^{j\theta_R}\ \overline{\imath}_R\right) = -R_R\ e^{j\theta_R}\ \overline{\imath}_R. \tag{5.59}$$

Differentiating the products and multiplying by $e^{-j\theta_R}$,

$$\begin{aligned} &e^{j(\theta_P - n_P\theta - \theta_R)}\frac{d}{dt}\left(M_P\ \overline{\imath}_P\right) + j\left(\omega_P - n_P\omega\right)\ e^{j(\theta_P - n_P\theta - \theta_R)}\left(M_P\ \overline{\imath}_P\right) \\ &+e^{j(n_C\theta - \theta_C - \theta_R)}\frac{d}{dt}\left(M_C\ \overline{\imath}_C\right) + j\left(n_C\omega - \omega_C\right)\ e^{j(n_C\theta - \theta_C - \theta_R)}\left(M_C\ \overline{\imath}_C\right) \\ &+\frac{d}{dt}\left(L_R\ \overline{\imath}_R\right) + j\omega_R\left(L_R\ \overline{\imath}_R\right) = -R_R\ \overline{\imath}_R. \end{aligned} \tag{5.60}$$

With the choices made on the reference frames (i.e., (5.51), (5.52), (5.56), and (5.57)), equation (5.60) becomes

$$\frac{d}{dt}\left(M_P\ \overline{\imath}_P + M_C\ \overline{\imath}_C + L_R\ \overline{\imath}_R\right) = -R_R\ \overline{\imath}_R - j\omega_R\left(M_P\ \overline{\imath}_P + M_C\ \overline{\imath}_C + L_R\ \overline{\imath}_R\right). \tag{5.61}$$

The torque in (5.46) with (5.47), (5.51), and (5.56) becomes

$$\tau_M = n_P M_P\ C_P^{-1}\ \mathrm{Im}\left(\overline{\imath}_P\ \overline{\imath}_R^*\right) - n_C M_C\ C_P^{-1}\ \mathrm{Im}\left(\overline{\imath}_C\ \overline{\imath}_R^*\right). \tag{5.62}$$

**Overall model:** combining (5.53), (5.58), (5.61), and (5.62), the complex model in the rotating reference frame is

$$\begin{aligned} &\begin{pmatrix} L_P & 0 & M_P \\ 0 & L_C & M_C \\ M_P & M_C & L_R \end{pmatrix}\frac{d}{dt}\begin{pmatrix} \overline{\imath}_P \\ \overline{\imath}_C \\ \overline{\imath}_R \end{pmatrix} \\ &= \begin{pmatrix} \overline{v}_P - R_P\ \overline{\imath}_P - j\omega_P\left(L_P\ \overline{\imath}_P + M_P\ \overline{\imath}_R\right) \\ \overline{v}_C - R_C\ \overline{\imath}_C + j\omega_C\left(L_C\ \overline{\imath}_C + M_C\ \overline{\imath}_R\right) \\ -R_R\ \overline{\imath}_R - j\omega_R\left(M_P\ \overline{\imath}_P + M_C\ \overline{\imath}_C + L_R\ \overline{\imath}_R\right) \end{pmatrix} \\ &\tau_M = n_P M_P\ C_P^{-1}\ \mathrm{Im}\left(\overline{\imath}_P\ \overline{\imath}_R^*\right) - n_C M_C\ C_P^{-1}\ \mathrm{Im}\left(\overline{\imath}_C\ \overline{\imath}_R^*\right). \end{aligned} \tag{5.63}$$

For the model to hold, the reference frames for the rotor and for the stator of the control machine must be tied to the reference frame of the stator of the power

machine, with

$$\begin{aligned} \theta_R &= \theta_P - n_P\theta, \quad \theta_C = n_C\theta - \theta_R = -\theta_P + (n_P + n_C)\,\theta, \\ \omega_R &= \omega_P - n_P\omega, \quad \omega_C = n_C\omega - \omega_R = -\omega_P + (n_P + n_C)\,\omega. \end{aligned} \tag{5.64}$$

The complex model of the CDFIM can be found in [13]. A small difference is that the definition of the control winding variables was adjusted here to remove complex conjugates in the electrical model.

## 5.5 Steady-state operation

The condition on the angular rates indicates that the steady-state speed associated with power and control frequencies $\omega_P$ and $\omega_C$ is given by

$$\omega = \frac{\omega_P + \omega_C}{n_P + n_C}. \tag{5.65}$$

Operation may require a control system to bring or keep the machine close to the steady-state speed. A special case corresponds $\omega_C = 0$ (DC currents in the control windings). Then,

$$\omega = \frac{\omega_P}{n_P + n_C} \tag{5.66}$$

is called the *natural speed*, or the *synchronous speed* of the CDFIM.

The CDFIM can also be operated in asynchronous mode [16]. The *simple induction mode* corresponds to $i_C = 0$ and the *cascade induction mode* corresponds to $v_C = 0$. The synchronous speed in asynchronous mode is $\omega_P/n_P$, with the actual speed of rotation determined by the load torque (as in a squirrel-cage induction machine). Then, (5.65) determines $\omega_C$ rather than $\omega$.

# Chapter 6

# Brushless Doubly-Fed Induction Machines

## 6.1 Objective

The objective of this chapter is to study *brushless doubly-fed induction machines* (BDFIM). The results of this chapter:

- apply winding function theory to fractional pitch windings.
- derive a model of the single-loop BDFIM.
- compute an equivalent two-phase model in the form of a complex variable model and show that the BDFIM is equivalent to a CDFIM. The BDFIM model is also shown to become equivalent to a DFIM model when the rotor resistance is neglected.
- extend the model to a general model in a rotating reference frame.
- extend the model to a BDFIM with nested loops and derive a reduced-order model similar to the single-loop model.

## 6.2 Winding function theory for fractional pitch windings

Before developing the model of a brushless doubly-fed induction machine, additional results are obtained using winding function theory.

**Self-inductance of a fractional pitch winding:** Fig. 6.1 shows a winding with one pole pair but spanning an angle $2\theta_1$ less than $\pi$, which was the case in

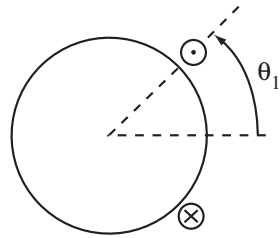


Figure 6.1: Fractional pitch winding

Fig. 2.1. The winding is referred to as a *fractional pitch winding*. Although one turn is shown, the number of turns will be taken to be equal to $N_1$.

Fig. 6.2 shows the winding function associated with Fig. 6.1. The result is similar to Fig. 2.2, except that the function is not symmetric with respect to the horizontal axis. The average of the function on the left is $N_1\theta_1/\pi$.

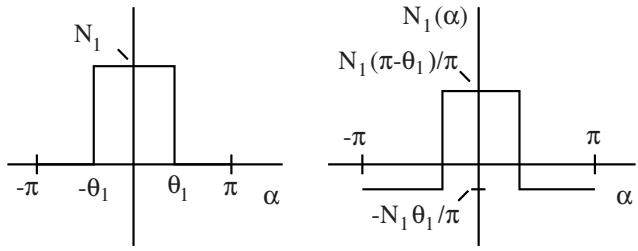


Figure 6.2: Winding function associated with Fig. 6.1

**Self-inductance of a fractional pitch winding:** using (2.6), the self-inductance of the winding is given by

$$\begin{aligned} L_{11} &= c\int_{-\pi}^{\pi} N_1^2(\alpha)\, d\alpha \\ &= cN_1^2\left(2\theta_1\left(\frac{\pi-\theta_1}{\pi}\right)^2 + 2(\pi-\theta_1)(-\frac{\theta_1}{\pi})^2\right) \\ &= \frac{2cN_1^2}{\pi}\,\theta_1\,(\pi-\theta_1)\,. \end{aligned} \tag{6.1}$$

**Mutual inductance between two fractional pitch windings without overlap:** assume that another fractional pitch winding is added that does not

overlap with the first winding. The case is shown on Fig. 6.3 (note that the centerlines of the windings are shown at 0° and 90°, but the angles are arbitrary).

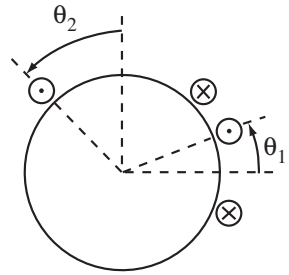


Figure 6.3: Fractional pitch windings without overlap

Using (2.6), the mutual inductance is composed of three terms

$$\begin{aligned} L_{12} &= cN_1N_2\left(2\theta_1\left(\frac{\pi-\theta_1}{\pi}\right)(-\frac{\theta_2}{\pi})+2\theta_2\left(\frac{\pi-\theta_2}{\pi}\right)(-\frac{\theta_1}{\pi})\right. \\ &\quad \left.+2\left(\pi-\theta_1-\theta_2\right)(-\frac{\theta_1}{\pi})(-\frac{\theta_2}{\pi})\right) \\ &= -\frac{2cN_1N_2}{\pi}\,\theta_1\theta_2. \end{aligned} \tag{6.2}$$

If the windings are identical

$$L_{12} = -\frac{2cN_1^2}{\pi}\,\theta_1^2. \tag{6.3}$$

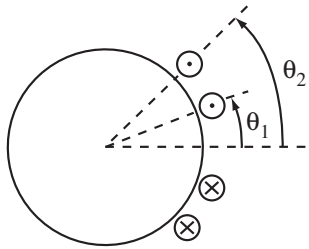


Figure 6.4: Fractional pitch windings with complete overlap

**Mutual inductance between two fractional pitch windings with complete overlap:** Fig. 6.4 shows two fractional pitch windings where winding 1 fits inside winding 2. Using (2.6), the mutual inductance is given by

$$\begin{aligned} L_{12} &= cN_1N_2\left(2\theta_1\left(\frac{\pi-\theta_1}{\pi}\right)(\frac{\pi-\theta_2}{\pi})+2(\theta_2-\theta_1)(-\frac{\theta_1}{\pi})\left(\frac{\pi-\theta_2}{\pi}\right)\right. \\ &\quad \left.+2\,(\pi-\theta_2)\,(-\frac{\theta_1}{\pi})(-\frac{\theta_2}{\pi})\right) \\ &= -\frac{2cN_1N_2}{\pi}\,\theta_1(\pi-\theta_2). \end{aligned} \tag{6.4}$$

**Mutual inductance between a fractional pitch winding and a sinusoidally-distributed winding:** assume that a fractional pitch winding is placed on a rotor at an angle $\theta$, as shown on Fig. 6.5. A sinusoidally-distributed winding with $N_2$ turns and $n_2$ pole pairs is placed on the stator at an angle $\varphi_2/n_2$.

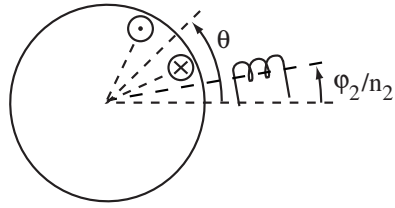


Figure 6.5: Coupling between a fractional pitch winding and a sinusoidally-distributed winding

Noting that integration can be performed over any interval of length $2\pi$ in (2.6), the mutual inductance between the fractional pitch winding and the sinusoidally-distributed winding is equal to

$$\begin{aligned} L_{12} &= c\int_{\theta-\theta_1}^{2\pi+\theta-\theta_1} N_1(\alpha)\frac{N_2}{2}\cos(n_2\alpha-\varphi_2)\;d\alpha \\ &= \frac{cN_1N_2}{2}\left(\int_{\theta-\theta_1}^{\theta+\theta_1}\left(\frac{\pi-\theta_1}{\pi}\right)\cos(n_2\alpha-\varphi_2)\;d\alpha\right. \\ &\quad \left.+\int_{\theta+\theta_1}^{2\pi+\theta-\theta_1}(-\frac{\theta_1}{\pi})\cos(n_2\alpha-\varphi_2)\;d\alpha\right) \\ &= \frac{cN_1N_2}{2\pi\;n_2}\left((\pi-\theta_1)\left[\sin(n_2\alpha-\varphi_2)\right]_{\alpha=\theta-\theta_1}^{\alpha=\theta+\theta_1}-\theta_1\left[\sin(n_2\alpha-\varphi_2)\right]_{\alpha=\theta+\theta_1}^{\alpha=2\pi+\theta-\theta_1}\right) \\ &= \frac{cN_1N_2}{2n_2}\left(\sin(n_2(\theta+\theta_1)-\varphi_2)-\sin(n_2(\theta-\theta_1)-\varphi_2)\right) \\ &= \frac{cN_1N_2}{n_2}\cos(n_2\theta-\varphi_2)\sin(n_2\theta_1). \end{aligned} \tag{6.5}$$

## 6.3 Model of a brushless doubly-fed induction machine

Fig. 6.6 shows a schematic representation of a brushless doubly-fed induction machine . The rotor has $n_R$ fractional pitch windings with spacing $2\pi/n_R$ ($n_R = 3$ on the figure). The span of each rotor winding is $2\theta_R$, which is slightly smaller than $2\pi/n_R$. The centerline of the first winding defines the angle $\theta$ of the rotor. The rotor windings are short-circuited, as in a squirrel-cage induction machine.

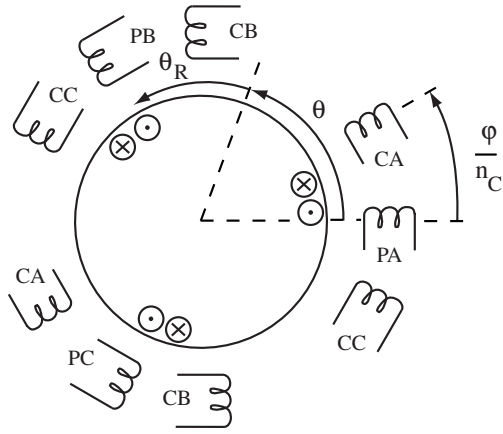


Figure 6.6: Schematic representation of a brushless doubly-fed induction machine

The configuration of Fig. 6.6 is a simplified representation of a *nested cage* brushless doubly-fed induction machine. In actual construction, the so-called nests include additional windings placed inside the span of the rotor windings shown on Fig. 6.6. The analysis presented here can either be extended to incorporate the additional windings, or used as an approximation of the machine with nested loops.

The stator is the same as the stator of the BDFRM in Fig. 4.1, with power and control windings. The figure shows a machine with $n_P = 1$ and $n_C = 2$. Other values of $n_P$ and $n_C$ are possible, but one needs $n_P \neq n_C$, and $n_P + n_C = n_R$. Also, performance depends on the specific values of $n_P$, $n_C$, and $n_R$. The choice $n_R = n_P - n_C$ or $n_R = n_C - n_P$ (whichever is positive) is also possible,

but is not considered here.

The power, control, and rotor windings have $N_P$, $N_C$, and $N_R$ turns per pole pair, respectively. The angle of the PA winding is zero, while the angle of the CA winding is $\varphi/n_C$.

The model of the machine is

$$\frac{d}{dt}\left(L(\theta)\begin{pmatrix} i_P \\ i_C \\ i_R \end{pmatrix}\right) = \begin{pmatrix} v_P - R_P i_P \\ v_C - R_C i_C \\ -R_R i_R \end{pmatrix}, \tag{6.6}$$

where the inductance matrix is of the form

$$L(\theta) = \begin{pmatrix} L_{PP} & 0 & L_{PR}(\theta) \\ 0 & L_{CC} & L_{CR}(\theta) \\ L_{PR}^T(\theta) & L_{CR}^T(\theta) & L_{RR} \end{pmatrix}. \tag{6.7}$$

The $L_{PC}$ sub-matrix is zero because $n_P \neq n_C$ and the airgap is uniform. $L_{PP}$ and $L_{CC}$ are given by

$$L_{PP} = \begin{pmatrix} L_{PW} & M_{PW} & M_{PW} \\ M_{PW} & L_{PW} & M_{PW} \\ M_{PW} & M_{PW} & L_{PW} \end{pmatrix},\ L_{CC} = \begin{pmatrix} L_{CW} & M_{CW} & M_{CW} \\ M_{CW} & L_{CW} & M_{CW} \\ M_{CW} & M_{CW} & L_{CW} \end{pmatrix}, \tag{6.8}$$

where

$$L_{PW} = \frac{cN_P^2\pi}{4},\ M_{PW} = -\frac{cN_P^2\pi}{8},\ L_{CW} = \frac{cN_C^2\pi}{4},\ M_{CW} = -\frac{cN_C^2\pi}{8}. \tag{6.9}$$

$L_{RR}$ is an $n_R \times n_R$ matrix given by

$$L_{RR} = \begin{pmatrix} L_{RW} & M_{RW} & \cdots & M_{RW} \\ M_{RW} & L_{RW} & \cdots & M_{RW} \\ \vdots & \vdots & \ddots & \vdots \\ M_{RW} & M_{RW} & \cdots & L_{RW} \end{pmatrix}, \tag{6.10}$$

where, according to (6.1) and (6.2),

$$L_{RW} = \frac{2cN_R^2}{\pi}\,\theta_R\,(\pi - \theta_R)\,,\ M_{RW} = -\frac{2cN_R^2}{\pi}\,\theta_R^2. \tag{6.11}$$

From (6.5), $L_{PR}(\theta)$ is the $n_R \times 3$ matrix

$$\begin{aligned} L_{PR}(\theta) \;=\; M_{PR}\begin{pmatrix} \cos(n_P\theta) & \cos(n_P(\theta + 2\pi/n_R)) \\ \cos(n_P\theta - 2\pi/3) & \cos(n_P(\theta + 2\pi/n_R) - 2\pi/3) \\ \cos(n_P\theta + 2\pi/3) & \cos(n_P(\theta + 2\pi/n_R) + 2\pi/3) \end{pmatrix} \\ \begin{matrix} \cdots & \cos(n_P(\theta + 2\pi(n_R-1)/n_R)) \\ \cdots & \cos(n_P(\theta + 2\pi(n_R-1)/n_R) - 2\pi/3) \\ \cdots & \cos(n_P(\theta + 2\pi(n_R-1)/n_R) + 2\pi/3) \end{matrix}\Bigg), \end{aligned} \tag{6.12}$$

where

$$M_{PR} = \frac{cN_PN_R}{n_P}\sin(n_P\theta_R). \tag{6.13}$$

Similarly

$$\begin{aligned} L_{CR}(\theta) &= M_{CR}\begin{pmatrix} \cos(n_C\theta-\varphi) & \cos(n_C(\theta+2\pi/n_R)-\varphi) \\ \cos(n_C\theta-2\pi/3-\varphi) & \cos(n_C(\theta+2\pi/n_R)-2\pi/3-\varphi) \\ \cos(n_C\theta+2\pi/3-\varphi) & \cos(n_C(\theta+2\pi/n_R)+2\pi/3-\varphi) \end{pmatrix} \\ &\quad \begin{pmatrix} \cdots & \cos(n_C(\theta+2\pi(n_R-1)/n_R)-\varphi) \\ \cdots & \cos(n_C(\theta+2\pi(n_R-1)/n_R)-2\pi/3-\varphi) \\ \cdots & \cos(n_C(\theta+2\pi(n_R-1)/n_R)+2\pi/3-\varphi) \end{pmatrix}, \end{aligned} \tag{6.14}$$

where

$$M_{CR} = \frac{cN_CN_R}{n_C}\sin(n_C\theta_R). \tag{6.15}$$

According to (1.7), the torque is given by

$$\begin{aligned} \tau_M &= \frac{1}{2}\begin{pmatrix} i_P^T & i_C^T & i_R^T \end{pmatrix}\frac{\partial L(\theta)}{\partial\theta}\begin{pmatrix} i_P \\ i_C \\ i_R \end{pmatrix} \\ &= i_P^T\frac{\partial L_{PR}(\theta)}{\partial\theta}i_R + i_C^T\frac{\partial L_{CR}(\theta)}{\partial\theta}i_R. \end{aligned} \tag{6.16}$$

**Special case:** for $n_P = 1$, $n_C = 2$, $n_R = 3$,

$$L_{PR}(\theta) = M_{PR}\begin{pmatrix} \cos(n_P\theta) & \cos(n_P\theta+2\pi/3) & \cos(n_P\theta-2\pi/3) \\ \cos(n_P\theta-2\pi/3) & \cos(n_P\theta) & \cos(n_P\theta+2\pi/3) \\ \cos(n_P\theta+2\pi/3) & \cos(n_P\theta-2\pi/3) & \cos(n_P\theta) \end{pmatrix} \tag{6.17}$$

and

$$\begin{aligned} L_{CR}(\theta) &= M_{CR}\begin{pmatrix} \cos(n_C\theta-\varphi) & \cos(n_C\theta-2\pi/3-\varphi) \\ \cos(n_C\theta-2\pi/3-\varphi) & \cos(n_C\theta+2\pi/3-\varphi) \\ \cos(n_C\theta+2\pi/3-\varphi) & \cos(n_C\theta-\varphi) \end{pmatrix} \\ &\qquad \begin{pmatrix} \cos(n_C\theta+2\pi/3-\varphi) \\ \cos(n_C\theta-\varphi) \\ \cos(n_C\theta-2\pi/3-\varphi) \end{pmatrix}. \end{aligned} \tag{6.18}$$

The structure of the BDFIM model in (6.6) and (6.7) and of the CDFIM model in (5.18) and (5.19) are the same. Further, the submatrices are the identical when $n_P = 1$, $n_C = 2$, and $n_R = 3$. In other words, the BDFIM is equivalent to a CDFIM in the special case of Fig. 6.6. The offset $\varphi$ of the CA winding in the BDFIM is tied to the offset $\theta_{CP}$ in the coupling of the CDFIM through (5.37). Using the complex model, we will show that the equivalence extends for other values of $n_P$, $n_C$, and $n_R$, as long as $n_P + n_C = n_R$.

## 6.4 Complex model of a BDFIM

**Complex variables and properties:** a model in complex variables is obtained by letting

$$\begin{aligned} \widetilde{v}_P &= C_V\ z_3^T\ v_P, & \widetilde{i}_P &= C_V\ z_3^T\ i_P, \\ \widetilde{v}_C &= C_V\ z_3^{*T}\ e^{-j\varphi}\ v_C, & \widetilde{i}_C &= C_V\ z_3^{*T}\ e^{-j\varphi}\ i_C, \\ \widetilde{v}_R &= C_{V,R}\ z_R^T\ v_R, & \widetilde{i}_R &= C_{V,R}\ z_R^T\ i_R, \end{aligned} \tag{6.19}$$

where $C_V$ is the coefficient of the 3-2 transformation and

$$z_3^T = \begin{pmatrix} 1 & e^{j2\pi/3} & e^{-j2\pi/3} \end{pmatrix}. \tag{6.20}$$

For the control winding, the transformation involves the complex conjugate of the variables, as for the CDFIM. A factor $e^{-j\varphi}$ was also inserted to account for the offset of the winding CA in Fig. 6.6. For the rotor, a new transformation with coefficient $C_{V,R}$ was introduced to account for a number $n_R$ of rotor windings that may be greater than 3. The vector $z_R$ is given by

$$z_R^T = \begin{pmatrix} 1 & e^{j2\pi n_P/n_R} & \cdots & e^{j2\pi n_P(n_R-1)/n_R} \end{pmatrix}. \tag{6.21}$$

The number of pole pairs also appears in the formula for the rotor variables.

The complex vector $z_3$ satisfies

$$\begin{aligned} &z_3^{*T}\ z_3 = 3, && z_3^T\ I_3 = z_3^T, && z_3^T\ O_3 = 0, \\ &z_3^T\ z_3 = 0, && z_3^{*T}\ I_3 = z_3^{*T}, && z_3^{*T}\ O_3 = 0, \end{aligned} \tag{6.22}$$

where $I_3$ is the $3 \times 3$ identity matrix and $O_3$ is a $3 \times 3$ matrix of 1's. On the other hand, for $n_R \geqslant 3$,

$$\begin{aligned} &z_R^{*T}\ z_R = n_R, && z_R^T\ I_R = z_R^T, && z_R^T\ O_R = 0, \\ &z_R^T\ z_R = 0, && z_R^{*T}\ I_R = z_R^{*T}, && z_R^{*T}\ O_R = 0, \end{aligned} \tag{6.23}$$

where $I_R$ is the $n_R \times n_R$ identity matrix and $O_R$ is a matrix of 1's with dimension $n_R \times n_R$. The fact that $z_R^T\ z_R = 0$ follows from

$$z_R^T\ z_R = \sum_{k=0}^{n_R-1} \left(e^{j4\pi k n_P/n_R}\right) = \sum_{k=0}^{n_R-1} \left(e^{j4\pi n_P/n_R}\right)^k, \tag{6.24}$$

and the standard formula

$$\sum_{k=0}^{n-1} a^k = \frac{1-a^n}{1-a}. \tag{6.25}$$

With $n_R > n_P$, it follows that

$$z_R^T \; z_R = \frac{1 - e^{j4\pi n_P}}{1 - e^{j4\pi n_P/n_R}} = 0. \tag{6.26}$$

**Properties of the inductance matrices:** define

$$\begin{aligned} L_P &= L_{PW} - M_{PW} = \frac{3cN_P^2\pi}{8} \\ L_C &= L_{CW} - M_{CW} = \frac{3cN_C^2\pi}{8} \\ L_R &= L_{RW} - M_{RW} = 2cN_R^2\theta_R. \end{aligned} \tag{6.27}$$

(6.8) and (6.10) become

$$\begin{aligned} L_{PP} &= L_P I_3 + M_{PW}\; O_3 \\ L_{CC} &= L_C I_3 + M_{CW}\; O_3 \\ L_{RR} &= L_R I_R + M_{RW}\; O_R. \end{aligned} \tag{6.28}$$

The following properties result

$$\begin{aligned} z_3^T \; L_{PP} &= L_P \; z_3^T \\ z_3^{*T} \; L_{CC} &= L_C \; z_3^{*T} \\ z_R^T \; L_{RR} &= L_R \; z_R^T. \end{aligned} \tag{6.29}$$

Further, from (6.12) and (6.22),

$$\begin{aligned} z_3^T \; L_{PR}(\theta) &= z_3^T \; M_{PR} \; \mathrm{Re}\left(e^{jn_P\theta} z_3^* \; z_R^T\right) \\ &= \frac{M_{PR}}{2} \; z_3^T \; \left(e^{jn_P\theta} z_3^* \; z_R^T + e^{-jn_P\theta} z_3 \; z_R^{*T}\right) \\ &= \frac{3M_{PR}}{2} \; e^{jn_P\theta} \; z_R^T. \end{aligned} \tag{6.30}$$

On the other hand, (6.12) and (6.23) give

$$\begin{aligned} z_R^T \; L_{PR}^T(\theta) &= z_R^T \; M_{PR} \; \mathrm{Re}\left(e^{jn_P\theta} z_R \; z_3^{*T}\right) \\ &= \frac{M_{PR}}{2} \; z_R^T \; \left(e^{jn_P\theta} z_R \; z_3^{*T} + e^{-jn_P\theta} z_R^* \; z_3^T\right) \\ &= \frac{n_R M_{PR}}{2} \; e^{-jn_P\theta} \; z_3^T. \end{aligned} \tag{6.31}$$

A most important property is that, for $n_R = n_P + n_C$,

$$\begin{aligned} z_R^T &= \left( 1 \quad e^{j2\pi n_P/n_R} \quad \dots \quad e^{j2\pi n_P(n_R-1)/n_R} \right) \\ &= \left( 1 \quad e^{j2\pi (n_R-n_C)/n_R} \quad \dots \quad e^{j2\pi (n_R-n_C)(n_R-1)/n_R} \right) \\ &= \left( 1 \quad e^{-j2\pi n_C/n_R} \quad \dots \quad e^{-j2\pi n_C(n_R-1)/n_R} \right). \end{aligned} \tag{6.32}$$

In other words, $n_P$ can be replaced by $-n_C$ in $z_R$. In the derivations, this change has a similar effect as the swapping of the phases in the CDFIM.

With (6.32), (6.14) implies that

$$\begin{aligned} z_3^{*T}\ L_{CR}(\theta) &= z_3^{*T}\ M_{CR}\ \mathrm{Re}\left(e^{j(n_C\theta-\varphi)} z_3^*\ z_R^{*T}\right) \\ &= \frac{M_{CR}}{2}\ z_3^{*T}\ \left(e^{j(n_C\theta-\varphi)} z_3^*\ z_R^{*T} + e^{-j(n_C\theta-\varphi)} z_3\ z_R^T\right) \\ &= \frac{3M_{CR}}{2}\ e^{-j(n_C\theta-\varphi)}\ z_R^T. \end{aligned} \tag{6.33}$$

On the other hand

$$\begin{aligned} z_R^T\ L_{CR}^T(\theta) &= z_R^T\ M_{CR}\ \mathrm{Re}\left(e^{j(n_C\theta-\varphi)} z_R^*\ z_3^{*T}\right) \\ &= \frac{M_{CR}}{2}\ z_R^T\ \left(e^{j(n_C\theta-\varphi)} z_R^*\ z_3^{*T} + e^{-j(n_C\theta-\varphi)} z_R\ z_3^T\right) \\ &= \frac{n_R M_{CR}}{2}\ e^{j(n_C\theta-\varphi)}\ z_3^{*T}. \end{aligned} \tag{6.34}$$

**Complex model:** using (6.19),

$$\begin{pmatrix} C_V\ z_3^T & 0 & 0 \\ 0 & C_V\ z_3^{*T}\ e^{-j\varphi} & 0 \\ 0 & 0 & C_{V,R}\ z_R^T \end{pmatrix} \begin{pmatrix} v_P - R_P i_P \\ v_C - R_C i_C \\ -R_R i_R \end{pmatrix} = \begin{pmatrix} \widetilde{v}_P - R_P \widetilde{i}_P \\ \widetilde{v}_C - R_C \widetilde{i}_C \\ -R_R \widetilde{i}_R \end{pmatrix}. \tag{6.35}$$

On the other hand, using (6.29), (6.30), (6.31), (6.33), and (6.34),

$$\begin{aligned} &\begin{pmatrix} C_V\ z_3^T & 0 & 0 \\ 0 & C_V\ z_3^{*T}\ e^{-j\varphi} & 0 \\ 0 & 0 & C_{V,R}\ z_R^T \end{pmatrix} \begin{pmatrix} L_{PP} & 0 & L_{PR}(\theta) \\ 0 & L_{CC} & L_{CR}(\theta) \\ L_{PR}^T(\theta) & L_{CR}^T(\theta) & L_{RR} \end{pmatrix} \begin{pmatrix} i_P \\ i_C \\ i_R \end{pmatrix} \\ &= \begin{pmatrix} L_P\ C_V\ z_3^T & 0 & \\ 0 & L_C\ C_V\ z_3^{*T}\ e^{-j\varphi} & \\ (n_R M_{PR}/2)\ e^{-jn_P\theta}\ C_{V,R}\ z_3^T & (n_R M_{CR}/2)\ e^{jn_C\theta}\ C_{V,R}\ z_3^{*T}\ e^{-j\varphi} & \end{pmatrix} \\ &\qquad \begin{pmatrix} (3M_{PR}/2)\ e^{jn_P\theta}\ C_V\ z_R^T \\ (3M_{CR}/2)\ e^{-jn_C\theta}\ C_V\ z_R^T \\ L_R\ C_{V,R}\ z_R^T \end{pmatrix} \begin{pmatrix} i_P \\ i_C \\ i_R \end{pmatrix} \\ &= \begin{pmatrix} L_P & 0 & M_P\ e^{jn_P\theta} \\ 0 & L_C & M_C\ e^{-jn_C\theta} \\ M_P'\ e^{-jn_P\theta} & M_C'\ e^{jn_C\theta} & L_R \end{pmatrix} \begin{pmatrix} \widetilde{i}_P \\ \widetilde{i}_C \\ \widetilde{i}_R \end{pmatrix}, \end{aligned} \tag{6.36}$$

where

$$\begin{aligned} M_P &= \frac{3M_{PR}}{2}\ \frac{C_V}{C_{V,R}},\ M_P' = \frac{n_R M_{PR}}{2}\ \frac{C_{V,R}}{C_V} \\ M_C &= \frac{3M_{CR}}{2}\ \frac{C_V}{C_{V,R}},\ M_C' = \frac{n_R M_{CR}}{2}\ \frac{C_{V,R}}{C_V}. \end{aligned} \tag{6.37}$$

Overall, the complex model is

$$\frac{d}{dt}\left(\begin{pmatrix} L_P & 0 & M_P\, e^{jn_P\theta} \\ 0 & L_C & M_C\, e^{-jn_C\theta} \\ M'_P\, e^{-jn_P\theta} & M'_C\, e^{jnC\theta} & L_R \end{pmatrix}\begin{pmatrix} \widetilde{\imath}_P \\ \widetilde{\imath}_C \\ \widetilde{\imath}_R \end{pmatrix}\right) = \begin{pmatrix} \widetilde{v}_P - R_P\widetilde{\imath}_P \\ \widetilde{v}_C - R_C\widetilde{\imath}_C \\ -R_R\widetilde{\imath}_R \end{pmatrix}. \tag{6.38}$$

**Special choice of 3-2 transformation for the rotor variables:** note that the transpose of the inductance matrix is equal to the complex conjugate of the matrix if and only if $M'_P = M_P$ and $M'_C = M_C$. The condition occurs when

$$\frac{3}{2}C_V^2 = \frac{n_R}{2}C_{V,R}^2, \tag{6.39}$$

or

$$C_{V,R} = \sqrt{\frac{3}{n_R}}C_V. \tag{6.40}$$

(6.39) can be interpreted to mean that the power coefficients $C_P$ and $C_{P,R}$ associated with the stator and rotor variables (generalized to $n_R$) are the same. Observe that $C_{V,R} = C_V$ if $n_R = 3$.

With (6.39), the parameters satisfy

$$\begin{aligned} M_P &= \frac{\sqrt{3n_R}}{2}M_{PR} = \frac{\sqrt{3n_R}}{2}\frac{cN_PN_R}{n_P}\sin(n_P\theta_R) \\ M_C &= \frac{\sqrt{3n_R}}{2}M_{CR} = \frac{\sqrt{3n_R}}{2}\frac{cN_CN_R}{n_C}\sin(n_C\theta_R). \end{aligned} \tag{6.41}$$

The electrical equations become

$$\frac{d}{dt}\left(\begin{pmatrix} L_P & 0 & M_P\, e^{jn_P\theta} \\ 0 & L_C & M_C\, e^{-jn_C\theta} \\ M_P\, e^{-jn_P\theta} & M_C\, e^{jnC\theta} & L_R \end{pmatrix}\begin{pmatrix} \widetilde{\imath}_P \\ \widetilde{\imath}_C \\ \widetilde{\imath}_R \end{pmatrix}\right) = \begin{pmatrix} \widetilde{v}_P - R_P\widetilde{\imath}_P \\ \widetilde{v}_C - R_C\widetilde{\imath}_C \\ -R_R\widetilde{\imath}_R \end{pmatrix}. \tag{6.42}$$

An interesting result is that the inductance matrix is Hermitian and independent of $C_V$ if (6.39) is satisfied.

**Torque computation:** following the initial steps of (6.30) and using (6.19),

the first term of the torque (6.16) is

$$\begin{aligned} i_P^T \frac{\partial L_{PR}(\theta)}{\partial \theta} i_R &= i_P^T \frac{\partial}{\partial \theta} \left( \frac{M_{PR}}{2} \left( e^{jn_P\theta} z_3^* \; z_R^T + e^{-jn_P\theta} z_3 \; z_R^{*T} \right) \right) i_R \\ &= \frac{M_{PR}}{2} \, jn_P \left( e^{jn_P\theta} i_P^T \; z_3^* \; z_R^T \; i_R - e^{-jn_P\theta} i_P^T \; z_3 \; z_R^{*T} \; i_R \right) \\ &= \frac{M_{PR}}{2 \; C_V \; C_{V,R}} \, jn_P \left( e^{jn_P\theta} \; \widetilde{i}_P^* \; \widetilde{i}_R - e^{-jn_P\theta} \; \widetilde{i}_P \; \widetilde{i}_R^* \right) \\ &= \frac{n_P M_{PR}}{C_V \; C_{V,R}} \, \mathrm{Im} \left( \widetilde{i}_P \; \left( \widetilde{i}_R \; e^{jn_P\theta} \right)^* \right). \end{aligned} \tag{6.43}$$

Similarly with (6.33) and (6.19), the second term of the torque (6.16) is

$$\begin{aligned} i_C^T \frac{\partial L_{CR}(\theta)}{\partial \theta} i_R &= i_C^T \frac{\partial}{\partial \theta} \left( \frac{M_{CR}}{2} \left( e^{j(n_C\theta - \varphi)} z_3^* \; z_R^{*T} + e^{-j(n_C\theta - \varphi)} z_3 \; z_R^T \right) \right) i_R \\ &= \frac{M_{CR}}{2} \, jn_C \left( e^{j(n_C\theta - \varphi)} i_C^T \; z_3^* \; z_R^{*T} \; i_R - e^{-j(n_C\theta - \varphi)} i_C^T \; z_3 \; z_R^T \; i_R \right) \\ &= \frac{M_{CR}}{2 \; C_V \; C_{V,R}} \, jn_C \left( e^{jn_C\theta} \; \widetilde{i}_C \; \widetilde{i}_R^* - e^{-jn_C\theta} \; \widetilde{i}_C^* \; \widetilde{i}_R \right) \\ &= -\frac{n_C M_{CR}}{C_V \; C_{V,R}} \, \mathrm{Im} \left( \widetilde{i}_C \; \left( \widetilde{i}_R \; e^{-jn_C\theta} \right)^* \right). \end{aligned} \tag{6.44}$$

With (6.37), the torque is

$$\begin{aligned} \tau_M &= n_P M_P \; C_P^{-1} \; \mathrm{Im} \left( \widetilde{i}_P \; \left( \widetilde{i}_R \; e^{jn_P\theta} \right)^* \right) \\ &\quad - n_C M_C \; C_P^{-1} \; \mathrm{Im} \left( \widetilde{i}_C \; \left( \widetilde{i}_R \; e^{-jn_C\theta} \right)^* \right), \end{aligned} \tag{6.45}$$

where $C_P = 3C_V^2/2$ is the coefficient of power of the $3-2$ transformation used for the power and control windings.

**Overall model:** assuming that (6.39) is satisfied, the complex model of the BDFIM is

$$\begin{aligned} \frac{d}{dt} \left( \begin{pmatrix} L_P & 0 & M_P \; e^{jn_P\theta} \\ 0 & L_C & M_C \; e^{-jn_C\theta} \\ M_P \; e^{-jn_P\theta} & M_C \; e^{jn_C\theta} & L_R \end{pmatrix} \begin{pmatrix} \widetilde{i}_P \\ \widetilde{i}_C \\ \widetilde{i}_R \end{pmatrix} \right) \\ = \begin{pmatrix} \widetilde{v}_P - R_P \widetilde{i}_P \\ \widetilde{v}_C - R_C \widetilde{i}_C \\ -R_R \widetilde{i}_R \end{pmatrix} \\ \tau_M = n_P M_P \; C_P^{-1} \; \mathrm{Im} \left( \widetilde{i}_P \; \left( \widetilde{i}_R \; e^{jn_P\theta} \right)^* \right) \\ - n_C M_C \; C_P^{-1} \; \mathrm{Im} \left( \widetilde{i}_C \; \left( \widetilde{i}_R \; e^{-jn_C\theta} \right)^* \right). \end{aligned} \tag{6.46}$$

## 6.5 BDFIM simulation using the complex model

Simulation and control of the BDFIM can be implemented in the complex domain. Fig. 6.7 shows a block diagram implementing the model in *Simulink*. The variables *vp*, *vc*, *ip*, *ic*, and *ir* are 3-dimensional vectors representing the corresponding variables. The BDFIM ODE block computes the derivatives *dip*, *dic*, and *dir* that are specified by the model. *om*, *th*, and *tau* represent $\omega$, $\theta$, and $\tau$.

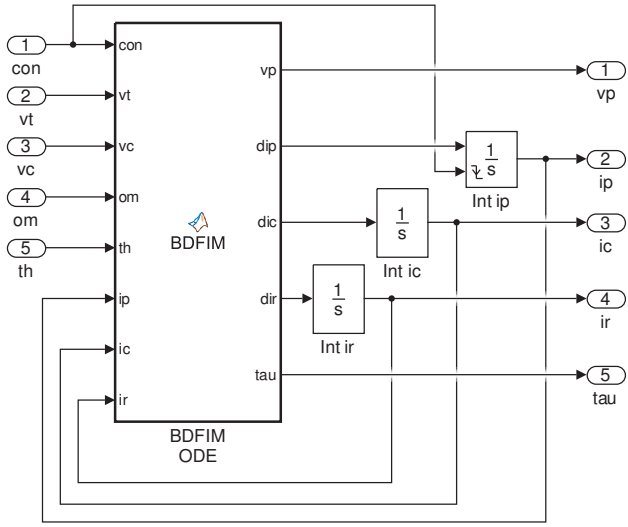


Figure 6.7: Simulink block representing the electrical equations of the BDFIM

A feature was added to enable the simulation with an open stator for a variable called *con* equal to 0. In that case, *vp* is the stator voltage induced on the power windings. For $con = 1$, the voltage applied to the power windings is $vt$ and $vp = vt$.

The code inside the BDFIM ODE block implements the complex-variable equations of the previous section and is given below using parameters from [23]. Control design and implementation using complex variables is discussed in [15].

```
function [vp,dip,dic,dir,tau] = BDFIM(con,vt,vc,om,th,ip,ic,ir)
% BDFIM electrical model
% Parameters
Rp=2.3;Lp=0.3498;Mp=3.1e-3;Rc=4;Lc=0.3637;Mc=2.2e-3;
```

```
Rr=1.2967e-4;Lr=4.4521e-5;npp=2;npc=4;phi=0;
% Three-phase to complex transformation
m3toc=sqrt(2/3)*[1 -1/2+1i*sqrt(3)/2 -1/2-1i*sqrt(3)/2];
cm3toc=conj(m3toc);ephi=exp(1i*phi);
vtx=m3toc*vt;ipx=m3toc*ip;irx=m3toc*ir;
vcx=cm3toc*vc*ephi';icx=cm3toc*ic*ephi';
% Complex model
nppom=npp*om;enppth=exp(1i*npp*th);
npcom=npc*om;enpcth=exp(1i*npc*th);
if con==0   % Open stator
    L=[Lc Mc*enpcth';Mc*enpcth Lr];
    di=L\[vcx-Rc*icx+1i*npcom*Mc*enpcth'*irx;...
        -Rr*irx-1i*npcom*Mc*enpcth*icx];
    dipx=0+0i;dicx=di(1);dirx=di(2);
    vpx=Mp*enppth*dirx+1i*nppom*Mp*enppth*irx;
else
    vpx=vtx;
    L=[Lp 0 Mp*enppth;0 Lc Mc*enpcth';Mp*enppth' Mc*enpcth Lr];
    di=L\[vpx-Rp*ipx-1i*nppom*Mp*enppth*irx;...
        vcx-Rc*icx+1i*npcom*Mc*enpcth'*irx;...
        -Rr*irx+1i*nppom*Mp*enppth'*ipx-1i*npcom*Mc*enpcth*icx];
    dipx=di(1);dicx=di(2);dirx=di(3);
end
tau=npp*Mp*imag(ipx*conj(irx*enppth))...
 -npc*Mc*imag(icx*conj(irx*enpcth'));
% Complex to three-phase transformation
dip=real(m3toc'*dipx);dic=real(cm3toc'*ephi*dicx);
dir=real(m3toc'*dirx);vp=real(m3toc'*vpx);
```

## 6.6 Equivalence between a BDFIM and a CDFIM

The complex models of the BDFIM in (6.46) and of the CDFIM in (5.46) are the same. Therefore, the two machines are equivalent under the assumptions made. Note that the offset $\varphi$ of the CA winding in the BDFIM is tied to the offset $\theta_{CP}$ in the coupling of the CDFIM through (5.37).

Parts of the derivation of the complex BDFIM model can be found in [1]. The

input/output model was obtained through a direct transformation to complex variables, without consideration for the homopolar variables. In the case of the rotor, the homopolar variables become a vector of $n_R - 2$ states that do not contribute to the torque. A more complete analysis of these variables is performed in [19].

## 6.7 Approximation of the BDFIM as a DFIM

Consider the multiplication of the electrical equations of (6.46) by a $2 \times 3$ matrix as follows

$$\begin{aligned}
&\begin{pmatrix} I & 0 & -M_P/L_R\, e^{jn_P\theta} \\ 0 & I & -M_C/L_R\, e^{-jn_C\theta} \end{pmatrix} \\
&\frac{d}{dt}\left(\begin{pmatrix} L_P & 0 & M_P\, e^{jn_P\theta} \\ 0 & L_C & M_C\, e^{-jn_C\theta} \\ M_P\, e^{-jn_P\theta} & M_C\, e^{jn_C\theta} & L_R \end{pmatrix}\begin{pmatrix} \widetilde{\imath}_P \\ \widetilde{\imath}_C \\ \widetilde{\imath}_R \end{pmatrix}\right) \\
= \;& \frac{d}{dt}\left(\begin{pmatrix} L_P - M_P^2/L_R & -M_PM_C/L_R\, e^{jn_R\theta} & 0 \\ -M_PM_C/L_R\, e^{-jn_R\theta} & L_C - M_C^2/L_R & 0 \end{pmatrix}\begin{pmatrix} \widetilde{\imath}_P \\ \widetilde{\imath}_C \\ \widetilde{\imath}_R \end{pmatrix}\right) \\
= \;& \begin{pmatrix} I & 0 & -M_P/L_R e^{jn_P\theta} \\ 0 & I & -M_C/L_R\, e^{-jn_C\theta} \end{pmatrix}\begin{pmatrix} \widetilde{v}_P - R_P\widetilde{\imath}_P \\ \widetilde{v}_C - R_C\widetilde{\imath}_C \\ -R_R\widetilde{\imath}_R \end{pmatrix}. \qquad (6.47)
\end{aligned}$$

If $R_R$ can be neglected, the equations become

$$\begin{aligned}
&\frac{d}{dt}\left(\begin{pmatrix} L_P - M_P^2/L_R & -M_PM_C/L_R\, e^{jn_R\theta} \\ -M_PM_C/L_R\, e^{-jn_R\theta} & L_C - M_C^2/L_R \end{pmatrix}\begin{pmatrix} \widetilde{\imath}_P \\ \widetilde{\imath}_C \end{pmatrix}\right) \\
&= \begin{pmatrix} \widetilde{v}_P - R_P\widetilde{\imath}_P \\ \widetilde{v}_C - R_C\widetilde{\imath}_C \end{pmatrix}. \qquad (6.48)
\end{aligned}$$

These equations are the same as those for the DFIM in (3.36) if the power and control variables become the stator and rotor variables of the DFIM, and the following substitutions are made.

| DFIM parameters | From the BDFIM parameters |
|---|---|
| $L_S$ | $L_P - M_P^2/L_R$ |
| $L_R$ | $L_C - M_C^2/L_R$ |
| $R_S$ | $R_P$ |
| $R_R$ | $R_C$ |
| $M$ | $-M_PM_C/L_R$ |
| $n_P$ | $n_R$ |

Note that the mutual inductance of the DFIM is negative, but a positive value can be obtained by switching the sign of the complex control voltage and current, or by shifting the angle $\theta$ by an offset $\pi/n_R$.

**Numerical example:** consider the BDFIM model of [23] with $L_P = 0.3498$ H, $L_C = 0.3637$ H, $M_P = 3.1$ mH, $M_C = 2.2$ mH, and $L_R = 4.4521\ 10^{-5}$ mH. The equivalent DFIM parameters of the approximation are $L_S = 0.1339$ H, $L_R = 0.255$ H, and $M = -0.1532$ H. Compared to the DFIM example on p. 15, $\sigma = 0.313$ and

$$\frac{M}{\sqrt{L_S L_R}} = \sqrt{1-\sigma} = 0.829. \tag{6.49}$$

The reduction of $M$ compared to the maximum value is greater for the BDFIM, because the magnetic coupling of the windings is smaller than for sinusoidally-distributed windings. The outcome is an apparent leakage, even when there is no leakage flux. A similar issue was encountered for the BDFRM in (4.14), but the reduction is smaller in this case.

**Caution:** as the equations of the BDFIM and DFIM are the same, the two models are equivalent. The DFIM approximation is sometimes referred to as the *reduced T-model*, in reference to the equivalent circuit [21]. Because the rotor resistance is small in a BDFIM, the approximation can be very useful. However, discrepancies can be observed in certain cases [9]. In particular, one should be cautious that the approximation is invalid if the rotor frequency approaches zero, i.e., for $\omega \simeq \omega_P/n_P$.

## 6.8 Complex model of a BDFIM in a rotating frame of reference

As in (5.47), define

$$\begin{aligned} \overline{v}_P &= e^{-j\theta_P}\ \widetilde{v}_P, \quad \overline{\imath}_P = e^{-j\theta_P}\ \widetilde{\imath}_P, \\ \overline{v}_C &= e^{j\theta_C}\ \widetilde{v}_C, \quad \overline{\imath}_C = e^{j\theta_C}\ \widetilde{\imath}_C, \\ \overline{v}_R &= e^{-j\theta_R}\ \widetilde{v}_R, \quad \overline{\imath}_R = e^{-j\theta_R}\ \widetilde{\imath}_R, \end{aligned} \tag{6.50}$$

where $\theta_P$ is arbitrary and

$$\theta_R = \theta_P - n_P\theta,\ \theta_C = n_C\theta - \theta_R. \tag{6.51}$$

Since the model is the same as the CDFIM in Section 5.3, the BDFIM in the rotating frame of reference is obtained from the results of Section 5.4 as

$$\begin{aligned}
\begin{pmatrix} L_P & 0 & M_P \\ 0 & L_C & M_C \\ M_P & M_C & L_R \end{pmatrix} \frac{d}{dt} \begin{pmatrix} \overline{\imath}_P \\ \overline{\imath}_C \\ \overline{\imath}_R \end{pmatrix} \\
= \begin{pmatrix} \overline{v}_P - R_P\,\overline{\imath}_P - j\omega_P\,(L_P\,\overline{\imath}_P + M_P\,\overline{\imath}_R) \\ \overline{v}_C - R_C\,\overline{\imath}_C + j\omega_C\,(L_C\,\overline{\imath}_C + M_C\,\overline{\imath}_R) \\ -R_R\,\overline{\imath}_R - j\omega_R\,(M_P\,\overline{\imath}_P + M_C\,\overline{\imath}_C + L_R\,\overline{\imath}_R) \end{pmatrix} \\
\tau_M = n_P M_P\, C_P^{-1}\ \mathrm{Im}\,(\overline{\imath}_P\,\overline{\imath}_R^*) - n_C M_C\, C_P^{-1}\ \mathrm{Im}\,(\overline{\imath}_C\,\overline{\imath}_R^*)\,. \qquad (6.52)
\end{aligned}$$

## 6.9 Model of a BDFIM with nested loops

In the BDFIM with nested loops, additional short-circuited rotor windings are placed inside the original windings of Fig. 6.6. The resulting rotor is shown schematically on Fig. 6.8. On the figure, there are three nests ($n_R = 3$) and each nest has three loops ($L = 3$).

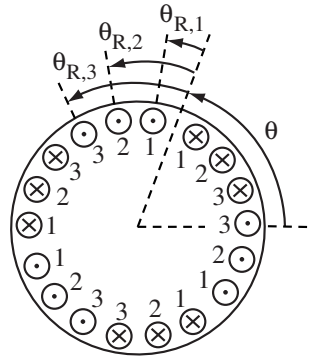


Figure 6.8: BDFIM with nested loops

The current vector $i_R$ is replaced by

$$i_{RL} = \begin{pmatrix} i_P \\ i_C \\ i_{R,1} \\ \vdots \\ i_{R,L} \end{pmatrix}, \qquad (6.53)$$

where $i_{R,1}, \cdots, i_{R,L}$ are vectors of dimension $n_R$ associated with the $L$ loops. The inductance matrix (6.7) becomes

$$L(\theta) = \begin{pmatrix} L_{PP} & 0 & L_{PRL}(\theta) \\ 0 & L_{CC} & L_{CRL}(\theta) \\ L_{PRL}^T(\theta) & L_{CRL}^T(\theta) & L_{RRL} \end{pmatrix}, \tag{6.54}$$

where

$$\begin{aligned} L_{PRL}(\theta) &= \begin{pmatrix} L_{PR,1}(\theta) & \cdots & L_{PR,L}(\theta) \end{pmatrix} \\ L_{CRL}(\theta) &= \begin{pmatrix} L_{CR,1}(\theta) & \cdots & L_{CR,L}(\theta) \end{pmatrix} \\ L_{RRL} &= \begin{pmatrix} L_{RR,11} & \cdots & L_{RR,1L} \\ \vdots & \ddots & \vdots \\ L_{RR,1L} & \cdots & L_{RR,LL} \end{pmatrix}. \end{aligned} \tag{6.55}$$

The matrices $L_{PP}$ and $L_{CC}$ are the same as for the single loop case, i.e., (6.8). The matrices $L_{PR,1}(\theta)$, ... , $L_{PR,L}(\theta)$, $L_{CR,1}(\theta)$, ... , $L_{CR,L}(\theta)$, and $L_{RR,11}$, ... , $L_{RR,LL}$ can be computed separately for each loop using the same formulas as for $L_{PR}(\theta)$, $L_{CR}(\theta)$, and $L_{RR}$ in (6.12), (6.14), and (6.10), respectively. The "off-diagonal" matrices $L_{RR,jk}$ have a similar structure as the matrices $L_{RR,kk}$, that is

$$L_{RR,jk} = \begin{pmatrix} L_{RW,jk} & M_{RW,jk} & \cdots & M_{RW,jk} \\ M_{RW,jk} & L_{RW,jk} & \cdots & M_{RW,jk} \\ \vdots & \vdots & \ddots & \vdots \\ M_{RW,jk} & M_{RW,jk} & \cdots & L_{RW,jk} \end{pmatrix}. \tag{6.56}$$

The parameter $L_{RW,jk}$ is the mutual inductance between two loops of different size in the same nest. Using the formula for two fractional windings with complete overlap (6.4),

$$\begin{aligned} L_{RW,jk} &= \frac{2cN_jN_k}{\pi}\,\theta_j(\pi - \theta_k), \text{ if } j < k \\ &= \frac{2cN_jN_k}{\pi}\,\theta_k(\pi - \theta_j), \text{ if } j > k. \end{aligned} \tag{6.57}$$

The parameter $M_{RW,jk}$ is the mutual inductance between two loops of different size in separate nests. Using the formula for two fractional windings without overlap (6.2),

$$M_{RW,jk} = -\frac{2cN_jN_k\theta_j\theta_k}{\pi}. \tag{6.58}$$

Note that $L_{RR,jk} = L_{RR,jk}^T = L_{RR,kj}$.

The transformation to complex variables (6.36) is extended in a straightforward manner to

$$\begin{pmatrix} C_V\ z_3^T & 0 & 0 & 0 & 0 \\ 0 & C_V\ z_3^{*T}\ e^{-j\varphi} & 0 & 0 & 0 \\ 0 & 0 & C_{V,R}\ z_R^T & 0 & 0 \\ \vdots & \vdots & \vdots & \ddots & \vdots \\ 0 & 0 & 0 & 0 & C_{V,R}\ z_R^T \end{pmatrix} L(\theta) \begin{pmatrix} i_P \\ i_C \\ i_{R,1} \\ \vdots \\ i_{R,L} \end{pmatrix}$$
$$= \begin{pmatrix} L_P & 0 & M_{PL}\ e^{jn_P\theta} \\ 0 & L_C & M_{CL}\ e^{-jn_C\theta} \\ M_{PL}^T\ e^{-jn_P\theta} & M_{CL}^T\ e^{jn_C\theta} & L_{RL} \end{pmatrix} \begin{pmatrix} \widetilde{i}_P \\ \widetilde{i}_C \\ \widetilde{i}_{RL} \end{pmatrix}, \tag{6.59}$$

where the previous scalar parameters become vectors and matrices

$$\begin{aligned} M_{PL} &= \begin{pmatrix} M_{P,1} & \cdots & M_{P,L} \end{pmatrix} \\ M_{CL} &= \begin{pmatrix} M_{C,1} & \cdots & M_{C,L} \end{pmatrix} \\ L_{RL} &= \begin{pmatrix} L_{R,11} & \cdots & L_{R,1L} \\ \vdots & \ddots & \vdots \\ L_{R,1L} & \cdots & L_{R,LL} \end{pmatrix}. \end{aligned} \tag{6.60}$$

Similar parameter definitions apply as for the single loop case.

The BDFIM model becomes

$$\frac{d}{dt}\left(\begin{pmatrix} L_P & 0 & M_{PL}\ e^{jn_P\theta} \\ 0 & L_C & M_{CL}\ e^{-jn_C\theta} \\ M_{PL}^T\ e^{-jn_P\theta} & M_{CL}^T\ e^{jn_C\theta} & L_{RL} \end{pmatrix} \begin{pmatrix} \widetilde{i}_P \\ \widetilde{i}_C \\ \widetilde{i}_{RL} \end{pmatrix}\right)$$
$$= \begin{pmatrix} \widetilde{v}_P - R_P\widetilde{i}_P \\ \widetilde{v}_C - R_C\widetilde{i}_C \\ -R_{RL}\widetilde{i}_R \end{pmatrix}$$
$$\tau_M = n_P\ C_P^{-1}\ \mathrm{Im}\left(\widetilde{i}_P\ \left(M_{PL}\ \widetilde{i}_{RL}\ e^{jn_P\theta}\right)^*\right)$$
$$-n_C\ C_P^{-1}\ \mathrm{Im}\left(\widetilde{i}_C\ \left(M_{CL}\ \widetilde{i}_{RL}\ e^{-jn_C\theta}\right)^*\right), \tag{6.61}$$

with the diagonal rotor resistance matrix

$$R_{RL} = \begin{pmatrix} R_{R,1} & \cdots & 0 \\ \vdots & \ddots & \vdots \\ 0 & \cdots & R_{R,L} \end{pmatrix}. \tag{6.62}$$

The model of the BDFIM with multiple loops has a higher order than the single loop model and is not equivalent to a CDFIM anymore.

**Numerical example:** consider the BDFIM model of [20]. The inductances of the complex model can be computed using the *Matlab* code below.

```
%
% BDFIM design parameters
%
r=0.1745/2;l=0.1899;g=6.35e-4;
np=2;nc=4;nr=np+nc;Np=80;Nc=80;Nr1=1;Nr2=1;Nr3=1;
thr1=pi*1/36;thr2=pi*3/36;thr3=pi*5/36;
%
% Compute inductance parameters
%
c=4e-7*pi*r*l/g;
Lpw=c*Np^2*pi/4,Mpw=-c*Np^2*pi/8
Lcw=c*Nc^2*pi/4,Mcw=-c*Nc^2*pi/8
Lrw11=2*c*Nr1^2*thr1*(pi-thr1)/pi+Lr1s,Mrw11=-2*c*Nr1^2*thr1^2/pi
Lrw12=2*c*Nr1*Nr2*thr1*(pi-thr2)/pi,Mrw12=-2*c*Nr1*Nr2*thr1*thr2/pi
Lrw13=2*c*Nr1*Nr3*thr1*(pi-thr3)/pi,Mrw13=-2*c*Nr1*Nr3*thr1*thr3/pi
Lrw22=2*c*Nr2^2*thr2*(pi-thr2)/pi+Lr2s,Mrw22=-2*c*Nr2^2*thr2^2/pi
Lrw23=2*c*Nr2*Nr3*thr2*(pi-thr3)/pi,Mrw23=-2*c*Nr2*Nr3*thr2*thr3/pi
Lrw33=2*c*Nr3^2*thr3*(pi-thr3)/pi+Lr3s,Mrw33=-2*c*Nr3^2*thr3^2/pi
Mpr=(c*Np/np)*[Nr1*sin(np*thr1) Nr2*sin(np*thr2) Nr3*sin(np*thr3)]
Mcr=(c*Nc/nc)*[Nr1*sin(nc*thr1) Nr2*sin(nc*thr2) Nr3*sin(nc*thr3)]
%
% Compute complex model parameters
%
Lp=Lpw-Mpw,Lc=Lcw-Mcw
Lrl=[Lrw11-Mrw11 Lrw12-Mrw12 Lrw13-Mrw13; ...
Lrw12-Mrw12 Lrw22-Mrw22 Lrw23-Mrw23; ...
Lrw13-Mrw13 Lrw23-Mrw23 Lrw33-Mrw33]
Mpl=(sqrt(3*nr)/2)*Mpr,Mcl=(sqrt(3*nr)/2)*Mcr
```

The results are:

```
Lp = 0.2472
Lc = 0.2472
Lrl = 1.0e-04 *
    0.0572    0.0572    0.0572
    0.0572    0.1717    0.1717
    0.0572    0.1717    0.2861
Mpl = 0.0005    0.0014    0.0021
Mcl = 0.0005    0.0012    0.0014
```

The parameters are similar to those reported in [20], but not identical because the stator windings were assumed to be sinusoidally-distributed instead of concentrated in [20]. Some other fine details were also neglected. On the other hand, all the inductance parameters were computed using simple analytical formulas. It is interesting to note that, with the assumption of sinusoidally-distributed stator windings and fractional-pitch rotor windings, pure sinusoidal steady-state operation is possible, and the computations do not require to discard any harmonic components..

## 6.10 Reduced-order model of a BDFIM with nested loops

It is common to derive a reduced-order model that has the same structure as the single-loop BDFIM. A technique proposed in [20] proceeds as follows. Observe that the matrix $L_{RL}$ must be symmetric positive semi-definite. Therefore, its eigenvalues are all real and positive, and the matrix can be decomposed as

$$L_{RL} = U\ D_{RL}\ U^T, \tag{6.63}$$

where $D_{RL}$ is a diagonal matrix containing the eigenvalues of $L_{RL}$ and $U$ is a matrix of orthogonal eigenvectors satisfying

$$U^{-1} = U^T. \tag{6.64}$$

Multiplying the last row of the model by $U^T$ and replacing $\widetilde{\imath}_{RL}$ by $UU^T\widetilde{\imath}_{RL}$, the model becomes

$$\begin{aligned}
\frac{d}{dt}\left(\begin{pmatrix} L_P & 0 & (M_{PL}U)\ e^{jn_P\theta} \\ 0 & L_C & (M_{CL}U)\ e^{-jn_C\theta} \\ (M_{PL}U)^T\ e^{-jn_P\theta} & (M_{CL}U)^T\ e^{jn_C\theta} & U^T L_{RL} U \end{pmatrix}\begin{pmatrix} \widetilde{\imath}_P \\ \widetilde{\imath}_C \\ U^T\,\widetilde{\imath}_{RL} \end{pmatrix}\right) \\
= \begin{pmatrix} \widetilde{v}_P - R_P\widetilde{\imath}_P \\ \widetilde{v}_C - R_C\widetilde{\imath}_C \\ -\left(U^T R_{RL} U\right)\ U^T\,\widetilde{\imath}_{RL} \end{pmatrix} \\
\tau_M = n_P\ C_P^{-1}\ \mathrm{Im}\left(\widetilde{\imath}_P\ \left(M_{PL}UU^T\,\widetilde{\imath}_{RL}\ e^{jn_P\theta}\right)^*\right) \\
-n_C\ C_P^{-1}\ \mathrm{Im}\left(\widetilde{\imath}_C\ \left(M_{CL}UU^T\,\widetilde{\imath}_{RL}\ e^{-jn_C\theta}\right)^*\right).
\end{aligned} \tag{6.65}$$

Assume that the eigenvalues have been ordered from the smallest to the largest in the matrix $D_{RL}$, and that the largest eigenvalue is much larger than the other eigenvalues. The model order reduction technique consists in retaining only the last rotor variable in the vector $U^T\,\widetilde{\imath}_{RL}$. Letting

$$x^T = \begin{pmatrix} 0 & \cdots & 0 & 1 \end{pmatrix}, \tag{6.66}$$

the model (6.46) is obtained where

$$\begin{aligned} M_P &= M_{PL}\, U\, x,\; M_C = M_{CL}\, U\, x \\ L_R &= x^T \left(U^T L_{RL} U\right) x = x^T D_{LL} x \\ R_R &= x^T \left(U^T R_{RL} U\right) x. \end{aligned} \tag{6.67}$$

Note that $L_R$ is the largest eigenvalue of $L_{RL}$.

**Numerical example:** the code below shows a *Matlab* implementation of the procedure (parameters from [20] are used, with some adjustments).

```
%
% Reduction of BDFIM model from three loops to one loop
%
Lrl=[0.72 0.576 0.576;0.576 1.878 1.727;0.576 1.727 3.037]*1e-5;
Rrl=[1.056 0 0;0 1.209 0;0 0 1.361]*1e-4;
Mpl=[0.5793 1.6693 2.5533]*1e-3;
Mcl=[0.5555 1.4137 1.6072]*1e-3;
[v,d]=eig(Lrl);
x=[0;0;1];
Lr=x'*d*x
Mp=Mpl*v*x
Mc=Mcl*v*x
Rr=x'*(v'*Rrl*v)*x
```

The code produces:

```
Lr = 4.4525e-05
Mp = 0.0031
Mc = 0.0022
Rr = 1.2969e-04
```

# Chapter 7

# Three-Phase Synchronous Machines

## 7.1 Objective

The objective of this chapter is to model a three-phase synchronous machine with field and damper windings, as shown schematically on Fig. 7.1 for a machine with one pole pair. The results of the chapter:

- derive a model of the machine in phase variables.
- deduce a DQ model for the machine.

## 7.2 Machine structure

The stator has a set of three-phase windings ($A$, $B$, and $C$). The rotor also has three windings, but they are organized differently. One winding ($F$) is called the *field winding*, and typically has a constant voltage applied to it. The resulting magnetic field is similar to the field produced by the permanent magnet (PM) in PM synchronous motors if the current is constant. In dynamic situations, however, the field and stator currents can interact in ways that are absent in PM machines. The direction used to define the position of the rotor is chosen to be aligned with the field winding. Two other windings ($D$ and $Q$) are present on the rotor: the first is placed along the same axis as the field winding, and the second is placed at a 90° angle. Both windings are typically short-circuited and produce a torque similar to squirrel-cage induction machines. The windings increase the damping of oscillations around the synchronous speed and are called *damper windings*.

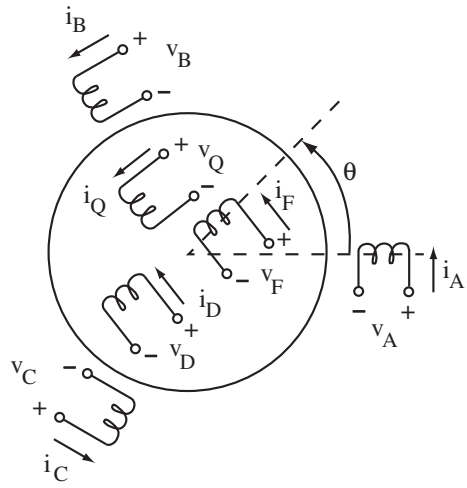


Figure 7.1: Schematic of a three-phase synchronous machine with field and damper windings

## 7.3 Inductances with salient rotor

The derivation of the model proceeds by expressing the flux linkages as functions of the currents, based on the geometry of the machine. The expressions are complicated by the fact that the rotor has salient poles (a schematic representation is shown on Fig. 7.2). The angle that will be used for the DQ transformation is the angle $\theta$ that defines the direction of the field winding. It will be assumed that the $D$-axis is also the direction of lowest reluctance. Figs. 7.1 and 7.2 show a machine with one pole pair. For multiple pole pairs, $\theta$ is replaced by $n_P\theta$.

The salient pole machine is modeled as a non-uniform airgap machine, as described in Section 2.4, where $n_R = 2n_P$ and $n_P$ is the number of pole pairs. In (2.22), inductances were obtained

$$\begin{aligned} L_{AA} &= L_0 + L_1\cos(2n_P\theta) & L_{AB} &= M_0 + L_1\cos(2n_P\theta - 2\pi/3) \\ L_{BB} &= L_0 + L_1\cos(2n_P\theta + 2\pi/3) & L_{BC} &= M_0 + L_1\cos(2n_P\theta) \\ L_{CC} &= L_0 + L_1\cos(2n_P\theta - 2\pi/3)) & L_{CA} &= M_0 + L_1\cos(2n_P\theta + 2\pi/3). \end{aligned} \tag{7.1}$$

$L_0$, $L_1$, and $M_0$ are parameters that depend on the winding characteristics. Without leakage flux, (2.22) gave $M_0 = -L_0/2$. Practically, $L_0$ is assumed to be slightly larger than $-2M_0$. One must also have $L_1 \leqslant L_0$.

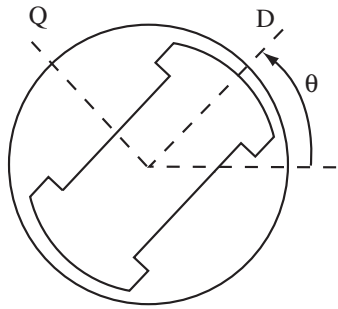


Figure 7.2: Rotor with salient poles ($n_P = 1$)

The inductance functions $L_{AA}$ and $L_{AB}$ are shown on Fig. 7.3 for $M_0 \simeq -L_0/2$. As expected, the self-inductance of winding $A$ reaches a maximum value when the rotor is aligned with winding $A$ (0°), and reaches a minimum for 90° (electrical). Interestingly, the mutual inductance peaks for $n_P\theta = 60°$, 150°, 240°, and 330°.

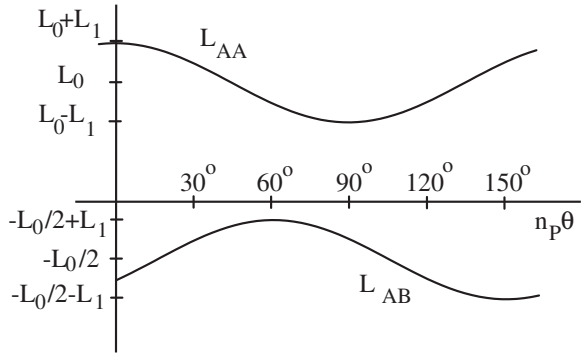


Figure 7.3: Self-inductance $L_{AA}$ and mutual inductance $L_{AB}$ as functions of the rotor angle

## 7.4 Model in phase variables

Define vectors of stator voltages, stator currents, and stator total flux linkages

$$v_S = \begin{pmatrix} v_A \\ v_B \\ v_C \end{pmatrix}, \; i_S = \begin{pmatrix} i_A \\ i_B \\ i_C \end{pmatrix}, \; \psi_S = \begin{pmatrix} \psi_A \\ \psi_B \\ \psi_C \end{pmatrix}. \tag{7.2}$$

Rotor variables are defined similarly with

$$v_R = \begin{pmatrix} v_F \\ v_D \\ v_Q \end{pmatrix}, \; i_R = \begin{pmatrix} i_F \\ i_D \\ i_Q \end{pmatrix}, \; \Psi_R = \begin{pmatrix} \psi_F \\ \psi_D \\ \psi_Q \end{pmatrix}. \tag{7.3}$$

The electrical equations describing the machine are

$$\frac{d\psi_S}{dt} = v_S - R_S i_S, \; \frac{d\psi_R}{dt} = v_R - \begin{pmatrix} R_F & 0 & 0 \\ 0 & R_D & 0 \\ 0 & 0 & R_Q \end{pmatrix} i_R, \tag{7.4}$$

where $R_S$ is the resistance of a stator winding, and $R_F$, $R_D$, and $R_Q$ are the resistances of the $F$, $D$, and $Q$ windings, respectively.

For the analysis of the machine, we assume linear expressions for the flux linkages as functions of the currents

$$\begin{pmatrix} \psi_S \\ \psi_R \end{pmatrix} = L(\theta) \begin{pmatrix} i_S \\ i_R \end{pmatrix}, \; L(\theta) = \begin{pmatrix} L_{SS}(\theta) & L_{SR}(\theta) \\ L_{SR}^T(\theta) & L_{RR} \end{pmatrix}. \tag{7.5}$$

The three stator windings are identical, except for shifts of 120°. From (7.1), $L_{SS}(\theta)$ has the form

$$L_{SS}(\theta) = \begin{pmatrix} L_0 + L_1\cos(2n_P\theta) & M_0 + L_1\cos(2n_P\theta - 2\pi/3) & M_0 + L_1\cos(2n_P\theta + 2\pi/3) \\ M_0 + L_1\cos(2n_P\theta - 2\pi/3) & L_0 + L_1\cos(2n_P\theta + 2\pi/3) & M_0 + L_1\cos(2n_P\theta) \\ M_0 + L_1\cos(2n_P\theta + 2\pi/3) & M_0 + L_1\cos(2n_P\theta) & L_0 + L_1\cos(2n_P\theta - 2\pi/3) \end{pmatrix}. \tag{7.6}$$

Based on the geometry of the machine, the other inductance matrices are assumed to have the form

$$L_{RR} = \begin{pmatrix} L_F & M_R & 0 \\ M_R & L_D & 0 \\ 0 & 0 & L_Q \end{pmatrix} \tag{7.7}$$

and

$$L_{SR}(\theta) = \begin{pmatrix} M_{SF}\cos(n_P\theta) & M_{SD}\cos(n_P\theta) & M_{SQ}\cos(n_P\theta + \pi/2) \\ M_{SF}\cos(n_P\theta - 2\pi/3) & M_{SD}\cos(n_P\theta - 2\pi/3) & M_{SQ}\cos(n_P\theta - \pi/6) \\ M_{SF}\cos(n_P\theta + 2\pi/3) & M_{SD}\cos(n_P\theta + 2\pi/3) & M_{SQ}\cos(n_P\theta - 5\pi/6) \end{pmatrix}. \tag{7.8}$$

In the model,

- $L_F$, $L_D$, $L_Q$ are the self-inductances of rotor windings $F$, $D$, and $Q$, respectively.
- $M_R$ is the mutual inductance between rotor winding $F$ and rotor winding $D$.
- $M_{SF}$, $M_{SD}$, and $M_{SQ}$ are the mutual inductances between a stator winding and the rotor windings $F$, $D$, and $Q$, respectively, when the windings are aligned (e.g., $M_{SF}$ is the mutual inductance between windings $A$ and $F$ when $\theta = 0$).

Considering that the damper windings are short-circuited, the electrical equations of the three-phase synchronous machine are

$$L(\theta)\frac{d}{dt}\begin{pmatrix} i_A \\ i_B \\ i_C \\ i_F \\ i_D \\ i_Q \end{pmatrix} = \begin{pmatrix} v_A - R_S i_A \\ v_B - R_S i_B \\ v_C - R_S i_C \\ v_F - R_F i_F \\ -R_D i_D \\ -R_Q i_Q \end{pmatrix} - \omega \frac{\partial L(\theta)}{\partial \theta}\begin{pmatrix} i_A \\ i_B \\ i_C \\ i_F \\ i_D \\ i_Q \end{pmatrix}, \tag{7.9}$$

where $L(\theta)$ is given by (7.5), and $L_{SS}(\theta)$, $L_{RR}$, and $L_{SR}(\theta)$ by (7.6), (7.7), and (7.8), respectively. The partial derivative is given by

$$\frac{\partial L(\theta)}{\partial \theta} = \begin{pmatrix} \partial L_{SS}(\theta)/\partial\theta & \partial L_{SR}(\theta)/\partial\theta \\ \partial L_{SR}^T(\theta)/\partial\theta & 0 \end{pmatrix}, \tag{7.10}$$

with

$$\frac{\partial L_{SS}(\theta)}{\partial \theta} = -2n_P L_1 \begin{pmatrix} \sin(2n_P\theta) & \sin(2n_P\theta - 2\pi/3) & \sin(2n_P\theta + 2\pi/3) \\ \sin(2n_P\theta - 2\pi/3) & \sin(2n_P\theta + 2\pi/3) & \sin(2n_P\theta) \\ \sin(2n_P\theta + 2\pi/3) & \sin(2n_P\theta) & \sin(2n_P\theta - 2\pi/3) \end{pmatrix}, \tag{7.11}$$

and

$$\frac{\partial L_{SR}(\theta)}{\partial \theta} = -n_P \begin{pmatrix} M_{SF}\sin(n_P\theta) & M_{SD}\sin(n_P\theta) & M_{SQ}\sin(n_P\theta + \pi/2) \\ M_{SF}\sin(n_P\theta - 2\pi/3) & M_{SD}\sin(n_P\theta - 2\pi/3) & M_{SQ}\sin(n_P\theta - \pi/6) \\ M_{SF}\sin(n_P\theta + 2\pi/3) & M_{SD}\sin(n_P\theta + 2\pi/3) & M_{SQ}\sin(n_P\theta - 5\pi/6) \end{pmatrix}. \tag{7.12}$$

The general formula for the torque of an electric machine (1.7) gives

$$\begin{aligned}\tau_M &= \frac{1}{2} i_S^T \frac{\partial L_{SS}(\theta)}{\partial \theta} i_S + i_S^T \frac{\partial L_{SR}(\theta)}{\partial \theta} i_R \\ &= -n_P L_1 \left(\sin(2n_P\theta) i_{SA}^2 + \sin(2n_P\theta + 2\pi/3) i_{SB}^2 + \sin(2n_P\theta - 2\pi/3) i_{SC}^2\right) \\ &\quad -2n_P L_1 \left(\sin(2n_P\theta - 2\pi/3) i_{SA} i_{SB} + \sin(2n_P\theta + 2\pi/3) i_{SA} i_{SC}\right. \\ &\quad \left. + \sin(2n_P\theta) i_{SB} i_{SC}\right) \\ &\quad -n_P \left(M_{SF} i_F + M_{SD} i_D\right) \left(\sin(n_P\theta) i_{SA} + \sin(n_P\theta - 2\pi/3) i_{SB}\right. \\ &\quad \left. + \sin(n_P\theta + 2\pi/3) i_{SC}\right) \\ &\quad -n_P M_{SQ} i_Q \left(\sin(n_P\theta + \pi/2) i_{SA} + \sin(n_P\theta - \pi/6) i_{SB}\right. \\ &\quad \left. + \sin(n_P\theta - 5\pi/6) i_{SC}\right). \end{aligned} \tag{7.13}$$

## 7.5 Model in DQ variables

Consider the matrix defining a three-phase DQ transformation, which is the combination of a 3-2 transformation (1.8) and a DQ transformation for the two-phase variables, leaving the homopolar variables the same [6],

$$M_{3-dq}(\theta) = \begin{pmatrix} \cos(n_P\theta) & \sin(n_P\theta) & 0 \\ -\sin(n_P\theta) & \cos(n_P\theta) & 0 \\ 0 & 0 & 1 \end{pmatrix} M_{3-2}. \tag{7.14}$$

The result is

$$M_{3-dq}(\theta) = C_V \begin{pmatrix} \cos(n_P\theta) & \cos(n_P\theta - 2\pi/3) & \cos(n_P\theta + 2\pi/3) \\ -\sin(n_P\theta) & -\sin(n_P\theta - 2\pi/3) & -\sin(n_P\theta + 2\pi/3) \\ 1/\sqrt{2} & 1/\sqrt{2} & 1/\sqrt{2} \end{pmatrix}. \tag{7.15}$$

New variables are defined using

$$\begin{pmatrix} \psi_d \\ \psi_q \\ \psi_h \end{pmatrix} = M_{3-dq}(\theta) \begin{pmatrix} \psi_A \\ \psi_B \\ \psi_C \end{pmatrix}, \quad \begin{pmatrix} v_d \\ v_q \\ v_h \end{pmatrix} = M_{3-dq}(\theta) \begin{pmatrix} v_A \\ v_B \\ v_C \end{pmatrix}, \quad \begin{pmatrix} i_d \\ i_q \\ i_h \end{pmatrix} = M_{3-dq}(\theta) \begin{pmatrix} i_A \\ i_B \\ i_C \end{pmatrix}. \tag{7.16}$$

With the DQ transformation, the total flux linkages become

$$\begin{aligned} \begin{pmatrix} \psi_d \\ \psi_q \\ \psi_h \end{pmatrix} &= M_{3-dq}(\theta) L_{SS}(\theta) M_{3-dq}^{-1}(\theta) \begin{pmatrix} i_d \\ i_q \\ i_h \end{pmatrix} + M_{3-dq}(\theta) L_{SR}(\theta) \begin{pmatrix} i_F \\ i_D \\ i_Q \end{pmatrix} \\ \begin{pmatrix} \psi_F \\ \psi_D \\ \psi_Q \end{pmatrix} &= L_{SR}^T(\theta) M_{3-dq}^{-1}(\theta) \begin{pmatrix} i_d \\ i_q \\ i_h \end{pmatrix} + L_{RR} \begin{pmatrix} i_F \\ i_D \\ i_Q \end{pmatrix}. \end{aligned} \tag{7.17}$$

Computing the products (see Section 7.6), one finds that

$$\begin{pmatrix} \psi_d \\ \psi_q \\ \psi_h \\ \psi_F \\ \psi_D \\ \psi_Q \end{pmatrix} = \begin{pmatrix} L_d & 0 & 0 & M_F & M_D & 0 \\ 0 & L_q & 0 & 0 & 0 & M_Q \\ 0 & 0 & L_h & 0 & 0 & 0 \\ M_F\ C_P^{-1} & 0 & 0 & L_F & M_R & 0 \\ M_D\ C_P^{-1} & 0 & 0 & M_R & L_D & 0 \\ 0 & M_Q C_P^{-1} & 0 & 0 & 0 & L_Q \end{pmatrix} \begin{pmatrix} i_d \\ i_q \\ i_h \\ i_F \\ i_D \\ i_Q \end{pmatrix}, \tag{7.18}$$

where $C_P$ is the coefficient of power associated with the $3-2$ transformation and

$$\begin{aligned} L_d &= L_0 - M_0 + \frac{3}{2}L_1,\ L_q = L_0 - M_0 - \frac{3}{2}L_1,\ L_h = L_0 + 2M_0, \\ M_F &= \frac{3C_V M_{SF}}{2},\ M_D = \frac{3C_V M_{SD}}{2},\ M_Q = \frac{3C_V M_{SQ}}{2}. \end{aligned} \tag{7.19}$$

Note that the inductance matrix is symmetric if and only if $C_P = 1$, i.e., if an equal power transformation is used. On the other hand, $M_F = M_{SF}$, $M_D = M_{SD}$, $M_Q = M_{SQ}$, $C_P^{-1} = 3/2$ if the equal magnitude transformation is used ($C_V = 2/3$). Both options are used in the power systems literature [3], [17].

Differentiating the total flux linkages with respect to time and computing the products

$$\begin{aligned} \frac{d}{dt}\begin{pmatrix} \psi_d \\ \psi_q \\ \psi_h \end{pmatrix} &= M_{3-dq}(\theta)\frac{d}{dt}\begin{pmatrix} \psi_A \\ \psi_B \\ \psi_C \end{pmatrix} + \omega\frac{\partial M_{3-dq}(\theta)}{\partial\theta}\begin{pmatrix} \psi_A \\ \psi_B \\ \psi_C \end{pmatrix} \\ &= M_{3-dq}(\theta)\begin{pmatrix} v_A - R_S i_A \\ v_B - R_S i_B \\ v_C - R_S i_C \end{pmatrix} + \omega\frac{\partial M_{3-dq}(\theta)}{\partial\theta}M_{3-dq}^{-1}(\theta)\begin{pmatrix} \psi_d \\ \psi_q \\ \psi_h \end{pmatrix} \\ &= \begin{pmatrix} v_d - R_S i_d \\ v_q - R_S i_q \\ v_h - R_S i_h \end{pmatrix} + n_P\omega\begin{pmatrix} \psi_q \\ -\psi_d \\ 0 \end{pmatrix}. \end{aligned} \tag{7.20}$$

The derivatives of the rotor fluxes are determined by (7.3) and (7.4) with $v_D = v_Q = 0$, i.e.,

$$\frac{d}{dt}\begin{pmatrix} \psi_F \\ \psi_D \\ \psi_Q \end{pmatrix} = \begin{pmatrix} v_F - R_F i_F \\ -R_D i_D \\ -R_Q i_Q \end{pmatrix}. \tag{7.21}$$

Note that the variables can be reordered to show a decoupling between the

DQ axes. Specifically,

$$\begin{pmatrix} \psi_d \\ \psi_F \\ \psi_D \\ \psi_q \\ \psi_Q \\ \psi_h \end{pmatrix} = \begin{pmatrix} L_d & M_F & M_D & 0 & 0 & 0 \\ M_F\, C_P^{-1} & L_F & M_R & 0 & 0 & 0 \\ M_D\, C_P^{-1} & M_R & L_D & 0 & 0 & 0 \\ 0 & 0 & 0 & L_q & M_Q & 0 \\ 0 & 0 & 0 & M_Q\, C_P^{-1} & L_Q & 0 \\ 0 & 0 & 0 & 0 & 0 & L_h \end{pmatrix} \begin{pmatrix} i_d \\ i_F \\ i_D \\ i_q \\ i_Q \\ i_h \end{pmatrix}. \tag{7.22}$$

Given that the inductance matrix is constant in the DQ variables,the system is described by

$$\begin{pmatrix} L_d & M_F & M_D \\ M_F\, C_P^{-1} & L_F & M_R \\ M_D\, C_P^{-1} & M_R & L_D \end{pmatrix} \frac{d}{dt} \begin{pmatrix} i_d \\ i_F \\ i_D \end{pmatrix} = \begin{pmatrix} v_d - R_S i_d + n_P \omega \left( L_q i_q + M_Q i_Q \right) \\ v_F - R_F i_F \\ -R_D i_D \end{pmatrix}$$

$$\begin{pmatrix} L_q & M_Q \\ M_Q\, C_P^{-1} & L_Q \end{pmatrix} \frac{d}{dt} \begin{pmatrix} i_q \\ i_Q \end{pmatrix} = \begin{pmatrix} v_q - R_S i_q - n_P \omega \left( L_d i_d + M_F i_F + M_D i_D \right) \\ -R_Q i_Q \end{pmatrix}$$

$$L_h \frac{di_h}{dt} = v_h - R_S i_h. \tag{7.23}$$

The torque can be obtained by converting (7.13) in the DQ variables, or

$$\begin{aligned} \tau_M &= \frac{1}{2} \begin{pmatrix} i_d & i_q & i_h \end{pmatrix} \left( M_{3-dq}^{-1}(\theta) \right)^T \frac{\partial L_{SS}(\theta)}{\partial \theta} M_{3-dq}^{-1}(\theta) \begin{pmatrix} i_d \\ i_q \\ i_h \end{pmatrix} \\ &\quad + \begin{pmatrix} i_d & i_q & i_h \end{pmatrix} \left( M_{3-dq}^{-1}(\theta) \right)^T \frac{\partial L_{SR}(\theta)}{\partial \theta} \begin{pmatrix} i_F \\ i_D \\ i_Q \end{pmatrix}. \end{aligned} \tag{7.24}$$

After simplifications

$$\tau_M = n_P\, C_P^{-1} \left( M_F i_F i_q + \left( L_d - L_q \right) i_d i_q + \left( M_D i_q i_D - M_Q i_d i_Q \right) \right). \tag{7.25}$$

The torque has three components:

- the first term, $n_P C_P^{-1} M_F i_F i_q$, is a *reaction* torque similar to the torque $K i_q$ produced by a permanent magnet synchronous motor [6]. In this case, the magnitude of the torque constant $n_P C_P^{-1} M_F i_F$ can be adjusted through the magnitude of the field current.

- the second term, $n_P C_P^{-1} (L_d - L_q)\, i_d i_q$, is a *reluctance* torque related to the saliency of the rotor. The same torque is found in reluctance or hybrid motors.

- the third term, $n_P C_P^{-1} (M_D i_q i_D - M_Q i_d i_Q)$ is an *induction* torque, similar to the torque found in two-phase induction motors with a reference frame attached to the rotor (with such motors, it is assumed that $M_D = M_Q$). The torque increases the damping of the motor and reduces speed fluctuations. It can also be used to start a synchronous motor from zero speed.

Note that the power absorbed through the electrical equations

$$P_E = -n_P \omega \left(L_q i_q + M_Q i_Q\right) i_d + n_P \omega \left(L_d i_d + M_F i_F + M_D i_D\right) i_q \tag{7.26}$$

is equal to the mechanical power $P_M = \tau_M\, \omega$ if the equal power transformation is used. For other transformations, $P_E = C_P P_M$.

## 7.6 Symbolic code

The code below produces the results of (7.15), (7.18), (7.20), and (7.25).

```
%
% Symbolic code for WFSM
%
syms lss l0 l1 m0 np th lrr lf mr ld lq lsr msf msd msq ...
    m3to2 cv mdq m3dq lssdq lsrdq lrsdq psidq psid psiq psih ...
    edq om idq id iq ih ir ifc iD iQ tm real
%
% Original model
%
a=2*pi/3;
lss=[l0+l1*cos(2*np*th) m0+l1*cos(2*np*th-a) m0+l1*cos(2*np*th+a);
     m0+l1*cos(2*np*th-a) l0+l1*cos(2*np*th+a) m0+l1*cos(2*np*th) ;
     m0+l1*cos(2*np*th+a) m0+l1*cos(2*np*th) l0+l1*cos(2*np*th-a)];
lrr=[lf mr 0;mr ld 0;0 0 lq];
lsr=[msf*cos(np*th) msd*cos(np*th) msq*cos(np*th+pi/2); ...
    msf*cos(np*th-a) msd*cos(np*th-a) msq*cos(np*th-a+pi/2);
    msf*cos(np*th+a) msd*cos(np*th+a) msq*cos(np*th+a+pi/2)];
%
```

```
% DQ model
%
m3to2=cv*[1 -1/2 -1/2;0 sqrt(3)/2 -sqrt(3)/2;1/sqrt(2) ...
    1/sqrt(2) 1/sqrt(2)];
mdq=[cos(np*th) sin(np*th) 0;-sin(np*th) cos(np*th) 0;0 0 1];
m3dq=simplify(mdq*m3to2)
lssdq=simplify(m3dq*lss*inv(m3dq))
lsrdq=simplify(m3dq*lsr)
lrsdq=simplify(lsr'*inv(m3dq))
psidq=[psid;psiq;psih];
edq=simplify(om*diff(m3dq,th)*inv(m3dq)*psidq)
idq=[id;iq;ih];ir=[ifc;iD;iQ];
tm=(1/2)*idq'*inv(m3dq)'*diff(lss,th)*inv(m3dq)*idq;
tm=simplify(tm+idq'*inv(m3dq)'*diff(lsr,th)*ir)
```

# Chapter 8

# $Y$ and $\Delta$- Connected Doubly-Fed Induction Machines

## 8.1 Objective

The objective of this chapter is to obtain models of $Y$ and $\Delta$-connected doubly-fed induction machines, and to show that the models of the machines are equivalent to each other.

## 8.2 Model for a $Y-$connected machine

Often, the windings of three-phase machines are connected in a $Y$ (or *star*) configuration, as shown in Fig. 8.1. With this connection, the line currents are equal to the winding currents

$$i_1 = i_{SA},\ i_2 = i_{SB},\ i_3 = i_{SC}, \tag{8.1}$$

and $i_{SA} + i_{SB} + i_{SC} = 0$. In the 3-2 transformation, $i_{Sh} = 0$, and (3.27) implies that $v_{Sh} = 0$.

For the voltages, one has

$$v_{SA} = v_1 - v_0,\ v_{SB} = v_2 - v_0,\ v_{SC} = v_3 - v_0, \tag{8.2}$$

where $v_0$ is the voltage at the neutral point (as shown on Fig. 8.1). Since $v_{Sh} = 0$

$$v_{SA} + v_{SB} + v_{SC} = v_1 + v_2 + v_3 - 3v_0 = 0. \tag{8.3}$$

Therefore

$$v_0 = \frac{v_1 + v_2 + v_3}{3}. \tag{8.4}$$

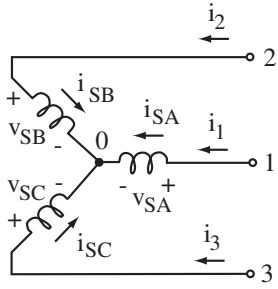


Figure 8.1: $Y-$connected machine

In other words, the neutral voltage is equal to the average of the line voltages. If the sum of the line voltages is zero, the winding voltages are equal to the line voltages and the neutral voltage is zero. If the sum of the line voltages is nonzero, the neutral voltage becomes the average of the line voltages, and the winding voltages are shifted by that amount. An important point to observe is that the currents and the torque are the same if all the voltages are offset by the same amount. Also, the two-phase equivalent voltages $v_a$ and $v_b$ remain the same if some voltage is added to (or subtracted from) the voltages $v_{SA}$, $v_{SB}$, and $v_{SC}$.

## 8.3 Model for a $\Delta$-connected machine

Another typical connection is the $\Delta$ (or *delta*) connection shown on Fig. 8.2. With this connection, one has $v_{SA} + v_{SB} + v_{SC} = 0$, which implies that $v_{Sh} = 0$. Then, (3.27) implies that $i_{Sh} = 0$, or converges exponentially to zero if initial conditions are different from zero.

From the figure

$$i_1 = i_{SA} - i_{SC},\ i_2 = i_{SB} - i_{SA},\ i_3 = i_{SC} - i_{SB}. \tag{8.5}$$

Using $i_{SA} + i_{SB} + i_{SC} = 0$,

$$i_1 - i_2 = 2i_{SA} - i_{SB} - i_{SC} = 3i_{SA} - (i_{SA} + i_{SB} + i_{SC}) = 3i_{SA}. \tag{8.6}$$

Repeating for the other variables, one finds that

$$i_{SA} = \frac{i_1 - i_2}{3},\ i_{SB} = \frac{i_2 - i_3}{3},\ i_{SC} = \frac{i_3 - i_1}{3}, \tag{8.7}$$

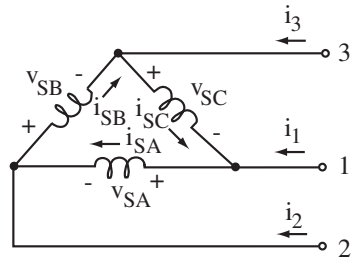


Figure 8.2: Δ-connected machine

or

$$\begin{pmatrix} i_{SA} \\ i_{SB} \\ i_{SC} \end{pmatrix} = M_\Delta \begin{pmatrix} i_1 \\ i_2 \\ i_3 \end{pmatrix}, \text{ where } M_\Delta = \frac{1}{3}\begin{pmatrix} 1 & -1 & 0 \\ 0 & 1 & -1 \\ -1 & 0 & 1 \end{pmatrix}. \tag{8.8}$$

For the voltages

$$v_{SA} = v_1 - v_2,\ v_{SB} = v_2 - v_3,\ v_{SC} = v_3 - v_1. \tag{8.9}$$

Note that

$$v_{SA} - v_{SC} = 2v_1 - v_2 - v_3 = 3v_1 - (v_1 + v_2 + v_3). \tag{8.10}$$

Define

$$v_0 = \frac{v_1 + v_2 + v_3}{3}. \tag{8.11}$$

Then

$$v_{SA} - v_{SC} = 3(v_1 - v_0). \tag{8.12}$$

As opposed to Section 8.2, the voltage $v_0$ is not the voltage of some physical location, but it is defined by the same equation. Repeating for the other variables,

$$\frac{v_{SA} - v_{SC}}{3} = v_1 - v_0,\ \frac{v_{SB} - v_{SA}}{3} = v_2 - v_0,\ \frac{v_{SC} - v_{SB}}{3} = v_3 - v_0, \tag{8.13}$$

or

$$M_\Delta^T \begin{pmatrix} v_{SA} \\ v_{SB} \\ v_{SC} \end{pmatrix} = \begin{pmatrix} v_1 - v_0 \\ v_2 - v_0 \\ v_3 - v_0 \end{pmatrix}. \tag{8.14}$$

With (3.3), the results imply that

$$\begin{aligned}\frac{d}{dt}\left(M_\Delta^T\psi_S\right) &= \begin{pmatrix}(v_{SA}-v_{SC})/3-(R_S/3)(i_{SA}-i_{SC})\\(v_{SB}-v_{SA})/3-(R_S/3)(i_{SB}-i_{SA})\\(v_{SC}-v_{SB})/3-(R_S/3)(i_{SC}-i_{SB})\end{pmatrix}\\ &= \begin{pmatrix}v_1-v_0-(R_S/3)i_1\\v_2-v_0-(R_S/3)i_2\\v_3-v_0-(R_S/3)i_3\end{pmatrix}. \qquad (8.15)\end{aligned}$$

Using the DFIM model (3.4)-(3.6) and computing the products (see Section 8.5),

$$\begin{aligned}M_\Delta^T\psi_S &= M_\Delta^T L_{SS} M_\Delta \begin{pmatrix}i_1\\i_2\\i_3\end{pmatrix} + M_\Delta^T L_{SR}(\theta)\begin{pmatrix}i_{RX}\\i_{RY}\\i_{RZ}\end{pmatrix}\\ &= \frac{1}{9}\begin{pmatrix}2(L_{SW}-M_{SW}) & M_{SW}-L_{SW} & M_{SW}-L_{SW}\\ M_{SW}-L_{SW} & 2(L_{SW}-M_{SW}) & M_{SW}-L_{SW}\\ M_{SW}-L_{SW} & M_{SW}-L_{SW} & 2(L_{SW}-M_{SW})\end{pmatrix}\begin{pmatrix}i_1\\i_2\\i_3\end{pmatrix}\\ &+ \frac{M_{SR}}{\sqrt{3}}\\ &\begin{pmatrix}\cos(n_P\theta-\pi/6) & \cos(n_P\theta+\pi/2) & \cos(n_P\theta-5\pi/6)\\ \cos(n_P\theta-5\pi/6) & \cos(n_P\theta-\pi/6) & \cos(n_P\theta+\pi/2)\\ \cos(n_P\theta+\pi/2) & \cos(n_P\theta-5\pi/6) & \cos(n_P\theta-\pi/6)\end{pmatrix}\begin{pmatrix}i_{RX}\\i_{RY}\\i_{RZ}\end{pmatrix}. \qquad (8.16)\end{aligned}$$

Given that $i_1+i_2+i_3=0$,

$$\frac{1}{9}\begin{pmatrix}L_{SW}+2M_{SW} & L_{SW}+2M_{SW} & L_{SW}+2M_{SW}\\ L_{SW}+2M_{SW} & L_{SW}+2M_{SW} & L_{SW}+2M_{SW}\\ L_{SW}+2M_{SW} & L_{SW}+2M_{SW} & L_{SW}+2M_{SW}\end{pmatrix}\begin{pmatrix}i_1\\i_2\\i_3\end{pmatrix}=0. \qquad (8.17)$$

Adding this term to the right-hand side of the previous equation gives

$$\begin{aligned}&\begin{pmatrix}(\psi_{SA}-\psi_{SC})/3\\(\psi_{SB}-\psi_{SA})/3\\(\psi_{SC}-\psi_{SB})/3\end{pmatrix} = \begin{pmatrix}L_{SW}/3 & M_{SW}/3 & M_{SW}/3\\ M_{SW}/3 & L_{SW}/3 & M_{SW}/3\\ M_{SW}/3 & M_{SW}/3 & L_{SW}/3\end{pmatrix}\begin{pmatrix}i_1\\i_2\\i_3\end{pmatrix}\\ &+\frac{M_{SR}}{\sqrt{3}}\begin{pmatrix}\cos(n_P\theta-\pi/6) & \cos(n_P\theta+\pi/2) & \cos(n_P\theta-5\pi/6)\\ \cos(n_P\theta-5\pi/6) & \cos(n_P\theta-\pi/6) & \cos(n_P\theta+\pi/2)\\ \cos(n_P\theta+\pi/2) & \cos(n_P\theta-5\pi/6) & \cos(n_P\theta-\pi/6)\end{pmatrix}\begin{pmatrix}i_{RX}\\i_{RY}\\i_{RZ}\end{pmatrix}. \qquad (8.18)\end{aligned}$$

On the side of the rotor,

$$\frac{d}{dt}\begin{pmatrix}\psi_{RX}\\\psi_{RY}\\\psi_{RZ}\end{pmatrix} = \begin{pmatrix}v_{RX}-R_R i_{RX}\\v_{RY}-R_R i_{RY}\\v_{RZ}-R_R i_{RZ}\end{pmatrix}, \qquad (8.19)$$

and

$$\begin{pmatrix} \psi_{RX} \\ \psi_{RY} \\ \psi_{RZ} \end{pmatrix} = L_{SR}^T(\theta) M_\Delta \begin{pmatrix} i_1 \\ i_2 \\ i_3 \end{pmatrix} + L_{RR} \begin{pmatrix} i_{RX} \\ i_{RY} \\ i_{RZ} \end{pmatrix}$$
$$= \frac{M_{SR}}{\sqrt{3}} \begin{pmatrix} \cos(n_P\theta - \pi/6) & \cos(n_P\theta - 5\pi/6) & \cos(n_P\theta + \pi/2) \\ \cos(n_P\theta + \pi/2) & \cos(n_P\theta - \pi/6) & \cos(n_P\theta - 5\pi/6) \\ \cos(n_P\theta - 5\pi/6) & \cos(n_P\theta + \pi/2) & \cos(n_P\theta - \pi/6) \end{pmatrix} \begin{pmatrix} i_1 \\ i_2 \\ i_3 \end{pmatrix}$$
$$+ L_{RR} \begin{pmatrix} i_{RX} \\ i_{RY} \\ i_{RZ} \end{pmatrix}. \tag{8.20}$$

(8.15), (8.18), (8.19) and (8.20) constitute the electrical model of the machine with a $\Delta$-connected stator.

## 8.4 Equivalence between $Y$ and $\Delta$- connected machines

$YY$ **vs.** $\Delta Y$: the equations describing a machine with a $\Delta$-connected stator and $Y$-connected rotor are the same as those describing a machine with $Y$-connected stator and $Y$-connected rotor if the following substitutions are made.

| Parameters of the $Y$-connected machine | Parameters of the equivalent $Y$-connected machine if the stator is reconnected in $\Delta$ |
|---|---|
| $R_S,\ L_{SW},\ M_{SW}$ | $R_S/3,\ L_{SW}/3,\ M_{SW}/3$ |
| $R_R,\ L_{RW},\ M_{RW}$ | $R_R,\ L_{RW},\ M_{RW}$ |
| $M_{SR}$ | $M_{SR}/\sqrt{3}$ |
| $n_P\theta$ | $n_P\theta - \pi/6$ |

For the additional parameters derived from the winding parameters, the following conversions apply.

| Parameters of the $Y$-connected machine | Parameters of the equivalent $Y$-connected machine if the stator is reconnected in $\Delta$ |
|---|---|
| $R_S,\ L_S$ | $R_S/3,\ L_S/3$ |
| $R_R,\ L_R$ | $R_R,\ L_R$ |
| $M$ | $M/\sqrt{3}$ |
| $n_P\theta$ | $n_P\theta - \pi/6$ |

$YY$ **vs.** $\Delta\Delta$: if the stator and rotor windings of a $Y$-connected machine are reconnected in $\Delta$, the matrix $L_{SR}$ transforms to $M_\Delta^T L_{SR}(\theta) M_\Delta = L_{SR}(\theta)/3$. $L_{RR}$ transforms to $M_\Delta^T L_{RR} M_\Delta = L_{RR}/3$. The machine becomes equivalent to the

$Y$-connected machine if the following adjustments are made to the parameters.

| Parameters of the $Y$-connected machine | Parameters of the equivalent $Y$-connected machine if the stator and rotor are reconnected in $\Delta$ |
|---|---|
| $R_S,\ L_S$ | $R_S/3,\ L_S/3$ |
| $R_R,\ L_R$ | $R_R/3,\ L_R/3$ |
| $M$ | $M/3$ |
| $n_P\theta$ | $n_P\theta$ |

## 8.5 Symbolic code

The code below produces the results of (8.16) and the $L_{SR}(\theta)$ matrix for the $\Delta - \Delta$ connection.

```
%
% Symbolic code for DFIM delta connection
%
syms lss lsw msw lrr lrw mrw lsr msr np th ...
     lssdy lsrdy aux checkzero lsrdd real
%
% Original model
%
a=2*pi/3;
lss=[lsw msw msw;msw lsw msw;msw msw lsw];
lrr=[lrw mrw mrw;mrw lrw mrw;mrw mrw lrw];
lsr=msr*[cos(np*th) cos(np*th+a) cos(np*th-a); ...
    cos(np*th-a) cos(np*th) cos(np*th+a);
    cos(np*th+a) cos(np*th-a) cos(np*th)];
%
% lsr for delta-Y conversion
%
md=[1/3 -1/3 0;0 1/3 -1/3;-1/3 0 1/3];
lssdy=simplify(md'*lss*md)
lsrdy=simplify(md'*lsr)
aux=(msr/sqrt(3))*[cos(np*th-pi/6) cos(np*th+pi/2)
    cos(np*th-5*pi/6);
    cos(np*th-5*pi/6) cos(np*th-pi/6) cos(np*th+pi/2);
    cos(np*th+pi/2) cos(np*th-5*pi/6) cos(np*th-pi/6)];
checkzero=simplify(lsrdy-aux)
%
```

```
% lsr for delta-delta conversion
%
lsrdd=simplify(md'*lsr*md)
checkzero=simplify(lsrdd-lsr/3)
```

# Chapter 9

# Three-Phase Induction Machines with a Two-Phase Rotor

## 9.1 Objective

The objective of this chapter is to derive a model for the machine shown schematically on Fig. 9.1. The stator has three windings that are identical to each other. The rotor has two windings, also identical to each other. The results of this chapter:

- derive a model of the machine.
- show that the machine is equivalent to a two-phase machine if an equal power transformation is used. Otherwise, an extra coefficient appears in the torque equation and the inductance matrix becomes non-symmetric.

## 9.2 Model in phase variables

Define vectors of stator voltages, stator currents, and stator total flux linkages

$$v_S = \begin{pmatrix} v_{SA} \\ v_{SB} \\ v_{SC} \end{pmatrix}, \; i_S = \begin{pmatrix} i_{SA} \\ i_{SB} \\ i_{SC} \end{pmatrix}, \; \psi_S = \begin{pmatrix} \psi_{SA} \\ \psi_{SB} \\ \psi_{SC} \end{pmatrix}. \tag{9.1}$$

Rotor variables are defined as

$$v_R = \begin{pmatrix} v_{RD} \\ v_{RQ} \end{pmatrix}, \; i_R = \begin{pmatrix} i_{RD} \\ i_{RQ} \end{pmatrix}, \; \psi_R = \begin{pmatrix} \psi_{RD} \\ \psi_{RQ} \end{pmatrix}. \tag{9.2}$$

The electrical equations describing the machine are

$$\frac{d\psi_S}{dt} = v_S - R_S i_S, \; \frac{d\psi_R}{dt} = v_R - R_D i_{R,} \tag{9.3}$$

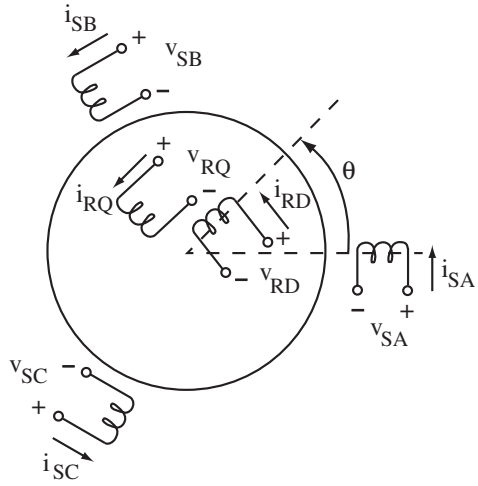


Figure 9.1: Schematic of a machine with a three-phase stator and a two-phase rotor

where $R_S$ is the resistance of a stator winding and $R_D$ is the resistance of a rotor winding.

An explicit model of the machine can be obtained by expressing the total flux linkages as functions of the currents. Based on the geometry of the machine in Fig. 9.1, we assume that

$$\begin{pmatrix} \psi_S \\ \psi_R \end{pmatrix} = L(\theta) \begin{pmatrix} i_S \\ i_R \end{pmatrix}, \; L(\theta) = \begin{pmatrix} L_{SS} & L_{SR}(\theta) \\ L_{SR}^T(\theta) & L_{RR} \end{pmatrix}, \tag{9.4}$$

where

$$L_{SS} = \begin{pmatrix} L_{SW} & M_{SW} & M_{SW} \\ M_{SW} & L_{SW} & M_{SW} \\ M_{SW} & M_{SW} & L_{SW} \end{pmatrix}, \; L_{RR} = \begin{pmatrix} L_D & 0 \\ 0 & L_D \end{pmatrix}, \tag{9.5}$$

and

$$L_{SR}(\theta) = M_D \begin{pmatrix} \cos(n_P\theta) & \cos(n_P\theta + \pi/2) \\ \cos(n_P\theta - 2\pi/3) & \cos(n_P\theta - \pi/6) \\ \cos(n_P\theta + 2\pi/3) & \cos(n_P\theta - 5\pi/6) \end{pmatrix}. \tag{9.6}$$

The variables of the model are:

- $\theta$, the angle of the rotor.
- $n_P$, the number of poles pairs ($n_P = 1$ on Fig. 9.1).

- $L_{SW}$, the self-inductance of a stator winding.
- $M_{SW}$, the mutual inductance between two stator windings.
- $L_D$, the self-inductance of a rotor winding.
- $M_D$, the mutual inductance between a stator winding and a rotor winding when the windings are aligned (e.g., between windings $A$ and $D$ when $\theta = 0$).

Using (9.3) and (9.4), the electrical equations of the machine consist of

$$\begin{aligned}\frac{d}{dt}\begin{pmatrix} i_S \\ i_R \end{pmatrix} &= L^{-1}(\theta)\left(\begin{pmatrix} v_S - R_S i_S \\ v_R - R_D i_R \end{pmatrix}\right. \\ &\quad \left. -\omega \begin{pmatrix} 0 & \partial L_{SR}(\theta)/\partial\theta \\ \partial L_{SR}^T(\theta)/\partial\theta & 0 \end{pmatrix}\begin{pmatrix} i_S \\ i_R \end{pmatrix}\right), \end{aligned} \tag{9.7}$$

where $\omega = d\theta/dt$ is the speed of the machine. Only $L_{SR}(\theta)$ contributes to the torque, so that the general formula for the torque of the machine (1.7) gives

$$\begin{aligned}\tau_M &= i_S^T \frac{\partial L_{SR}(\theta)}{\partial\theta} i_R \\ &= -n_P M_D \\ &\quad ((\sin(n_P\theta) i_{SA} + \sin(n_P\theta - 2\pi/3) i_{SB} + \sin(n_P\theta + 2\pi/3) i_{SC})\, i_{RD}) \\ &\quad + (\sin(n_P\theta + \pi/2) i_{SA} + \sin(n_P\theta - \pi/6) i_{SB} + \sin(n_P\theta - 5\pi/6) i_{SC})\, i_{RQ}). \end{aligned} \tag{9.8}$$

## 9.3 Two-phase equivalent machine

The three-phase machine can be transformed into an equivalent two-phase machine using a three-phase to two-phase transformation (1.8). The rotor variables do not need to be transformed, since the rotor is two-phase. With the transformation, the stator fluxes become

$$\begin{pmatrix} \psi_{Sa} \\ \psi_{Sb} \\ \psi_{Sh} \end{pmatrix} = M_{3-2} L_{SS} M_{3-2}^{-1} \begin{pmatrix} i_{Sa} \\ i_{Sb} \\ i_{Sh} \end{pmatrix} + M_{3-2} L_{SR}(\theta) \begin{pmatrix} i_{RD} \\ i_{RQ} \end{pmatrix}. \tag{9.9}$$

Computing the products (see Section 9.4), one finds that

$$\begin{aligned}\begin{pmatrix} \psi_{Sa} \\ \psi_{Sb} \\ \psi_{Sh} \end{pmatrix} &= \begin{pmatrix} L_S & 0 & 0 \\ 0 & L_S & 0 \\ 0 & 0 & L_{Sh} \end{pmatrix}\begin{pmatrix} i_{Sa} \\ i_{Sb} \\ i_{Sh} \end{pmatrix} \\ &\quad + M \begin{pmatrix} \cos(n_P\theta) & -\sin(n_P\theta) \\ \sin(n_P\theta) & \cos(n_P\theta) \\ 0 & 0 \end{pmatrix}\begin{pmatrix} i_{RD} \\ i_{RQ} \end{pmatrix}, \end{aligned} \tag{9.10}$$

where

$$L_S = L_{SW} - M_{SW},\ L_{Sh} = L_{SW} + 2M_{SW},\ M = \frac{3C_V}{2}M_D. \tag{9.11}$$

In a similar manner, the following equations can obtained for the rotor fluxes

$$\begin{aligned}\begin{pmatrix} \psi_{RD} \\ \psi_{RQ} \end{pmatrix} &= L_{RR}\begin{pmatrix} i_{RD} \\ i_{RQ} \end{pmatrix} + L_{SR}^T(\theta)M_{3-2}^{-1}\begin{pmatrix} i_{Sa} \\ i_{Sb} \\ i_{Sh} \end{pmatrix} \\ &= \begin{pmatrix} L_D & 0 \\ 0 & L_D \end{pmatrix}\begin{pmatrix} i_{RD} \\ i_{RQ} \end{pmatrix} \\ &\quad + M\ C_P^{-1}\begin{pmatrix} \cos(n_P\theta) & \sin(n_P\theta) & 0 \\ -\sin(n_P\theta) & \cos(n_P\theta) & 0 \end{pmatrix}\begin{pmatrix} i_{Sa} \\ i_{Sb} \\ i_{Sh} \end{pmatrix}. \end{aligned} \tag{9.12}$$

Due to the fact that the three-phase to two-phase transformation is linear and independent of time, the transformed stator variables satisfy electrical equations similar to the three-phase variables, and with identical stator resistances. Specifically

$$\frac{d}{dt}\begin{pmatrix} \psi_{Sa} \\ \psi_{Sb} \\ \psi_{Sh} \end{pmatrix} = \begin{pmatrix} v_{Sa} - R_S i_{Sa} \\ v_{Sb} - R_S i_{Sb} \\ v_{Sh} - R_S i_{Sh} \end{pmatrix}. \tag{9.13}$$

Therefore, the two-phase variables satisfy

$$\frac{d}{dt}\left(L_2(\theta)\begin{pmatrix} i_{Sa} \\ i_{Sb} \\ i_{RD} \\ i_{RQ} \end{pmatrix}\right) = \begin{pmatrix} v_{Sa} - R_S\ i_{Sa} \\ v_{Sb} - R_S\ i_{Sb} \\ v_{RD} - R_D\ i_{RD} \\ v_{RQ} - R_D\ i_{RQ} \end{pmatrix}, \tag{9.14}$$

with $L_2(\theta)$ given by

$$L_2(\theta) = \begin{pmatrix} L_S & 0 \\ 0 & L_S \\ M\ C_P^{-1}\cos(n_P\theta) & M\ C_P^{-1}\sin(n_P\theta) \\ -M\ C_P^{-1}\sin(n_P\theta) & M\ C_P^{-1}\cos(n_P\theta) \\ M\cos(n_P\theta) & -M\sin(n_P\theta) \\ M\sin(n_P\theta) & M\cos(n_P\theta) \\ L_D & 0 \\ 0 & L_D \end{pmatrix}. \tag{9.15}$$

The torque is equal to

$$\begin{aligned}\tau_M &= \begin{pmatrix} i_{Sa} & i_{Sb} & i_{Sh} \end{pmatrix}\left(M_{3-2}^{-1}\right)^T \frac{\partial L_{SR}(\theta)}{\partial\theta} i_R \\ &= n_P M\ C_P^{-1}\ (-\sin(n_P\theta)i_{RD}i_{Sa} - \cos(n_P\theta)i_{RQ}i_{Sa} \\ &\quad \cos(n_P\theta)i_{RD}i_{Sb} - \sin(n_P\theta)i_{RQ}i_{Sb}). \end{aligned} \tag{9.16}$$

Equations (9.14), (9.15), and (9.16) are the same as the equations defining a two-phase machine with windings $a$, $b$, $D$, and $Q$ when $C_P = 1$, i.e., for the equal power 3-2 transformation. For other transformations, the equations are similar, but an extra factor $C_P^{-1}$ must be included in the torque and in the inductance matrix, which ceases to be symmetric.

For the homopolar variables

$$L_{Sh}\frac{di_{Sh}}{dt} = v_{Sh} - R_S i_{Sh}. \tag{9.17}$$

The variables with the subscript $h$ (called homopolar variables) satisfy the equation of a stable first-order system that is independent of the equations for the two-phase variables. The homopolar variables do not affect the torque and are independent of the main two-phase variables.

## 9.4 Symbolic code

The code below produces the results of (9.10), (9.12), and (9.16).

```
%
% Symbolic code for DFIM with 3-ph stator and 2-ph rotor
%
syms lss lsw msw lrr ld lsr md np th m3to2 cv ...
     l2ss l2sr l2rs is2 isa isb ish ir ird irq tm real
%
% Original model
%
a=2*pi/3;b=pi/2;
lss=[lsw msw msw;msw lsw msw;msw msw lsw];
lrr=[ld 0;0 ld];
lsr=md*[cos(np*th) cos(np*th+b) ; cos(np*th-a) cos(np*th-a+b);
    cos(np*th+a) cos(np*th+a+b)];
%
% 2-phase equivalent model
%
m3to2=cv*[1 -1/2 -1/2;0 sqrt(3)/2 -sqrt(3)/2;1/sqrt(2) ...
    1/sqrt(2) 1/sqrt(2)];
l2ss=simplify(m3to2*lss*inv(m3to2))
l2sr=simplify(m3to2*lsr)
l2rs=simplify(lsr'*inv(m3to2))
```

```
is2=[isa;isb;ish];ir=[ird;irq];
tm=simplify(is2'*inv(m3to2)'*diff(lsr,th)*ir)
```

# Chapter 10

# Three-Phase Induction Machines with Single-Phase Excitation

## 10.1 Objective

The objective of this chapter is to consider several problems where a single-phase supply is applied to three-phase machines. The results show that:

- a three-phase rotor with line-to-line excitation is equivalent to a single-phase rotor.
- the voltage induced on the stator applying a constant line-to-line rotor current at non-zero speed or applying a sinusoidal current at standstill can be used to determine the mutual inductance parameter of a doubly-fed induction machine.
- a three-phase rotor with line-to-2 line excitation is equivalent to a two-phase rotor with one phase excited and the other phase short-circuited.

## 10.2 Single-phase line-to-line excitation on a three-phase rotor

Consider the model of a machine with a three-phase rotor derived in Section 3.2. Assume that single-phase excitation is applied to the rotor from winding $Y$ to winding $Z$, with winding $X$ left open. Let $v_{RQ}$ and $i_{RQ}$ be the voltage and the current applied to the rotor in this manner. Then

$$v_{RY} - v_{RZ} = v_{RQ},\ i_{RX} = 0,\ i_{RY} = -i_{RZ} = i_{RQ}. \tag{10.1}$$

The expressions for the stator fluxes (3.4)-(3.6) give (see Section 10.5),

$$\begin{aligned}\psi_S &= L_{SS}i_S + L_{SR}(\theta)\begin{pmatrix}0\\1\\-1\end{pmatrix} i_{RQ}\\ &= L_{SS}i_S + M_D\begin{pmatrix}\cos(n_P\theta+\pi/2)\\ \cos(n_P\theta-\pi/6)\\ \cos(n_P\theta-5\pi/6)\end{pmatrix} i_{RQ},\end{aligned} \tag{10.2}$$

where $M_D = \sqrt{3}M_{SR}$. On the side of the rotor, let

$$\psi_{RQ} = \psi_{RY} - \psi_{RZ}, \tag{10.3}$$

so that

$$\begin{aligned}\psi_{RQ} &= \begin{pmatrix}0 & 1 & -1\end{pmatrix} L_{SR}^T(\theta) i_S + \begin{pmatrix}0 & 1 & -1\end{pmatrix} L_{RR}\begin{pmatrix}0\\1\\-1\end{pmatrix} i_{RQ}\\ &= M_D\begin{pmatrix}\cos(n_P\theta+\pi/2) & \cos(n_P\theta-\pi/6) & \cos(n_P\theta-5\pi/6)\end{pmatrix} i_S\\ &+ L_D i_{RQ},\end{aligned} \tag{10.4}$$

where $L_D = 2(L_{RW} - M_{RW})$. Also

$$\begin{aligned}\frac{d\psi_{RQ}}{dt} &= \begin{pmatrix}0 & 1 & -1\end{pmatrix}\left(v_R - R_R\begin{pmatrix}0\\1\\-1\end{pmatrix} i_{RQ}\right)\\ &= v_{RQ} - R_D i_{RQ},\end{aligned} \tag{10.5}$$

where $R_D = 2R_R$.

The characteristics are the same as those of the machine with a two-phase rotor of Section 9.2, where the $D$ winding is open ($i_{RD} = 0$) and the $Q$ winding is connected to a supply. The total rotor flux linkages are

$$\psi_{RD} = \psi_{RX},\ \psi_{RQ} = \psi_{RY} - \psi_{RZ}, \tag{10.6}$$

but the differential equation for $\psi_{RD}$ can be omitted since there is no associated current in the $D$ axis ($i_{RD} = 0$). Parameters are converted using

$$R_D = 2R_R,\ L_D = 2(L_{RW} - M_{RW}) = 2L_R,\ M_D = \sqrt{3}M_{SR} = \frac{2}{\sqrt{3}}M. \tag{10.7}$$

As expected, the line-to-line resistance and the line-to-line inductance are 2 times the winding resistance and the winding inductance, respectively

## 10.3 Open-stator response with line-to-line rotor excitation

With an open stator, the stator currents are zero and (10.5) gives

$$\psi_S = M_D \begin{pmatrix} \cos(n_P\theta + \pi/2) \\ \cos(n_P\theta - \pi/6) \\ \cos(n_P\theta - 5\pi/6) \end{pmatrix} i_{RQ}. \tag{10.8}$$

Therefore

$$\begin{aligned} \psi_{SA} - \psi_{SB} &= \sqrt{3} M_D \cos(n_P\theta + 2\pi/3) i_{RQ} \\ &= 2M \cos(n_P\theta + 2\pi/3) i_{RQ}. \end{aligned} \tag{10.9}$$

The line-to-line voltage is

$$\begin{aligned} v_{AB} &= v_{SA} - v_{SB} = \frac{d\psi_{SA}}{dt} - \frac{d\psi_{SB}}{dt} \\ &= 2M \cos(n_P\theta + 2\pi/3) \frac{di_{RQ}}{dt} - 2n_P\omega M \sin(n_P\theta + 2\pi/3) i_{RQ}. \end{aligned} \tag{10.10}$$

The result can be used to measure $M$ as follows:

1. The machine rotates at constant speed $\omega$ with a DC current $I_{DC}$ applied line-to-line to the rotor. The induced line-to-line stator voltage is a sinusoid of frequency $\omega_S = n_P\omega$ and peak magnitude

$$V_{pk} = 2\omega_S M \; I_{DC}. \tag{10.11}$$

2. The machine is at standstill with a sinusoidal rotor current of frequency $\omega_S$ and peak magnitude $I_{pk}$

$$i_{RQ} = I_{pk} \sin(\omega_S t). \tag{10.12}$$

Then,

$$v_{AB} = 2\omega_S M \cos(n_P\theta + 2\pi/3) I_{pk} \sin(\omega_S t). \tag{10.13}$$

3. Note that

$$\begin{aligned} v_{BC} &= 2\omega_S M \cos(n_P\theta) I_{pk} \sin(\omega_S t) \\ v_{CA} &= 2\omega_S M \cos(n_P\theta - 2\pi/3) I_{pk} \sin(\omega_S t). \end{aligned} \tag{10.14}$$

If the rotor is moved so that the largest voltage is observed between two lines of the stator (so that $n_P\theta + 2\pi/3 = 0$), the peak magnitude of the line-to-line voltage is

$$V_{pk} = 2\omega_S M\ I_{pk}. \tag{10.15}$$

If the rotor is turned until $v_{BC} = 0$ (obtained for $n_P\theta = \pi/2$), the peak magnitude of the line-to-line voltage $v_{AB}$ is

$$V_{pk} = 2\omega_S M\,|\cos(7\pi/6)|\,I_{pk} = \sqrt{3}\omega_S M\ I_{pk}. \tag{10.16}$$

$V_{pk}$ is the same as the peak voltage for $v_{CA}$. The second procedure may be preferable because it is more precise to align the rotor using a zero crossing than using a maximum.

## 10.4 Single-phase line-to-2 line excitation on a three-phase rotor

Assume that single-phase excitation is applied to the rotor from winding $X$ to windings $Y$ and $Z$ tied together. Let $v_{RD}$ and $i_{RD}$ be the voltage and the current applied to the rotor in this manner. Then

$$v_{RX} - v_{RY} = v_{RD},\ v_{RY} = v_{RZ},\ i_{RX} = -(i_{RY} + i_{RZ}) = i_{RD}. \tag{10.17}$$

Let

$$i_{RQ} = (i_{RY} - i_{RZ})/\sqrt{3}. \tag{10.18}$$

Then,

$$i_{RY} = \frac{-i_{RD} + \sqrt{3}i_{RQ}}{2},\ i_{RZ} = \frac{-i_{RD} - \sqrt{3}i_{RQ}}{2}. \tag{10.19}$$

Overall

$$\begin{pmatrix} i_{RX} \\ i_{RY} \\ i_{RZ} \end{pmatrix} = M_{L2L} \begin{pmatrix} i_{RD} \\ i_{RQ} \end{pmatrix},\ \text{where } M_{L2L} = \begin{pmatrix} 1 & 0 \\ -1/2 & \sqrt{3}/2 \\ -1/2 & -\sqrt{3}/2 \end{pmatrix}. \tag{10.20}$$

The expressions for the stator fluxes (3.4)-(3.6) become

$$\begin{aligned} \psi_S &= L_{SS} i_S + L_{SR}(\theta) M_{L2L} \begin{pmatrix} i_{RD} \\ i_{RQ} \end{pmatrix} \\ &= L_{SS} i_S + M_D \begin{pmatrix} \cos(n_P\theta) & \cos(n_P\theta + \pi/2) \\ \cos(n_P\theta - 2\pi/3) & \cos(n_P\theta - \pi/6) \\ \cos(n_P\theta + 2\pi/3) & \cos(n_P\theta - 5\pi/6) \end{pmatrix} \begin{pmatrix} i_{RD} \\ i_{RQ} \end{pmatrix}. \end{aligned} \tag{10.21}$$

where $M_D = (3/2)M_{SR} = M$. On the side of the rotor, let

$$\begin{pmatrix} \psi_{RD} \\ \psi_{RQ} \end{pmatrix} = M_{L2L}^T \begin{pmatrix} \psi_{RX} \\ \psi_{RY} \\ \psi_{RZ} \end{pmatrix}, \tag{10.22}$$

so that

$$\begin{aligned} \begin{pmatrix} \psi_{RD} \\ \psi_{RQ} \end{pmatrix} &= M_{L2L}^T L_{SR}^T(\theta) i_S + M_{L2L}^T L_{RR} M_{L2L} \begin{pmatrix} i_{RD} \\ i_{RQ} \end{pmatrix} \\ &= M_D \begin{pmatrix} \cos(n_P\theta) & \cos(n_P\theta - 2\pi/3) & \cos(n_P\theta + 2\pi/3) \\ \cos(n_P\theta + \pi/2) & \cos(n_P\theta - \pi/6) & \cos(n_P\theta - 5\pi/6) \end{pmatrix} i_S \\ &\quad + \begin{pmatrix} L_D & 0 \\ 0 & L_Q \end{pmatrix} \begin{pmatrix} i_{RD} \\ i_{RQ} \end{pmatrix}, \end{aligned} \tag{10.23}$$

where $L_D = L_Q = (3/2)(L_{RW} - M_{RW}) = (3/2)L_R$. Also,

$$\begin{aligned} \frac{d}{dt} \begin{pmatrix} \psi_{RD} \\ \psi_{RQ} \end{pmatrix} &= M_{L2L}^T \left( v_R - R_R i_R \right) \\ &= \begin{pmatrix} v_{RD} \\ 0 \end{pmatrix} - R_R M_{L2L}^T M_{L2L} \begin{pmatrix} i_{RD} \\ i_{RQ} \end{pmatrix} \\ &= \begin{pmatrix} v_{RD} - R_D i_{RD} \\ -R_Q i_{RQ} \end{pmatrix}, \end{aligned} \tag{10.24}$$

where $R_D = R_Q = (3/2)R_R$.

The characteristics are the same as those of the machine with a two-phase rotor in Section 9.2, with the $D$ winding connected to the supply and the $Q$ winding short-circuited ($v_{RQ} = v_{RY} - v_{RZ} = 0$). Parameters are converted using $R_D = (3/2)R_R$, $L_D = (3/2)(L_{RW} - M_{RW}) = (3/2)L_R$, and $M_D = (3/2)M_{SR} = M$. As expected, the line-to-2 line resistance and the line-to-2 line inductance are 1.5 times the winding resistance and the winding inductance. The parameter $M_D$ is smaller than in the line-to-line connection. Thus, the stator voltage induced for a given rotor current is smaller for the line-to-2 line connection than for the line-to-line connection. Note that the transformation using $M_{L2L}$ is similar to the equal vector $3-2$ transformation, but it represents here a physical connection of the machine, as opposed to an algebraic definition.

## 10.5 Symbolic code

The code below produces the results of (10.2), (10.4), (10.21), and (10.23).

```
%
% Symbolic code for DFIM with single-phase excitation
```

```
%
syms lsr msr np th lrr lrw mrw lsrll lrrll lsrl2l lrrl2l real
%
% Original model
%
a=2*pi/3;
lsr=msr*[cos(np*th) cos(np*th+a) cos(np*th-a); ...
    cos(np*th-a) cos(np*th) cos(np*th+a);
    cos(np*th+a) cos(np*th-a) cos(np*th)];
lrr=[lrw mrw mrw;mrw lrw mrw;mrw mrw lrw];
%
% Line-to-line excitation
%
lsrll=simplify(lsr*[0;1;-1])
lrrll=simplify([0 1 -1]*lrr*[0;1;-1])
%
% Line-to-2 line excitation
%
ml2l=[1 0;-1/2 sqrt(3)/2;-1/2 -sqrt(3)/2];
lsrl2l=simplify(lsr*ml2l)
lrrl2l=simplify(ml2l'*lrr*ml2l)
```

# Chapter 11

# Non-Symmetric 2-Phase Induction Machines

## 11.1 Objective

The objective of this chapter is to obtain a model for the two-phase induction machine shown in Fig. 11.1, where the rotor windings are assumed to be identical, but the stator windings are different from each other. The configuration arises with capacitor-start single-phase induction motors, or with generators using these machines [18]. The results of the chapter:

- give a model of the machine in phase variables.
- derive a simpler model in stator coordinates.
- show that a special configuration of a three-phase machine is equivalent to a non-symmetric two-phase machine.

## 11.2 Model in phase variables

Define vectors of stator voltages, stator currents, and stator total flux linkages

$$v_S = \begin{pmatrix} v_{SA} \\ v_{SB} \end{pmatrix},\ i_S = \begin{pmatrix} i_{SA} \\ i_{SB} \end{pmatrix},\ \psi_S = \begin{pmatrix} \psi_{SA} \\ \psi_{SB} \end{pmatrix}. \tag{11.1}$$

Rotor variables are defined as

$$v_R = \begin{pmatrix} v_{RX} \\ v_{RY} \end{pmatrix},\ i_R = \begin{pmatrix} i_{RX} \\ i_{RY} \end{pmatrix},\ \psi_R = \begin{pmatrix} \psi_{RX} \\ \psi_{RY} \end{pmatrix}. \tag{11.2}$$

The electrical equations describing the machine are

$$\frac{d\psi_S}{dt} = v_S - \begin{pmatrix} R_A & 0 \\ 0 & R_B \end{pmatrix} i_S,\ \frac{d\psi_R}{dt} = v_R - R_R i_{R,} \tag{11.3}$$

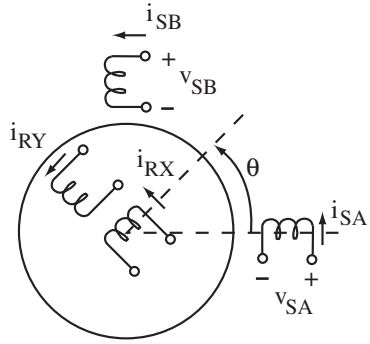


Figure 11.1: Two-phase induction motor

where $R_A$, $R_B$ are the resistances of the stator windings, and $R_R$ is the resistance of the rotor windings.

Based on the geometry of the motor, we assume that the total flux linkages have the form

$$\begin{pmatrix} \psi_S \\ \psi_R \end{pmatrix} = L(\theta) \begin{pmatrix} i_S \\ i_R \end{pmatrix}, \tag{11.4}$$

where

$$L(\theta) = \begin{pmatrix} L_{SS} & L_{SR}(\theta) \\ L_{SR}^T(\theta) & L_{RR} \end{pmatrix}, \tag{11.5}$$

and

$$\begin{aligned} L_{SS} &= \begin{pmatrix} L_A & 0 \\ 0 & L_B \end{pmatrix}, \; L_{RR} = \begin{pmatrix} L_R & 0 \\ 0 & L_R \end{pmatrix} \\ L_{SR}(\theta) &= \begin{pmatrix} M_A \cos(n_P\theta) & -M_A \sin(n_P\theta) \\ M_B \sin(n_P\theta) & M_B \cos(n_P\theta) \end{pmatrix}. \end{aligned} \tag{11.6}$$

The self-inductances of the stator and rotor windings are denoted $L_A$, $L_B$, and $L_R$, respectively. The mutual inductances between stator and rotor windings, when aligned, are denoted $M_A$ and $M_B$. It is assumed that there is no mutual inductance between stator windings $A$ and $B$, as well as between rotor windings $X$ and $Y$.

The electrical equations of the machine are

$$\frac{d}{dt}\left( L(\theta) \begin{pmatrix} i_{SA} \\ i_{SB} \\ i_{RX} \\ i_{RY} \end{pmatrix} \right) = \begin{pmatrix} v_{SA} - R_A i_{SA} \\ v_{SB} - R_B i_{SB} \\ v_{RX} - R_R i_{RX} \\ v_{RY} - R_R i_{RY} \end{pmatrix}. \tag{11.7}$$

An explicit model is

$$\frac{d}{dt}\begin{pmatrix} i_{SA} \\ i_{SB} \\ i_{RX} \\ i_{RY} \end{pmatrix} = L^{-1}(\theta)\left(\begin{pmatrix} v_{SA} - R_A i_{SA} \\ v_{SB} - R_B i_{SB} \\ v_{RX} - R_R i_{RX} \\ v_{RY} - R_R i_{RY} \end{pmatrix} + n_P\omega \begin{pmatrix} M_A\left(i_{RX}\sin(n_P\theta) + i_{RY}\cos(n_P\theta)\right) \\ M_B\left(-i_{RX}\cos(n_P\theta) + i_{RY}\sin(n_P\theta)\right) \\ M_A i_{SA}\sin(n_P\theta) - M_B i_{SB}\cos(n_P\theta) \\ M_A i_{SA}\cos(n_P\theta) + M_B i_{SB}\sin(n_P\theta) \end{pmatrix}\right). \tag{11.8}$$

The general formula for the torque of an electric machine (1.7) gives

$$\begin{aligned} \tau_M &= \begin{pmatrix} i_{SA} & i_{SB} \end{pmatrix} \frac{\partial L_{SR}(\theta)}{\partial\theta} \begin{pmatrix} i_{RX} \\ i_{RY} \end{pmatrix} \\ &= -n_P M_A i_{SA}\ \left(i_{RX}\sin(n_P\theta) + i_{RY}\ \cos(n_P\theta)\right) \\ &\quad +n_P M_B i_{SB}\ \left(i_{RX}\cos(n_P\theta) - i_{RY}\sin(n_P\theta)\right). \end{aligned} \tag{11.9}$$

## 11.3 Model in stator coordinates

The rotor currents may be expressed in a coordinate frame attached to the stator, so that

$$\begin{pmatrix} i_{RA} \\ i_{RB} \end{pmatrix} = U^T(\theta)\begin{pmatrix} i_{RX} \\ i_{RY} \end{pmatrix}, \tag{11.10}$$

where

$$U^T(\theta) = \begin{pmatrix} \cos(n_P\theta) & -\sin(n_P\theta) \\ \sin(n_P\theta) & \cos(n_P\theta) \end{pmatrix}. \tag{11.11}$$

Then, (11.4)-(11.6) give

$$\begin{aligned} \psi_{SA} &= L_A i_{SA} + M_A i_{RA} \\ \psi_{SB} &= L_B i_{SB} + M_B i_{RB} \end{aligned} \tag{11.12}$$

and

$$\begin{aligned} L_A\frac{d}{dt}i_{SA} + M_A\frac{d}{dt}i_{RA} &= v_{SA} - R_A\ i_{SA} \\ L_B\frac{d}{dt}i_{SB} + M_B\frac{d}{dt}i_{RB} &= v_{SB} - R_B\ i_{SB}. \end{aligned} \tag{11.13}$$

On the rotor side

$$\begin{aligned} \begin{pmatrix} \psi_{RA} \\ \psi_{RB} \end{pmatrix} &= U^T(\theta)\begin{pmatrix} \psi_{RX} \\ \psi_{RY} \end{pmatrix} \\ &= U^T(\theta)L_{SR}^T(\theta)\begin{pmatrix} i_{SA} \\ i_{SB} \end{pmatrix} + U^T(\theta)L_{RR}\begin{pmatrix} i_{RX} \\ i_{RY} \end{pmatrix}, \end{aligned} \tag{11.14}$$

which gives

$$\begin{aligned} \psi_{RA} &= M_A i_{SA} + L_R i_{RA} \\ \psi_{RB} &= M_B i_{SB} + L_R i_{RB}. \end{aligned} \tag{11.15}$$

For the time derivative

$$\begin{aligned} \frac{d}{dt}\begin{pmatrix} \psi_{RA} \\ \psi_{RB} \end{pmatrix} &= U^T(\theta)\frac{d}{dt}\begin{pmatrix} \psi_{RX} \\ \psi_{RY} \end{pmatrix} + \frac{d}{dt}\left(U^T(\theta)\right)\begin{pmatrix} \psi_{RX} \\ \psi_{RY} \end{pmatrix} \\ &= U^T(\theta)\begin{pmatrix} v_{RX} \\ v_{RY} \end{pmatrix} - R_R U^T(\theta)\begin{pmatrix} i_{RX} \\ i_{RY} \end{pmatrix} \\ &\quad + n_P\omega\begin{pmatrix} 0 & -1 \\ 1 & 0 \end{pmatrix} U^T(\theta)\begin{pmatrix} \psi_{RX} \\ \psi_{RY} \end{pmatrix} \\ &= \begin{pmatrix} v_{RA} - R_R i_{RA} - n_P\omega\psi_{RB} \\ v_{RB} - R_R i_{RB} + n_P\omega\psi_{RA} \end{pmatrix}. \end{aligned} \tag{11.16}$$

Combining (11.15) and (11.16)

$$\begin{aligned} \frac{d}{dt}\psi_{RA} = M_A\frac{d}{dt}i_{SA} + L_R\frac{d}{dt}i_{RA} = v_{RA} - R_R i_{RA} - n_P\omega(M_B i_{SB} + L_R i_{RB}) \\ \frac{d}{dt}\psi_{RB} = M_B\frac{d}{dt}i_{SB} + L_R\frac{d}{dt}i_{RB} = v_{RB} - R_R i_{RB} + n_P\omega(M_A i_{SA} + L_R i_{RA}). \end{aligned} \tag{11.17}$$

**Overall model:** the electrical equations of the machine become

$$\begin{aligned} &\begin{pmatrix} L_A & 0 & M_A & 0 \\ 0 & L_B & 0 & M_B \\ M_A & 0 & L_R & 0 \\ 0 & M_B & 0 & L_R \end{pmatrix}\frac{d}{dt}\begin{pmatrix} i_{SA} \\ i_{SB} \\ i_{RA} \\ i_{RB} \end{pmatrix} \\ &= \begin{pmatrix} v_{SA} - R_A\, i_{SA} \\ v_{SB} - R_B\, i_{SB} \\ v_{RA} - R_R\, i_{RA} - n_P\omega\,(M_B i_{SB} + L_R i_{RB}) \\ v_{RB} - R_R\, i_{RB} + n_P\omega\,(M_A i_{SA} + L_R i_{RA}) \end{pmatrix}. \end{aligned} \tag{11.18}$$

The torque (11.9) becomes

$$\tau_M = n_P\ \left(M_B i_{SB} i_{RA} - M_A i_{SA} i_{RB}\right). \tag{11.19}$$

## 11.4 Three-phase machine as a non-symmetric two-phase machine

Consider a three-phase induction machine with a stator connection as shown on Fig. 11.2. Note that one must have access to the individual windings for this

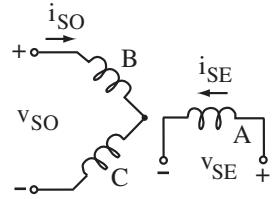


Figure 11.2: Three-phase machine operated as a two-phase machine

implementation, or to the neutral if the machine is $Y$-connected. The configuration has been considered for power generation, where excitation is applied at the terminal with voltage $v_{SE}$ and current $i_{SE}$, and power is produced at the terminal with voltage $v_{SO}$ and current $i_{SO}$ [11].

The connection is such that

$$\left( \begin{array}{c} v_{SE} \\ v_{SO} \end{array} \right) = \left( \begin{array}{c} v_{SA} \\ v_{SB} - v_{SC} \end{array} \right), \left( \begin{array}{c} i_{SE} \\ i_{SO} \end{array} \right) = \left( \begin{array}{c} i_{SA} \\ i_{SB} \end{array} \right), \; i_{SC} = -i_{SB}. \tag{11.20}$$

Define

$$v_T = \left( \begin{array}{c} v_{SE} \\ v_{SO} \end{array} \right), i_T = \left( \begin{array}{c} i_{SE} \\ i_{SO} \end{array} \right). \tag{11.21}$$

With $v_S$ and $i_S$ denoting the vectors of stator voltages and currents of the three-phase machine, one has that

$$v_T = M_1 v_S, \; i_T = M_2 i_S, \tag{11.22}$$

where

$$M_1 = \left( \begin{array}{ccc} 1 & 0 & 0 \\ 0 & 1 & -1 \end{array} \right), M_2 = \left( \begin{array}{ccc} 1 & 0 & 0 \\ 0 & 1 & 0 \end{array} \right). \tag{11.23}$$

Given that $i_{SC} = -i_{SB}$, one also has that

$$i_S = M_1^T i_T. \tag{11.24}$$

Chapter 9 showed that three-phase and two-phase rotors were equivalent. Modeling the squirrel-cage rotor as a two-phase rotor for convenience (with $v_R = 0$),

$$\frac{d}{dt} \left( \left( \begin{array}{cc} L_{SS} & L_{SR}(\theta) \\ L_{SR}^T(\theta) & L_{RR} \end{array} \right) \left( \begin{array}{c} i_S \\ i_R \end{array} \right) \right) = \left( \begin{array}{c} v_S - R_S i_S \\ -R_D i_R \end{array} \right), \tag{11.25}$$

where the inductance matrices are given by (9.5) and (9.6). Multiplying the first line of (11.25) by $M_1$, and using (11.22) with (11.24), the equations transform to

$$\frac{d}{dt}\left(\begin{pmatrix} M_1 L_{SS} M_1^T & M_1 L_{SR}(\theta) \\ L_{SR}^T(\theta) M_1^T & L_{RR} \end{pmatrix} \begin{pmatrix} i_T \\ i_R \end{pmatrix}\right) = \begin{pmatrix} v_T - M_1 R_S M_1^T i_T \\ -R_D i_R \end{pmatrix}. \tag{11.26}$$

Computing the expressions and returning to the components of the vectors, one finds that

$$\frac{d}{dt}\left(L_2(\theta)\begin{pmatrix} i_{SE} \\ i_{SO} \\ i_{RD} \\ i_{RQ} \end{pmatrix}\right) = \begin{pmatrix} v_{SE} - R_S\, i_{SE} \\ v_{SO} - 2R_S\, i_{SO} \\ -R_D\, i_{RD} \\ -R_D\, i_{RQ} \end{pmatrix}, \tag{11.27}$$

where

$$L_2(\theta) = \begin{pmatrix} L_{SW} & 0 & M_D\cos(n_P\theta) & -M_D\sin(n_P\theta) \\ 0 & 2(L_{SW}-M_{SW}) & \sqrt{3}M_D\sin(n_P\theta) & \sqrt{3}M_D\cos(n_P\theta) \\ M_D\cos(n_P\theta) & \sqrt{3}M_D\sin(n_P\theta) & L_D & 0 \\ -M_D\sin(n_P\theta) & \sqrt{3}M_D\cos(n_P\theta) & 0 & L_D \end{pmatrix}. \tag{11.28}$$

The equations of the machine are the same as those of the non-symmetric two-phase machine (11.5), (11.6), (11.7), if one replaces $E$, $O$, $D$, $Q$ by $A$, $B$, $X$, $Y$, $L_2(\theta)$ by $L(\theta)$, and use the parameters

$$\begin{aligned} R_A &= R_S,\ R_B = 2R_S,\ L_A = L_{SW},\ L_B = 2(L_{SW} - M_{SW}), \\ M_A &= M_D,\ M_B = \sqrt{3}M_D,\ R_R = R_D,\ L_R = L_D. \end{aligned} \tag{11.29}$$

## 11.5 Symbolic code

The code below produces the results of (11.28).

```
%
% Symbolic code for a 3-phase induction machine
% operated as a 2-phase machine
%
syms lss lsw msw lrr ld lsr md np th rs l2ss l2sr r2s real
%
```

```
% Original model
%
a=2*pi/3;b=pi/2;
lss=[lsw msw msw;msw lsw msw;msw msw lsw];
lrr=[ld 0;0 ld];
lsr=md*[cos(np*th) cos(np*th+b); ...
        cos(np*th-a) cos(np*th-a+b); ...
        cos(np*th+a) cos(np*th+a+b)];
%
% Transformed model
%
m1=[1 0 0;0 1 -1];
m2=[1 0 0;0 1 0];
l2ss=simplify(m1*lss*m1'),
l2sr=simplify(m1*lsr),
r2s=simplify(m1*rs*m1'),
```

# Chapter 12

# Hybrid Motor

## 12.1 Objective

The objective of this chapter is to derive a model for the hybrid motor shown in Fig. 12.1. The motor is a two-phase permanent magnet synchronous motor with reluctance torque. The schematic is also representative of *interior permanent magnet motors* (IPM). The results of the chapter:

- give a model of the machine in phase variables.
- derive a model in DQ variables.

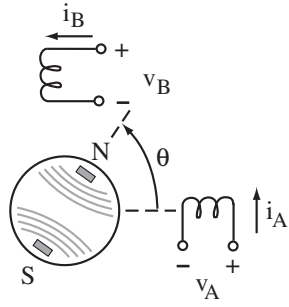


Figure 12.1: Hybrid motor

## 12.2 Model in phase variables

The model of the motor is

$$\frac{d\psi_A}{dt} = v_A - Ri_A, \ \frac{d\psi_B}{dt} = v_B - Ri_B. \tag{12.1}$$

According to (1.2), assume that

$$\begin{pmatrix} \psi_A \\ \psi_B \end{pmatrix} = \psi_0 D(\theta) + L(\theta) \begin{pmatrix} i_A \\ i_B \end{pmatrix}, \tag{12.2}$$

where $\psi_0$ is the flux linkage in a winding due to the PM when the magnet is aligned with the winding, and

$$D(\theta) = \begin{pmatrix} \cos(n_P\theta) \\ \sin(n_P\theta) \end{pmatrix}. \tag{12.3}$$

Using (2.21),

$$L(\theta) = \begin{pmatrix} L_0 + L_1\cos(2n_P\theta) & L_1\sin(2n_P\theta) \\ L_1\sin(2n_P\theta) & L_0 - L_1\cos(2n_P\theta) \end{pmatrix}, \tag{12.4}$$

for some $L_0 > L_1 > 0$.

The model can be expressed as

$$L(\theta)\frac{d}{dt}\begin{pmatrix} i_A \\ i_B \end{pmatrix} = \begin{pmatrix} v_A - Ri_A \\ v_B - Ri_B \end{pmatrix} - \omega\psi_0\frac{\partial D(\theta)}{\partial\theta} - \omega\frac{\partial L(\theta)}{\partial\theta}\begin{pmatrix} i_A \\ i_B \end{pmatrix}, \tag{12.5}$$

where

$$\begin{aligned} \frac{\partial D(\theta)}{\partial\theta} &= n_P\begin{pmatrix} -\sin(n_P\theta) \\ \cos(n_P\theta) \end{pmatrix} \\ \frac{\partial L(\theta)}{\partial\theta} &= 2n_P L_1\begin{pmatrix} -\sin(2n_P\theta) & \cos(2n_P\theta) \\ \cos(2n_P\theta) & \sin(2n_P\theta) \end{pmatrix}. \end{aligned} \tag{12.6}$$

Using (1.7), the torque is

$$\begin{aligned} \tau_M &= \psi_0\begin{pmatrix} i_A & i_B \end{pmatrix}\frac{\partial D(\theta)}{\partial\theta} + \frac{1}{2}\begin{pmatrix} i_A & i_B \end{pmatrix}\frac{\partial L(\theta)}{\partial\theta}\begin{pmatrix} i_A \\ i_B \end{pmatrix} \\ &= -Ki_A\sin(n_P\theta) + Ki_B\cos(n_P\theta) \\ &\quad + n_P L_1\left(\left(-i_A^2 + i_B^2\right)\sin(2n_P\theta) + 2i_A i_B\cos(2n_P\theta)\right), \end{aligned} \tag{12.7}$$

where $K = n_P\psi_0$.

## 12.3 Model in DQ variables

The DQ model is obtained using the DQ transformation

$$\begin{pmatrix} \psi_d \\ \psi_q \end{pmatrix} = U(\theta)\begin{pmatrix} \psi_A \\ \psi_B \end{pmatrix}, \tag{12.8}$$

where

$$U(\theta) = \begin{pmatrix} \cos(n_P\theta) & \sin(n_P\theta) \\ -\sin(n_P\theta) & \cos(n_P\theta) \end{pmatrix}. \tag{12.9}$$

The inverse transformation is

$$\begin{pmatrix} \psi_A \\ \psi_B \end{pmatrix} = U^T(\theta) \begin{pmatrix} \psi_d \\ \psi_q \end{pmatrix}. \tag{12.10}$$

In other words, $U^{-1}(\theta) = U^T(\theta)$.

Differentiating (12.10), one finds

$$\frac{d}{dt}\begin{pmatrix} \psi_A \\ \psi_B \end{pmatrix} = U^T(\theta)\frac{d}{dt}\begin{pmatrix} \psi_d \\ \psi_q \end{pmatrix} + \omega\frac{\partial U^T(\theta)}{\partial\theta}\begin{pmatrix} \psi_d \\ \psi_q \end{pmatrix}, \tag{12.11}$$

where

$$\frac{\partial U(\theta)}{\partial\theta} = n_P \begin{pmatrix} -\sin(n_P\theta) & \cos(n_P\theta) \\ -\cos(n_P\theta) & -\sin(n_P\theta) \end{pmatrix}. \tag{12.12}$$

Therefore

$$\begin{aligned} \frac{d}{dt}\begin{pmatrix} \psi_d \\ \psi_q \end{pmatrix} &= U(\theta)\frac{d}{dt}\begin{pmatrix} \psi_A \\ \psi_B \end{pmatrix} - \omega U(\theta)\frac{\partial U^T(\theta)}{\partial\theta}\begin{pmatrix} \psi_d \\ \psi_q \end{pmatrix} \\ &= U(\theta)\begin{pmatrix} v_A - Ri_A \\ v_B - Ri_B \end{pmatrix} - n_P\omega\begin{pmatrix} 0 & -1 \\ 1 & 0 \end{pmatrix}\begin{pmatrix} \psi_d \\ \psi_q \end{pmatrix} \\ &= \begin{pmatrix} v_d - Ri_d + n_P\omega\psi_q \\ v_q - Ri_q - n_P\omega\psi_d \end{pmatrix}. \end{aligned} \tag{12.13}$$

The DQ fluxes are given by

$$\begin{aligned} \begin{pmatrix} \psi_d \\ \psi_q \end{pmatrix} &= \psi_0 U(\theta)D(\theta) + U(\theta)L(\theta)U^T(\theta)\begin{pmatrix} i_d \\ i_q \end{pmatrix} \\ &= \begin{pmatrix} \psi_0 \\ 0 \end{pmatrix} + \begin{pmatrix} L_d & 0 \\ 0 & L_q \end{pmatrix}\begin{pmatrix} i_d \\ i_q \end{pmatrix}, \end{aligned} \tag{12.14}$$

where

$$L_d = L_0 + L_1,\ L_q = L_0 - L_1. \tag{12.15}$$

The DQ model of the hybrid motor becomes

$$\begin{aligned} L_d\frac{di_d}{dt} &= v_d - Ri_d + n_P\omega L_q i_q \\ L_q\frac{di_q}{dt} &= v_q - Ri_q - n_P\omega L_d i_d - K\omega. \end{aligned} \tag{12.16}$$

After simplifications, the torque is

$$\begin{aligned} \tau_M &= \psi_0 \begin{pmatrix} i_d & i_q \end{pmatrix} U(\theta)\frac{\partial D(\theta)}{\partial\theta} + \frac{1}{2}\begin{pmatrix} i_d & i_q \end{pmatrix} U(\theta)\frac{\partial L(\theta)}{\partial\theta}U^T(\theta)\begin{pmatrix} i_d \\ i_q \end{pmatrix} \\ &= K\ i_q + n_P(L_d - L_q)\ i_d\ i_q. \end{aligned} \tag{12.17}$$

The first component of the torque is due to the permanent magnet, while the second component is the reluctance torque.

## 12.4 Symbolic code

The code below produces the results of (12.13), (12.14), and (12.17).

```
%
% Symbolic code for the hybrid motor
%
syms u np th d l l0 l1 du dl dd udut ulut idq id iq ...
     tm psi0 ud delta udldqudt ifg ifc ig tm k real
%
u=[cos(np*th) sin(np*th);-sin(np*th) cos(np*th)];
d=[cos(np*th);sin(np*th)];
l=[l0+l1*cos(2*np*th) l1*sin(2*np*th);l1*sin(2*np*th) ...
   l0-l1*cos(2*np*th)];
du=diff(u,th);dd=diff(d,th);dl=diff(l,th);
udut=simplify(u*du')
ulut=simplify(u*l*u')
idq=[id;iq];
tm=simplify(psi0*idq'*u*dd+0.5*idq'*u*dl*u'*idq)
```

# Bibliography


[1] S. Atallah, D. Benattous, & M.-S. Nait-Said, "Complex vector model of the brushless doubly fed machine in unified reference frame," *International Conference on Electronics & Oil: From Theory to Applications*, Ouargla, Algeria, 2013.

[2] H. J. Baesmat & M. Bodson, "Pole placement control for doubly-fed induction generators using compact representations in complex variables," *IEEE Trans. on Energy Conversion*, vol. 34, no. 2, pp. 750-760, 2019.

[3] A. R. Bergen & V. Vittal, *Power systems analysis*, 2nd edition, Prentice-Hall, Upper Saddle River, NJ, 2000.

[4] R.E. Betz & M. Jovanovic, "Introduction to the space vector modeling of the brushless doubly fed reluctance machine," *Electric Power Components and Systems*, vol. 31, no. 8, pp. 729-755, 2003.

[5] M. Bodson, "Speed control for doubly fed induction motors with and without current feedback," *IEEE Trans. on Control Systems Technology*, vol. 28, no. 3, pp. 898-907, 2020.

[6] M. Bodson, *Control of electric motors*, to appear.

[7] M. Bodson & M. A. Hossain, "Integrated control of a motor/generator set composed of doubly-fed induction machines," *IEEE Journal of Emerging and Selected Topics in Power Electronics*, vol. 8, no. 2, pp. 1858-1869, 2020.

[8] M. Bodson & O. Kiselychnyk, "The complex Hurwitz test for the analysis of spontaneous self-excitation in induction generators," *IEEE Trans. on Automatic Control*, vol. 58, no. 2, pp. 449-454, 2013.

[9] M. Cheng, R. Luo, & X. Wei, "Design and analysis of current control methods for brushless doubly fed induction machines," *IEEE Trans. on Industrial Electronics*, vol. 66, no. 1, pp. 717-727, 2019.

[10] J. Chiasson, *Modeling and high-performance control of electric machines*, IEEE Press & Wiley-Interscience, New York, NY, 2005.

[11] P. Chrin, P. Maussion, M. Pietrzak-David, B. Dagues, & L. Bun, "Modeling of 3-phase induction machine as single phase generator for electricity generation from renewable energies in rural areas," *2015 IEEE International Electric Machines & Drives Conference (IEMDC)*, Coeur d'Alene, ID, 2015, pp. 405-411.

[12] A. Dòria-Cerezo, M. Bodson, C. Batlle, & R. Ortega, "Study of the stability of a direct stator current controller for a doubly fed induction machine using the complex Hurwitz test," *IEEE Trans. on Control Systems Technology*, vol. 21, no. 6, pp. 2323-2331, 2013.

[13] P. Han, M. Cheng, & Z. Chen, "Single-electrical-port control of cascaded doubly-fed induction machine for EV/HEV applications," *IEEE Trans. on Power Electronics*, vol. 32, no. 9, pp. 7233-7243, 2017.

[14] M. A. Hossain & M. Bodson, "Control of a PMSM using the rotor-side converter of a doubly fed induction generator for hybrid-electric propulsion," *IEEE Trans. on Control Systems Technology*, vol. 30, no. 4, pp. 1758-1765, 2022.

[15] M. A. Hossain & M. Bodson, "Control of brushless doubly-fed induction motors with real-time torque optimization," to appear.

[16] M. Kong, X. Wang, Z. Li, & P. Nie, "Asynchronous operation characteristics and soft-starting method for the brushless doubly-fed motor," *IET Electric Power Applications*, vol. 11, pp. 1276-1283, 2017.

[17] P. Kundur, *Power system stability and control*, Mc Graw Hill, 1994.

[18] M. Myers, M. Bodson, & F. Khan, "Design of drives for inverter-assisted induction generators," *IEEE Trans. on Industry Applications*, vol. 48, no. 6, pp. 2147-2156, 2012.

[19] P. C. Roberts, *A study of brushless doubly-fed (induction) machines*, Ph.D. dissertation, University of Cambridge, 2005

[20] P. C. Roberts, T. Long, R. A. McMahon, S. Shao, E. Abdi, & J. M. Maciejowski, "Dynamic modelling of the brushless doubly fed machine," *IET Electric Power Applications*, vol. 7, no. 7, pp. 544–556, 2013.

[21] R. Sadeghi, S. M. Madani, T. A. Lipo, M. R. A. Kashkooli, M. Ataei, & S. Ademi, "Voltage-dip analysis of brushless doubly fed induction generator using reduced T-model," *IEEE Trans. on Industrial Electronics*, vol. 66, no. 10, pp. 7510-7519, 2019.

[22] N. L. Schmitz & D. W. Novotny, *Introductory electromechanics*, Ronald Press, 1965.

[23] S. Shao, E. Abdi, F. Barati, & R. McMahon, "Stator-flux-oriented vector control for brushless doubly fed induction generator," *IEEE Trans. on Industrial Electronics*, vol. 56, no. 10, pp. 4220-4228, 2009.

[24] L. Xu, B. Guan, H. Liu, L. Gao, & K. Tsai, "Design and control of a high-efficiency doubly-fed brushless machine for wind power generator application," *2010 IEEE Energy Conversion Congress and Exposition*, 2010, pp. 2409-2416.